doi.org/10.26434/chemrxiv.13293356.v1

Concise asymmetric syntheses of streptazone A and abikoviromycin

Gustav J. Wørmer, Nikolaj L. Villadsen, Peter Nørby, Thomas Poulsen

Submitted date: 26/11/2020 • Posted date: 27/11/2020

Citation information: Wørmer, Gustav J.; Villadsen, Nikolaj L.; Nørby, Peter; Poulsen, Thomas (2020): Concise asymmetric syntheses of streptazone A and abikoviromycin. ChemRxiv. Preprint. https://doi.org/10.26434/chemrxiv.13293356.v1

Streptazone A and abikoviromycin are related alkaloids that both feature an unusual arrangement of reactive functionalities within an underlying compact tricyclic ring system. Here, we report a highly concise asymmetric synthesis of both natural products. The developed route first constructs another member of the streptazones, streptazone B1, using a rhodium-catalyzed distal selective allene-ynamide Pauson-Khand reaction as the key transformation. A regio- and enantioselective epoxidation under chiral phase-transfer catalytic conditions was then achieved to directly make streptazone A in 8 steps overall. A chemoselective, iridium-catalyzed reduction of the enaminone-system was employed to make abikoviromycin in one additional step. Studies of the intrinsic reactivity of streptazone A towards the cysteine mimic, N-acetylcysteamine, revealed unanticipated transformations, resulting in thiol conjugation to both the hindered tertiary carbon of the double allylic epoxide and in bis-thiol conjugation which may proceed via formation of a cyclopentadienone intermediate. With flexible access to these compounds, studies aimed to identify their direct biological targets are now possible.

Concise asymmetric syntheses of streptazone A and abikoviromycin

Gustav J. Wørmer, Nikolaj L. Villadsen, Peter Nørby, Thomas B. Poulsen*

Department of Chemistry, Aarhus University, Langelandsgade 140, DK-8000, Aarhus C, Denmark.

ABSTRACT: Streptazone A and abikoviromycin are related alkaloids that both feature an unusual arrangement of reactive functionalities within an underlying compact tricyclic ring system. Here, we report a highly concise asymmetric synthesis of both natural products. The developed route first constructs another member of the streptazones, streptazone B1, using a rhodium-catalyzed distal selective allene-ynamide Pauson-Khand reaction as the key transformation. A regio- and enantioselective epoxidation under chiral phase-transfer catalytic conditions was then achieved to directly make streptazone A in 8 steps overall. A chemoselective, iridium-catalyzed reduction of the enaminone-system was employed to make abikoviromycin in one additional step. Studies of the intrinsic reactivity of streptazone A towards the cysteine mimic, *N*-acetylcysteamine, revealed unanticipated transformations, resulting in thiol conjugation to both the hindered tertiary carbon of the double allylic epoxide and in bis-thiol conjugation which may proceed via formation of a cyclopentadienone intermediate. With flexible access to these compounds, studies aimed to identify their direct biological targets are now possible.

Natural products that feature unusual constellations of reactive chemical groups are fascinating outcomes of microbial biosynthesis and may constitute unique opportunities for discovery of interesting biological activity.[1] The streptazones[2,3] (Fig. 1A) are members of a larger family of piperidine alkaloids with diverse biological activity[4-9] that share an interesting [4.3.0] bicyclic core (Fig. 1A,B). Streptazoline **3**[4,10] has been the subject of sustained interest from a series of laboratories due to the challenging tricyclic urethane core structure and the (*Z*)-exocyclic ethylidene side chain.[11] Overall, the different family members are defined by variations in oxidation state and modifications to the underlying hexahydrocyclopenta[*b*]pyridine scaffold. We have taken special interest in streptazone A (**1**) which is reported to be a potent inhibitor of liver cancer cell growth (HepG2, GI_{50} = <0.1 μM).[2] **1** features the unique constellation of an enaminone, a Michael acceptor, and a bis-allylic epoxide. We were intrigued by the compact nature of the multiple electrophilic sites embedded in this small molecule (MW = 177 g/mol) as well as the absence of information about direct biological targets, and the lack of known methods to assemble the structure. Notably, other members of the family that feature a related fused epoxide-core, kobutimycin A-B[7], hatomamicin[8], and abikoviromycin (**4**)[6,12] have also been associated with potent biological activity, with **4** differing from **1** by a different oxidation state at C7. In this communication, we report the first asymmetric synthesis of (+)-streptazone A (**1**) in 8 steps, the assignment of its absolute configuration, and the discovery of conditions for selectively transforming **1** into abikoviromycin (**4**) in a single operation. Finally, we uncover an unanticipated spectrum of thiol-reactivity inherent within the streptazone A ring system.

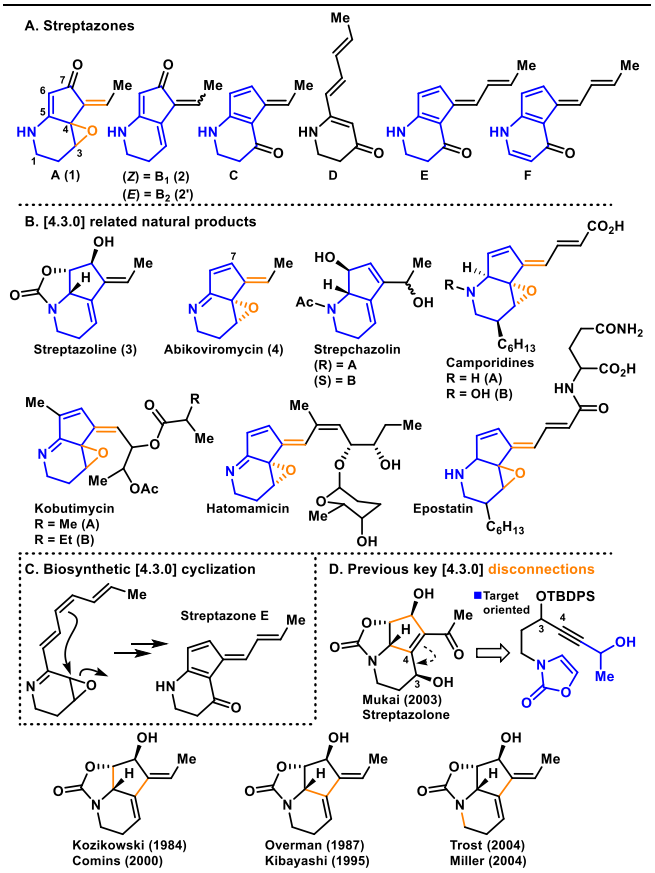

Figure 1. Chemical structures of (A) the streptazones and (B) additional family members. (C) [4.3.0]-assembly during the biosynthesis of streptazone E. (D) Different synthesis strategies towards streptazolin and streptazolone.

In contrast to the plethora of syntheses of **3**, no synthesis has been reported for any epoxide-containing member of the family.[11] It has been proposed that an epoxide facilitates the formation of the [4.3.0] core by a ring-opening event during the biosynthesis of streptazone E[13] and the camporidines[9] (Fig. 1C), however, the subsequent events that result in re-closure/re-installation of the epoxide and further oxidations are not known in detail. Arguably, any synthetic strategies targeting this functionality are likely to be challenging due to the expected tendency for carbocation formation as a result of the double allylic tertiary position at C4 (Scheme 1). Indeed, **4** has been reported to be highly unstable and to undergo polymerization even at -50 °C when handled too concentrated[12c], thus pointing to an intrinsic structural lability of such systems.

Scheme 1. Retrosynthetic analysis

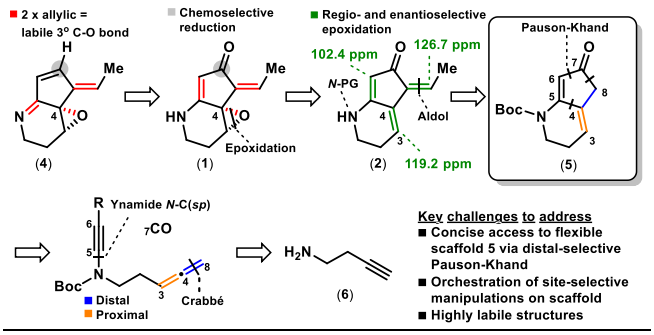

Mindful of the expected challenges associated with the epoxide, we opted to pursue a strategy that would install this group at the final stages. Indeed, we realized the potential for developing a direct approach in which **2** could be converted first to **1** and then further to **4** through sequential selective epoxidation and reduction. However, based on the reported ^{13}C NMR chemical shifts of **2**[2], the potential for conducting a selective C3-C4 epoxidation was hard to predict and methodologies describing the subsequent reduction was absent in the literature. This disconnection is therefore directly addressing two challenging and fundamental transformations for this class of compounds. Access to **2** would be possible via the highly simplified [4.3.0] bicyclic core **5** that was revealed by disconnecting the ethylidene sidechain (Scheme 1).

To develop an efficient route to **5**, we judiciously evaluated the prior syntheses of **3** and streptazolone (Fig. 1D) and found the intramolecular oxazolidinone Pauson-Khand cycloaddition utilized by Mukai and co-workers[11e] appealing, however, not directly applicable to our purpose: First, the cyclic urethane is central for the construction of the tricyclic ring system and variations to this particular core were unlikely to be trivial. Second, the Pauson-Khand cycloaddition product obtained would require a challenging isomerization of the olefin to the desired C3-C4 position. Instead, we envisioned that the olefin could be positioned advantageously by a distal selective intramolecular allene-ynamide Pauson-Khand cyclization, which, interestingly, is unprecedented in the literature for [4.3.0] scaffolds. The ynamide functionality has been studied extensively by several groups to construct the rather difficult *N*-C(*sp*) bond directly and different protecting groups may be applied in the transformation.[14] This analysis then converged to commercial but-3-yn-1-amine hydrochloride **6** as an optimal starting material.

The synthesis was initiated using the Crabbé homologation[15] of Boc-protected **6** to deliver allene **7** in 76% yield in multigram quantities (16 g isolated) over two steps. Next, we turned our attention to establish the acyclic bulky carbamate *N*-C(*sp*) bond. Several methodologies were evaluated[14] which generally failed to provide reproducible results for a scalable synthesis. Initial attempts based on TMS-bromoacetylene employing the 2nd generation copper catalyzed ynamide synthesis delivered the allene tethered ynamide **8a** in <1% yield whereas the TIPS-bromoacetylene and the TES-bromoacetylene, resulting in **8b** and **8c** respectively, performed significantly better after optimization (see Table 1 in SI).[16] Our initial intramolecular allene-ynamide Pauson-Khand cyclization was tested on all three ynamides (**8a**-**8c**) using the commonly employed $[Rh(CO)_2Cl]_2$ for regioselectively favoring the distal π-bond of the allene in the cyclization.[17-19] Furthermore, for safe handling of CO gas, we studied the reaction utilizing a two-chamber system developed by Skrydstrup et al. where stoichiometric CO is delivered ex situ from a palladium catalyzed decarbonylation of a solid precursor (see SI).[20] Indeed, we found that the cyclization worked on all three substrates which establishes ynamides as functional precursors for rhodium-catalyzed Pauson-Khand cyclization to deliver [4.3.0] scaffolds. To our knowledge, only catalytic molybdenum has been employed in an intramolecular allene-ynamide cyclization, however, to access [3.3.0] scaffolds.[21] In our hands, **8c** was balanced appropriately for both ynamide accessibility and performance in the early cyclization attempts. After evaluation of several distal selective catalysts (scheme 2, step d), we found $[Rh(CO)Cl(dppp)]_2$ the most suitable for a scalable synthesis (66% yield on a 19 mmol scale). With rapid access to the [4.3.0] core secured, installation of the C8-ethylidene group was next. Following our retrosynthetic analysis, the aldol disconnection was initiated by C8 alkylation using the lithium enolate generated with LiHMDS that could subsequently be treated with acetaldehyde to afford a 60:40 dr mixture of β-hydroxy ketones in 74% yield. The mixture of diastereoisomers could readily undergo dehydration using Burgess reagent to predominantly afford the *syn* eliminated α,β-unsaturated ketones **11** in 82% yield as a 55:45 *cis*/*trans* mixture.[22] To our delight, protodesilylation and *N*-Boc deprotection could be achieved in a single operation using diluted TFA which upon basic work-up delivered **2** and **2'** in 89% yield.

Progressing forward, **2** and **2'** were separated using standard chromatography which enabled us to study the direct epoxidation of **2**. An extensive work was put into this particular transformation – testing both racemic and a range of established asymmetric procedures to probe the overall reactivity of the tris-olefins in **2**/**2'**. Generally, we found that electrophilic epoxidations using *m*-CPBA, DMDO etc. under different conditions delivered complex mixtures,

presumably as a direct consequence of the more nucleophilic free enaminone system. Next we speculated whether the C3-C4 olefin (scheme 1) principally could be viewed as a γ-δ unsaturated ketone and become activated under Lewis acid- or Brøndsted acid catalysis. In our hands, however, such conditions either resulted in decomposition or reisolation of starting material. Jacobsen's manganese based system[23] (Scheme 2, step h, entry 1) did allow us to identify trace formation of **1** but unfortunately, the methodology failed to deliver improvement after substantial experimentation and was furthermore limited by irreproducible results on scales greater than 0.05 mmol. To our delight, we found that Shibasaki's lanthanum-BINOL system[24] (entry 2) indeed delivered **1**, though as a racemic mixture. Upon rational exclusion of each component in the system, it was clear that lanthanum was irrelevant for the epoxidation while cumene hydroperoxide (CHP) at elevated temperature sluggishly could deliver **1** regioselectively. With catalytic DBU, we started to obtain promising results (entry 3) and conversion of **2** was further improved using TBAI as phase-transfer catalyst (PTC), although **1** was still only formed in small amounts (entry 4). This prompted us to investigate cinchona-based PTCs.[25] Gratifyingly, the yield of **2** increased significantly and stereoinduction was also obtained (entry 5-6). After further optimization (see Table 2 in SI) we found that the commercial catalyst **12** could deliver **1** in 62% yield with 72% ee (>99% ee after recrystallization). Subsequent derivatization of (+)-**1** with ferrocene-CO_2Cl enabled us to determine the absolute configuration of (+)-**1** by X-ray crystallography.

Scheme 2. Synthesis of streptazone A and abikoviromycin

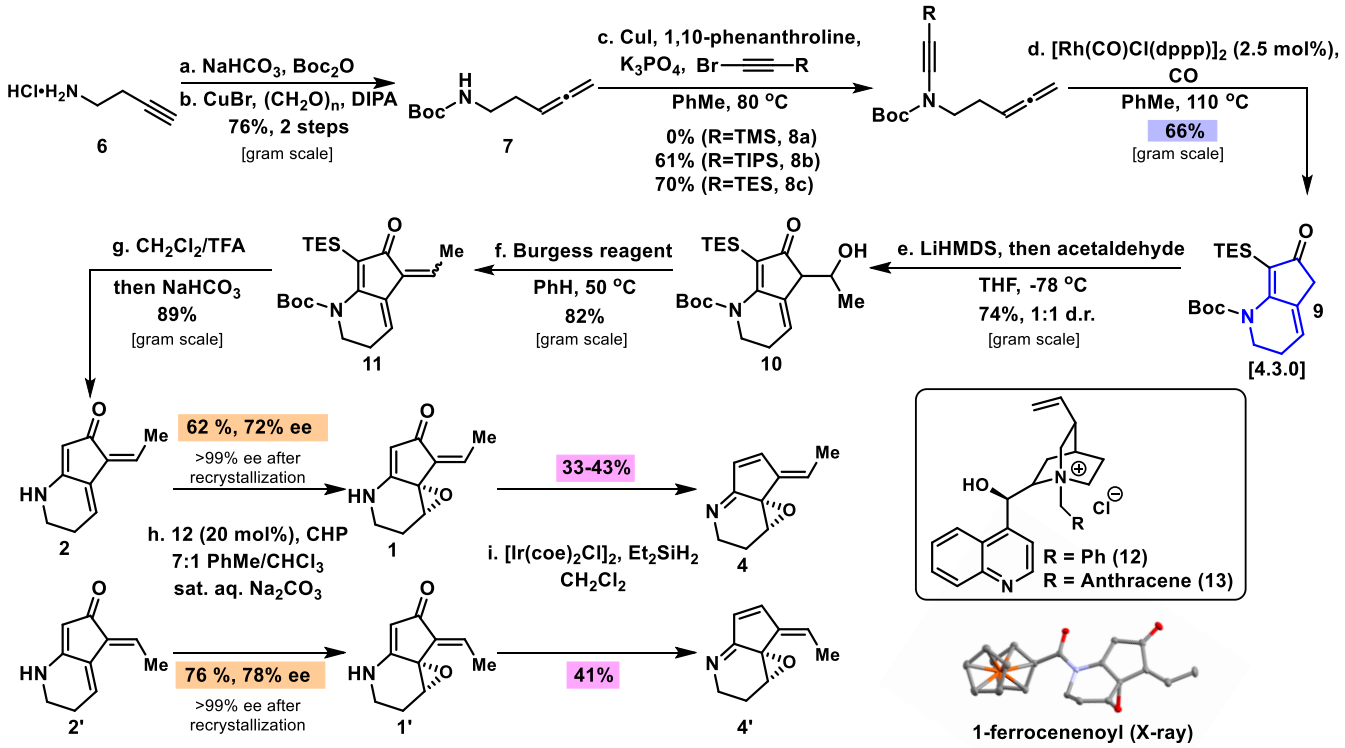

Step d

Entry	Catalyst	Isolated (9/8c)
1	$[Rh(CO)_2Cl]_2$ (2.5 mol%)	24/0
2	$[Ir(cod)Cl]_2$ (2.5 mol%)	11/30
3	$[Ir(coe)_2Cl]_2$ (2.5 mol%)	11/12
4	$[Rh(cod)B(Ph)_4]$ (2.5 mol%)	32/5
5	$[Rh(CO)Cl(dppp)]_2$ (2.5 mol%)	56/0, (66/4)*

Screening was performed in two-chamber
* Conducted on 19.3 mmol scale

Step h

Entry	Conditions	Yield (2/1)#	ee%
1	Jacobsen's $Mn^{(III)}$	0/trace	89
2	Shibasaki's La-BINOL	89/11*	0
3	CHP, DBU	28/23	-
4	TBAI	0/7	-
5	12	0/56	76
6	13	6/26	32

HNMR yield, * ratio between 2/1

Step i

Entry	Conditions	Result
1	Tf_2O then $Pd(OAc)_2$, TPP, Et_3N, HCO_2H	Decomposition
2	Tf_2O then $Pd(PPh_3)_4$, LiCl, Bu_3SnH	Decomposition
3	Schwartz reagent	1' recovered
4	$Zn(OAc)_2$, $(EtO)_3SiH$	1' recovered
5	$LiAlH(OtBu)_3$, CuBr	1' recovered
6	Stryker's reagent, $PhMe_2SiH$	1' recovered
7	$[Ir(coe)_2Cl]_2$, Et_2SiH_2	1' recovered + 4'

1 and **4** differ only by oxidation level. Although the potential biosynthetic connection between these two compounds currently remains elusive, access to **1** prompted the question if a single, selective reduction to form **4** could be realized to directly access the imine [4.3.0] subclass. Albeit a highly appealing synthetic option, the direct conversion from a free cyclic enaminone to the corresponding conjugated imine is, however, to our knowledge not precedented in the literature. This particular transformation is complicated by several factors: 1) multiple sites in **1** are prone to alternate reductions, hereof the labile epoxide and the Michael acceptor, 2) feasible over-reduction upon generation of the conjugated imine, 3) the product **4**, is reportedly highly unstable.

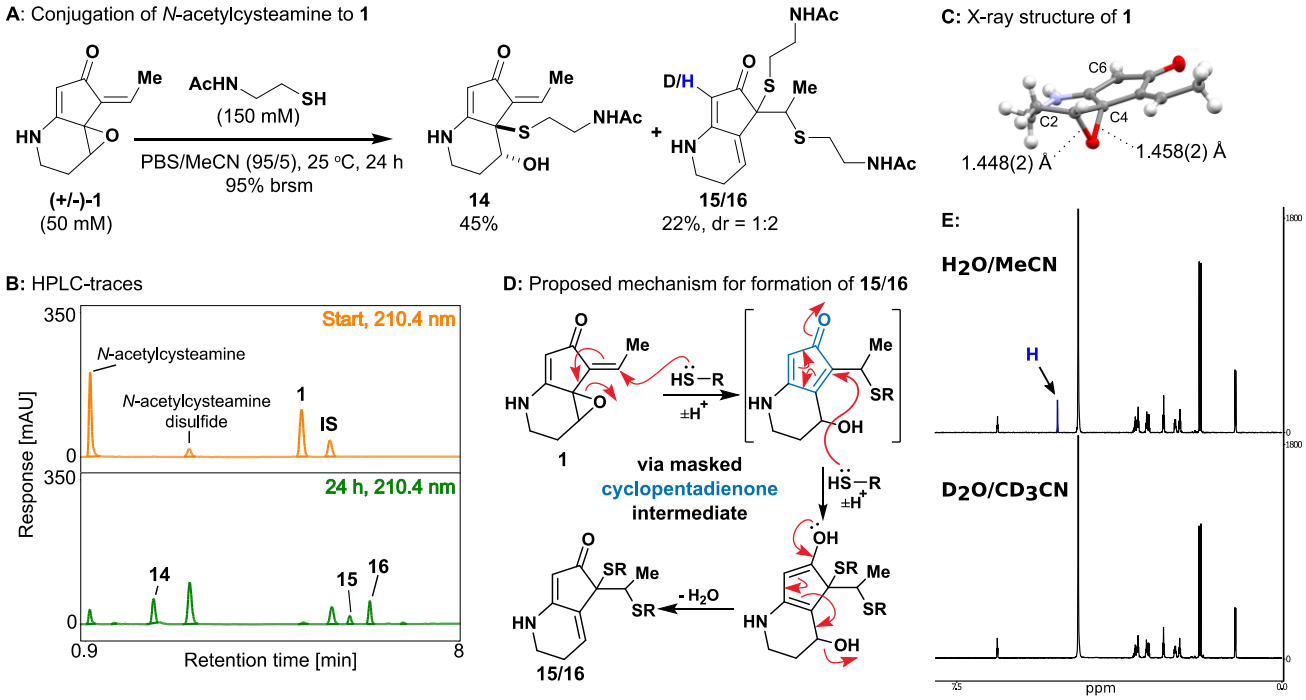

Figure 2. Studies of thiol-conjugation to streptazone A reveals dichotomous reactivity.

We decided to engage in a screen for reduction conditions utilizing the geometric isomer **1'** under the assumption that the overall outcome would be representative also for **1**. Our initial effort was based on the hypothesis that enaminones have increased electron density at the carbonyl which should render the system more susceptible for *O*-activation. When **1'** was subjected to Tf_2O, we indeed observed formation of the *O*-triflated triflate salt which was immediately subjected to reductive conditions under palladium catalysis (Scheme 1, step i, entry 1-2)[26,27], however, only decomposition of the starting material was observed. Next we tested methodologies reported for secondary amide reduction by metal catalyzed reductions (entry 3-4)[28,29] with neither indication of imine nor amine formation. Moreover, we evaluated the possibility of a 3-step sequence by initial 1,4-hydride copper-catalyzed reduction of the enaminone, triflation and reduction and lastly relying on the reported enzymatic reoxidation to **4** by SF-973B oxidoreductase.[30-32] This idea, however, fell short of the goal already in the initial 1,4 hydride reduction (entry 5-6). Finally, inspired by the recently reported total synthesis of Herquline B and C by Baran and co-workers employing the iridium-diethylsilane system developed by Cheng and Brookhart, we ultimately found the reduction-system applicable to directly deliver the imine product **4'** (entry 7) (see Table 3 in SI for evaluation of reductions).[33-34] In the case of **1**, the reduction proceeded slower but it nonetheless afforded **4** in 43% overall best yield, (see SI for a discussion of general stability of **4**). In the case of **1'**, simply increasing the reaction time pushed the reaction toward the dihydro adduct whereas **1** required additional reductant to deliver dihydroabikoviromycin (see SI).[6,35] Hence, the system may be employed to afford both the imine- and the amine [4.3.0] bicyclic classes by careful reaction control.

Finally, we investigated the electrophilic properties of **1** towards a biological thiol mimetic, *N*-acetylcysteamine, at physiological pH (Fig. 2A). 95% conversion was obtained after 24 h thereby confirming the intrinsic reactivity of the natural product towards thiols. Surprisingly, we were able to identify three major thiol conjugates by analytical RP-HPLC, which we successfully isolated with the major thiol conjugate corresponding to epoxide opening (Fig. 2A,B). As evident by careful 2D NMR analysis, the epoxide was curiously opened at the tertiary position, not the secondary. We speculate that the observed regioselectivity is a direct consequence of the double allylic contribution to the σ^* C-O bond that in turn favors the tertiary carbon for incoming nucleophiles. To further elaborate on this effect, we were able to crystallize the natural product which indeed revealed that this particular C-O bond was slightly elongated in comparison to the other (Fig. 2C). The remaining two conjugates corresponded to a set of diastereoisomers (**15/16**) and were unmistakably the product of double addition of *N*-acetylcysteamine (Fig. 2A,B). Again,

we were surprised by the behavior performed by **1**, as it became evident from HMBC couplings, that the additions corresponded to a completely different reaction path, in this case initiated via the Michael acceptor. We speculate that initial 1,4-addition induces epoxide opening via the corresponding enolate and, in turn, unmasks a highly reactive cyclopentadienone electrophile (possibly stabilized by the fused amine) that undergoes a subsequent nucleophilic addition at the α-position and ultimately results in dehydration (Fig. 2D). To gain mechanistic insight of the α-addition, we conducted the conjugation in D_2O/CD_3CN and found that C6 had undergone full deuterium exchange, thereby suggesting that α-addition principally may be viewed as a 1,6-addition (Fig. 2E). To our knowledge, this is the first evidence supporting a masked cyclopentadienone natural product electrophile.

From a biological perspective, this data supports that **1** likely acts as a cysteine-reactive natural product that furthermore demonstrate the reactivity characteristic for some "molecular glues" by having multiple electrophilic sites.[36] We anticipate that this highly peculiar reactivity will manifest itself in biological studies of this natural product family. Attempts to reproduce the reported toxicity against HepG2 liver cancer cells were, in our hands, not successful with **1** (of any of its isomers) showing negligible toxicity. This, along with the intrinsic reactivity of **1** that we have observed, underscores the importance of mapping the covalent targets of **1**.

In summary, we have developed the first synthesis of streptazone B_1/B_2, streptazone A, abikoviromycin and dihydroabikoviromycin in 7, 8 and 9 steps, respectively. During our studies, we discovered a new intramolecular Pauson-Khand cycloaddition performed on an allene-tethered ynamide substrate to deliver a bicyclo[4.3.0] core. Furthermore, we present a highly regioselective epoxidation employing chiral phase-transfer catalysis to epoxidize streptazone B_1 to A. This in turn enabled the direct reduction of an unprecedented cyclic enaminone functionality using iridium catalysis to access abikoviromycin and dihydroabikoviromycin. Finally, we demonstrate that streptazone A possess several electrophilic sites by *in vitro* thiol-conjugation studies. This includes formation of surprising double thiol-adducts that are potentially the result of a cyclopentadienone intermediate.

ASSOCIATED CONTENT

The Supporting Information is available free of charge at XXX

Experimental details, spectroscopic data, supporting Tables 1–3, general stabilities etc. is found in supporting information.

AUTHOR INFORMATION

Corresponding Author

* **Thomas B. Poulsen** – Department of Chemistry, Aarhus University, 8000 Aarhus C, Denmark; orcid.org/ 0000-0002-0763-9996; E-mail: thpou@chem.au.dk

Authors

Gustav J. Wørmer - Department of Chemistry, Aarhus University, 8000 Aarhus C, Denmark

Nikolaj L. Villadsen† - Department of Chemistry, Aarhus University, 8000 Aarhus C, Denmark

Peter Nørby - Department of Chemistry, Aarhus University, 8000 Aarhus C, Denmark

Present Addresses

† Process Chemistry Development, H. Lundbeck A/S, 2500 Valby, Denmark.

Notes

The authors declare no competing financial interest.

ACKNOWLEDGMENTS

This work was supported by grants from the Novo Nordisk Foundation (grant NNF19OC0054782 to T.B.P.) and the Carlsberg Foundation (grant CF17-0800 to T.B.P.). We further thank the K.A. Jørgensen lab for access to chiral stationary phase UPC² and Anders Bodholt Nielsen and Dennis Wilkens Juhl for technical assistance with NMR spectroscopy. Lastly, we thank Troels Skrydstrup lab for technical assistance using the two-chamber system and Jens Christian Kondrup for scientific glassware design.

REFERENCES

(1) (a) Nomura, D. K.; Maimone, T. J. Target Identification of Bioactive Covalently Acting Natural Products. *Curr. Top Microbiol. Immunol.* **2019**, *420*, 351–374. (b) Gersch, M.; Kreuzer, J.; Sieber, S. A. Electrophilic natural products and their biological targets. *Nat. Prod. Rep.* **2012**, *29*, 659-682.

(2) Puder, C.; Krastel P.; Zeeck, A. Streptazones A, B1, B2, C, and D: New Piperidine Alkaloids from Streptomycetes. *J. Nat. Prod.* **2000**, *63*, 9, 1258-1260.

(3) Liu, Q.-F.; Wang, J.-D.; Wang X.-J.; Liu, C.-X.; Zhang, J.; Pang, Y.-W.; Yu, C.; Xiang, W.-S. Two new piperidine alkaloids from Streptomyces sp. NEAU-Z4. *J. Asian Nat. Prod. Res.* **2013**, *15*, 221–224.

(4) Perry, J. A.; Koteva, K.; Verschoor, C. P.; Wang, W.; Bowdish, D. M.; Wright, G. D. A macrophage-stimulating compound from a screen of microbial natural products. *J. Antibiot.* **2014**, *68*, 1, 40–46.

(5) Akiyama, T.; Harada, S.; Kojima, F.; Kinoshita, N.; Hamada, M.; Muraoka, Y.; Aoyagi, T.; Takeuchi, T. Epostatin, new inhibitor of dipeptidyl peptidase II, produced by Streptomyces sp. MJ995-OF5. *J. Antibiot*. **1998**, 51, 3, 253–260.

(6) (a) Maruyama, H.; Okamoto, S.; Kubo, Y.; Tsuji, G.; Fujii, I.; Ebizuka, Y.; Furihata, K.; Hayakawa, Y.; Nagasawa, H.; Sakuda, S. Isolation of abikoviromycin and dihydroabikoviromycin as inhibitors of polyketide synthase involved in melanin biosynthesis by Colletotrichum lagenarium. *J. Antibiot.* **2003**, 56, 9, 801–804. (b) Takahashi, S., Serita, K., Enokita, R., Okaza, T. and Haneishi, T. A new antibiotic, *N*-Hydroxydihydroabikoviromycin. *Sankyo Kenkyusho Nempo.* **1986**, 38, 105–108.

(7) Kanbe, K.; Naganawa, H.; Okami, Y.; Takeuchi, T. Kobutimycins A and B, new alkaloid antibiotics produced by a streptomyces strain. *J. Antibiot.* **1992**, *45*, 10, 1700–1702.

(8) Imai, H.; Fujita, S.; Suzuki, K.; Morioka, M.; Tokunaga, T.; Shimizu, M.; Kadota, S.; Furuya, T.; Saito, T. Hatomamicin (YL-0358M-A), a new alkaloid antibiotic: Fermentation, isolation, structure and biological properties. *J. Antibiot.* **1989**, *42*, 7, 1043–1048.

(9) Hong, S.-H.; Ban, Y. H.; Byun, W. S.; Kim, D.; Jang, Y.-J.; An, J. S.; Shin, B.; Lee, S. K.; Shin, J.; Yoon, Y. J.; Oh, D.-C. Camporidines A and B: antimetastatic and anti-inflammatory polyketide alkaloids from a gut bacterium of Camponotus kiusiuensis. *J. Nat. Prod*. **2019**, *82*, 4, 903-910.

(10) Drautz, H.; Zahner, H.; Kupfer, E.; Kellerschierlein, W. Metabolism products of microorganisms 205. Isolation and structure of streptazolin. *Helv. Chim. Acta.* **1981**, *64*, 1752-1765.

(11) (a) Kozikowski, A. P.; Uk Park, P. Total synthesis of streptazolin - an application of the aza-analogue of the ferrier rearrangement. *J. Am. Chem. Soc.* **1985**, *107*, 6, 1763-1765. (b) Flann, C. J.; Overman, L. E. Enantioselective total synthesis of streptazolin. The tandem use of iminium ion vinylsilane cyclizations and intramolecular acylations. *J. Am. Chem. Soc.* **1987**, *109*, 20, 6115–6118. (c) Yamada, H.; Aoyagi, S.; Kibayashi, C. Stereoselective total synthesis of natural (+)-streptazolin via a palladium-catalyzed enyne bicyclization approach. *J. Am. Chem. Soc.* **1996**, *118*, 5, 1054–1059. (d) Huang, S.; Comins, D. L. Total synthesis of (+)-streptazolin. *Chem. Commun*. **2000**, *7*, 569–570. (e) Nomura, I.; Mukai, C. Total synthesis of (±)-8α-hydroxystreptazolone. *Org. Lett.* **2002**, *4*, 24, 4301–4304. (f) Trost, B. M.; Chung, C. K.; Pinkerton, A. B. Stereocontrolled total synthesis of (+)-streptazolin by a palladium-catalyzed reductive diyne cyclization. *Angew. Chem. Int. Ed*. **2004**, *43*, 33, 4327–4329. (g) Li, F.; Warshakoon, N. C.; Miller, M. J. Synthetic application of acylnitroso Diels–Alder derived aminocyclopentenols: Total synthesis of (+)-streptazolin. *J. Org. Chem*. **2004**, 69, 25, 8836–8841. (h) Mitchell, D.; Liebeskind, L. S. (+/-)-Benzoabikoviromycin, a Potential Antiviral Agent Synthesized by the Palladium-Catalyzed Ring Expansion of 2-Alkynyl-2-Hydroxybenzocyclobutenones. *J. Am. Chem. Soc*. **1990**, 112, 1, 291–296.

(12) Abikoviromycin has also been referred to as latumcidin in some earlier papers. In this manuscript, we refer to the compound as abikoviromycin. (a) Sakagami, Y.; Yamaguchi, I.; Yonehara, H.; Okimoto, Y.; Yamanouchi, S.; Takiguchi, K.; Sakai, H., Latumcidin, a new antibiotic from Streptomyces sp. *J. Antibiot. Ser. A*. **1958**, *11*, 6-13. (b) Umezawa, H.; Tazaki, T.; Fukuyama, S., An antiviral substance, abikoviromycin, produced by Streptomyces species. *J. Antibiot*. **1952**, 5, 469-476. (c) Gurevich, A.; Kolosov, M.; Korobko, V.; Onoprienko, V. The structure of abikoviromycin. *Tetrahedron Lett*. **1968**, *9*, 2209–2212.

(13) Ohno, S.; Katsuyama, Y.; Tajima, Y.; Izumikawa, M.; Takagi, M.; Fujie, M.; Satoh, N.; Shin-ya, K.; Ohnishi, Y. Identification and characterization of the streptazone E biosynthetic gene cluster in Streptomyces sp. MSC090213JE08. *ChemBioChem.* **2015**, *16*, 2385–2391.

(14) Selected examples: (a) Witulski, B.; Stengel, T. N-functionalized 1-Aalkynylamides: New building blocks for transition metal mediated inter- and intramolecular [2+2+1] cycloadditions. *Angew. Chem. Int. Ed.* **1998**, *37*, 489–492. (b) Frederick, M. O.; Mulder, J. A.; Tracey, M. R.; Hsung, R. P.; Huang, J.; Kurtz, K. C.; Shen, L.; Douglas, C. J. A copper-catalyzed C–N bond formation involving sp-hybridized carbons. A direct entry to chiral ynamides via N-alkynylation of amides. *J. Am. Chem. Soc*. **2003**, 125, 2368–2369. (c) Dunetz, J. R.; Danheiser, R. L. Copper-mediated N-alkynylation of carbamates, ureas, and sulfonamides. A general method for the synthesis of ynamides. *Org. Lett*. **2003**, 5, 4011–4014. (d) Istrate, F. M.; Buzas, A. K.; Jurberg, I. D.; Odabachian, Y.; Gagosz, F. Synthesis of functionalized oxazolones by a sequence of Cu(II)- and Au(I)-catalyzed transformations. *Org. Lett*. **2008**, *10*, 925–928. (e) Mansfield, S. J.; Smith, R. C.; Yong, J. R. J.; Garry, O. L.; Anderson, E. A. A general copper-catalyzed synthesis of ynamides from 1,2-dichloroenamides. *Org. Lett*. **2019**, 21, 2918-2922. (f) Riddell, N.; Villeneuve, K.; Tam, W. Ruthenium-catalyzed [2 + 2] cycloadditions of ynamides. *Org. Lett*. **2005**, 7, 3681–3684.

(15) (a) Crabbé, P.; Fillion, H.; André, D.; Luche, J.-L. Efficient homologation of acetylenes to allenes. *J. Chem. Soc., Chem. Commun*. **1979**, 19, 859–860. (b) Li, M.; Dixon, D. J. Stereoselective spirolactam synthesis via palladium catalyzed arylative allene carbocyclization cascades. *Org. Lett*. **2010**, *12*, 3784–3787.

(16) (a) Zhang, Y.; Hsung, R. P.; Tracey, M. R.; Kurtz, K. C. M.; Vera, E. L. Copper sulfate-pentahydrate-1,10-phenanthroline catalyzed amidations of alkynyl bromides. Synthesis of heteroaromatic amine substituted ynamides. *Org. Lett*. **2004**, *6*, 1151–1154. (b) Zhang, X.; Zhang, Y.; Huang, J.; Hsung, R. P.; Kurtz, K. C. M.; Oppenheimer, J.; Petersen, M. E.; Sagamanova, I. K.; Shen, L.; Tracey, M. R. Copper(II)-catalyzed amidations of alkynyl bromides as a general synthesis of ynamides and *Z*-enamides. An intramolecular amidation for the synthesis of macrocyclic ynamides. *J. Org. Chem*. **2006**, *71*, 4170–4177. (c) Dooleweerdt, K.; Birkedal, H.; Ruhland, T.; Skrydstrup, T. Irregularities in the effect of potassium phosphate in ynamide synthesis. *J. Org. Chem*. **2008**, *73*, 9447–9450.

(17) Brummond, K. M.; Chen, H.; Fisher, K. D.; Kerekes, A. D.; Rickards, B.; Sill, P. C.; Geib, S. J. An allenic Pauson–Khand-type reaction: A reversal in π-bond selectivity and the formation of seven-membered rings. *Org. Lett*. **2002**, *4*, 1931–1934.

(18) Kitagaki, S.; Inagaki, F.; Mukai, C. [2+2+1] Cyclization of allenes. *Chem. Soc. Rev*. **2014**, 43, 2956-2978.

(19) Bayden, A. S.; Brummond, K. M.; Jordan, K. D. Computational insight concerning catalytic decision points of the transition

metal catalyzed [2 + 2 + 1] cyclocarbonylation reaction of allenes. *Organometallics*, **2006**, *25*, 5204-5206.
(20) Hermange, P.; Lindhardt, A. T.; Taaning, R. H.; Bjerglund, K.; Lupp, D.; Skrydstrup, T. Ex situ generation of stoichiometric and substoichiometric ^{12}CO and ^{13}CO and its efficient incorporation in palladium catalyzed aminocarbonylations. *J. Am. Chem. Soc*. **2011**, *133*, 6061–6071.
(21) Gupta, A. K.; Park, D. I.; Oh, C. H. The exclusive formation of cyclopentenones from molybdenum hexacarbonyl-catalyzed Pauson–Khand reactions of 5-allenyl-1-ynes. *Tetrahedron Lett*. **2005**, *46*, 4171–4174.
(22) Hjerrild, P.; Tørring, T.; Poulsen, T. B. Dehydration Reactions in Polyfunctional Natural Products. *Nat. Prod. Rep*. **2020**, 37, 8, 1043–1064.
(23) (a) Zhang, W.; Loebach, J. L.; Wilson, S. R.; Jacobsen, E. N. Enantioselective epoxidation of unfunctionalized olefins catalyzed by (salen)manganese complexes. *J. Am. Chem. Soc*. **1990**, 112, 2801–2803. (b) Brandes, B. D.; Jacobsen, E. N. Highly enantioselective, catalytic epoxidation of trisubstituted olefins. *J. Org. Chem*. **1994**, 59, 4378–4380.
(24) Bougauchi, M.; Watanabe, S.; Arai, T.; Sasai, H.; Shibasaki, M. Catalytic asymmetric epoxidation of α,β-unsaturated ketones promoted by lanthanoid complexes. *J. Am. Chem. Soc*. **1997**, 119, 2329–2330.
(25) (a) Hummelen, J. C.; Wynberg, H. Alkaloid assisted asymmetric synthesis IV additional routes to chiral epoxides. *Tetrahedron Lett*. **1978**, 19, 1089–1092. (b) Lygo, B.; Wainwright, P. G. Asymmetric Phase-Transfer Mediated Epoxidation of α,β-Unsaturated Ketones Using Catalysts Derived from Cinchona Alkaloids. *Tetrahedron Lett*. **1998**, 39, 12, 1599–1602. (c) Lygo, B.; Wainwright, P. G. Phase-Transfer Catalysed Asymmetric Epoxidation of Enones Using *N*-Anthracenylmethyl-Substituted Cinchona Alkaloids. *Tetrahedron*, **1999**, 55, 20, 6289–6300.
(26) Cacchi, S.; Morera, E.; Ortar, G. Palladium-catalyzed reduction of enol triflates to alkenes. *Tetrahedron Lett*. **1984**, *25*, 4821–4824.
(27) Scott, W. J.; Stille, J. K. Palladium-catalyzed coupling of vinyl triflates with organostannanes. Synthetic and mechanistic studies. *J. Am. Chem. Soc*. **1986**, *108*, 3033–3040.
(28) Das, S.; Addis, D.; Zhou, S.; Junge, K.; Beller, M. Zinc-catalyzed reduction of amides: Unprecedented selectivity and functional group tolerance. *J. Am. Chem. Soc.* **2010**, *132*, 1770–1771.
(29) Schedler, D. J. A.; Godfrey, A. G.; Ganem, B. Reductive deoxygenation by Cp_2ZrHCl: Selective formation of imines via zirconation/hydrozirconation of amides. *Tetrahedron Lett*. **1993**, *34*, 5035–5038.
(30) Focken, T.; Charette, A. B. stereoselective synthesis of pyridinones: application to the synthesis of (–)-barrenazines. *Org. Lett*. **2006**, *8*, 2985–2988.
(31) Lipshutz, B. H.; Chrisman, W.; Noson, K.; Papa, P.; Sclafani, J. A.; Vivian, R. W.; Keith, J. M., Copper hydride-catalyzed tandem 1,4-reduction/alkylation reactions. *Tetrahedron*, **2000**, *56*, 2779–2788.
(32) Tsuruoka, T.; Shomura, T.; Ogawa, Y.; Ezaki, N.; Watanabe, H.; Amano, S.; Inouye, S.; Niida, T. Some properties of SF-973 B substance, the enzyme catalyzing the conversion of dihydroabikoviromycin to abikoviromycin. *J. Antibiot*. **1973**, *26*, 168–174.
(33) He, C.; Stratton, T. P.; Baran, P. S. Concise total synthesis of herqulines B and C. *J. Am. Chem. Soc*. **2018**, *141*, 29–32.
(34) Cheng, C.; Brookhart, M. Iridium-catalyzed reduction of secondary amides to secondary amines and imines by diethylsilane. *J. Am. Chem. Soc*. **2012**, 134, 11304–11307.
(35) (a) Holmalahti, J.; Mäki-Paakkanen, J.; Kangas, L.; von Wright, A. Genotoxicity of dihydroabikoviromycin, a secondary metabolite of Streptomyces Anulatus. *Mutat. Res-Genet. Tox*. **1996**, 368, 157–163. (b) Holmalahti, J.; Raatikainen O.; von Wright, A.; Laatsch, H.; Spohr, A.; Lyngberg, O. K.; Nielsen, J. Production of dihydroabikoviromycin by Streptomyces Anulatus: Production parameters and chemical characterization of genotoxicity. *J. App. Microbiol*. **1998**, *85*, 61–68.
(36) Isobe, Y.; Okumura, M.; McGregor, L. M.; Brittain, S. M.; Jones, M. D.; Liang, X.; White, R.; Forrester, W.; McKenna, J. M.; Tallarico, J. A.; Schirle, M.; Maimone, T. J.; Nomura, D. K. Manumycin polyketides act as molecular glues between UBR7 and P53. *Nat. Chem. Biol*. **2020**, 16, 1189–1198.

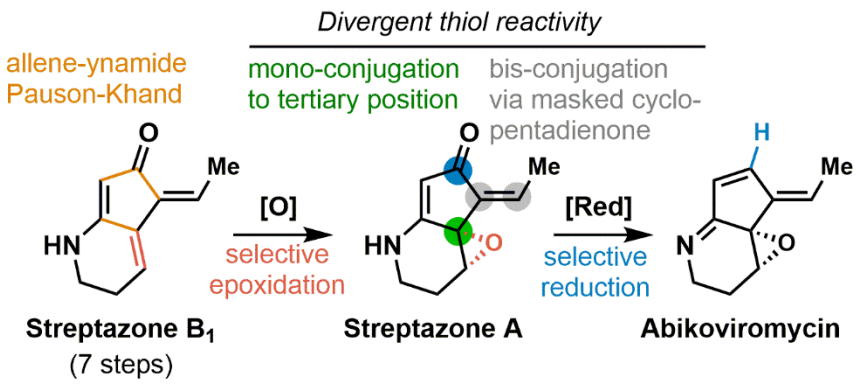
Divergent thiol reactivity
allene-ynamide
Pauson-Khand
mono-conjugation
to tertiary position
bis-conjugation
via masked cyclo-
pentadienone
O
Me
HN
[O]
selective
epoxidation
O
Me
HN
O
[Red]
selective
reduction
H
Me
N
O
Streptazone B1
(7 steps)
Streptazone A
Abikoviromycin

Supporting information

Contents

Organic synthesis - general information

All reactions were conducted in flame-dried glassware under an atmosphere of dry argon unless otherwise stated. CH_2Cl_2, THF and PhMe were dried over aluminium oxide via an MBraun SPS-800 solvent purification system. 1,4-dioxane was purchased as anhydrous. The dryness of solvents was controlled via Karl Fischer titration. Reagents were used as received from commercial suppliers unless otherwise stated (Sigma Aldrich, Merck, AK Scientific, Acros Organics, TCI and Fluorochem). DIPEA was dried by stirring for at least 30 minutes over CaH_2 followed by distillation onto preactivated molecular sieves (4 Å). Concentration *in vacuo* was performed using a rotary evaporator with the water bath temperature at 30 °C, or 40 °C, followed by further concentration using a high vacuum pump. TLC analysis was carried out on silica coated aluminum foil plates (Merck Kieselgel 60 F254). The TLC plates were visualized by UV irradiation and/or by staining with $KMnO_4$ stain ($KMnO_4$(5.0 g), 5% NaOH (aq., 8.3 mL) and K_2CO_3(33.3 g) in H_2O (500 mL)). Molecular sieves were activated by drying in the oven at 120 °C for at least 24 hours, before they were heated in a microwave at maximum power for 2 minutes, followed by evaporation of the formed vapor on a high vacuum line. This was repeated 3-4 times, and finished by gently flame-drying the flask containing the molecular sieves. Flash column chromatography (FCC) was carried out using silica gel (230-400 mesh particle size, 60 Å pore size) as stationary phase. Automated flash column chromatography (AFCC) was carried out with Interchim PuriFlash 420 or Interchim PuriFlash 5.050 using 30 µm prepacked columns. Infrared spectra (IR) were acquired on a PerkinElmer Spectrum TwoTM UATR. Mass spectra (HRMS) were recorded on a Bruker Daltonics MicrOTOF time-of-flight spectrometer with positive electrospray ionization, or negative ionization when stated. Nuclear magnetic resonance (NMR) spectra were recorded on a Bruker BioSpin Co. AVANCE III 500 MHz spectrometer, a Varian Mercury 400 MHz spectrometer or a Bruker BioSpin GmbH 400 MHz spectrometer, running at 500/400 and 125/101 MHz for ^{1}H and ^{13}C, respectively. Chemical shifts (δ) are reported in ppm relative to the residual solvent signals ($CDCl_3$: 7.26 ppm ^{1}H NMR, 77.16 ppm ^{13}C NMR etc.). Multiplicities are indicated using the following abbreviations: s = singlet, d = doublet, t = triplet, q = quartet, h = heptet, m = multiplet, b = broad. MPLC was performed using Interchim PuriFlash 5.050. Analytical HPLC analysis was conducted using Agilent 1260 infinity II.

X-ray crystallography

Crystallographic single crystal X-ray data for **1'** and **1**-ferrocenenoyl were collected on a Bruker Kappa Apex2 diffractometer equipped with a Mo source. The crystals were cooled to 100(1) K using an Oxford Cryosystems liquid nitrogen Cryostream device. Absorption correction for the structures were done with SADABS. Cell refinement and data reduction were done in SAINT-plus.[1] The structures were solved and refined with SHELXT and SHELXL, respectively, in Olex2. [2-4]

Crystallographic single crystal X-ray data for **1**, *syn*-**10** and *anti*-**10** were collected using an Oxford Diffraction Supernova instrument equipped with a Mo micro-focus X-ray source, an Atlas charge-coupled device detector, and a four-circle goniometer. The crystals were cooled to 100(1) K using an Oxford Cryosystems liquid nitrogen Cryostream device. The intensities were empirically corrected for absorption using SCALE3 ABSPACK implemented in CrysAlisPRO.[5] The unit cell parameters were determined, and the Bragg intensities were integrated using CrysAlisPRO. The structures were solved and refined with SHELXT and SHELXL, respectively, in Olex2.[2-4]

Synthetic procedures

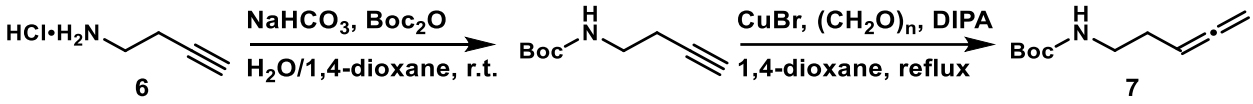

But-3-yn-1-amine hydrochloride (12.016 g, 0.114 mol, 1 equiv.) was charged to a flask and dissolved in water (240 mL) and then cooled to 0 °C. Solid $NaHCO_3$ (19.159 g, 0.228 mol, 2 equiv.) was added and the reaction mixture was allowed to warm to r.t. slowly and then stirred for 10 min. The reaction mixture was cooled to 0 °C again followed by addition of 1,4-dioxane (60 mL) and then a solution of di-*tert*-butyl dicarbonate (32.42 g, 0.149 mol, 1.3 equiv.) in 1,4-dioxane (60 mL) was added and the reaction mixture was allowed to warm to r.t. The reaction mixture was stirred for 12 h at r.t. and then extracted with Et_2O (3 x 150 mL) and the combined organics were dried over Na_2SO_4, filtered through a plug of sand and celite and then concentrated *in vacuo*.

The crude material was redissolved in anhydrous 1,4-dioxane (720 mL) followed by addition of CuBr (8.18 g, 0.057 mol, 0.5 equiv.)[*], paraformaldehyde (8.57 g, 0.285 mol, 2.5 equiv.) and diisopropylamine (32 mL, 0.228 mol, 2 equiv.). The flask was equipped with a CondenSyn Waterless Condenser and the suspension was heated to reflux for 14 h and then cooled to r.t. The orange suspension was poured into 0.5 M aq. HCl (1 L) and then extracted (3 x 300 mL) with Et_2O. The combined organics were dried over Na_2SO_4, filtered through a plug of sand and celite and then concentrated *in vacuo* to obtain a thick orange oil. The crude material was purified by FCC (pentane to 7:3 pentane/Et_2O) to obtain **7** as a clear oil with a yellow hint (15.96 g, 76% over 2 steps).

R_f (3:1 heptane/EtOAc, $KMnO_4$ stain) 0.55.

^{1}H NMR (400 MHz, Chloroform-d) δ_H (ppm) 5.08 (p, *J* = 6.6 Hz, 1H), 4.72 (dt, *J* = 6.6, 3.2 Hz, 2H), 4.62 (bs, 1H), 3.22 (q, *J* = 6.6 Hz, 2H), 2.18 (qt, *J* = 6.6, 3.2 Hz, 2H), 1.44 (s, 9H).

^{13}C NMR (101 MHz, Chloroform-d) δ_C (ppm) 209.0, 156.0, 87.2, 79.3, 75.5, 39.9, 28.9, 28.5.

$\tilde{\nu}_{max}$ (ATR): 3349, 2978, 2932, 1957, 1691, 1521, 1452, 1392, 1366, 1275, 1250, 1172, 845.

HRMS (ESI): Calc. for $C_{10}H_{18}O_2N^+$ 184.1332; found 184.1331.

The obtained data is in accordance with literature.[6]

[*] 99.99% trace metals basis, beads -10 mesh

General procedure for alkyne halogenation.

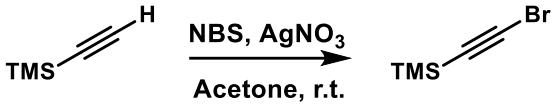

Acetone (160 mL) was added to a flask charged with NBS (17.11 g, 0.09613 mol, 1.3 equiv.) followed by addition of ethynyltrimethylsilane (10 mL, 0.072 mol, 1.0 equiv.) and $AgNO_3$ (1.41 g, 8.30 mmol, 0.12 equiv.) at r.t. After 4 h, the mixture was poured over ice (~ 250 mL) in a separatory funnel and the ice was allowed to melt. The mixture was extracted with pentane (3 x 150 mL) and the combined organics were dried over Na_2SO_4, filtered through sand and celite and concentrated *in vacuo*. The obtained material was run through a plug of silica to yield TMS acetylene bromide as a colorless oil (8.61 g, 67%). This material was employed without further purification.

^{1}H NMR (400 MHz, Chloroform-d) δ_H (ppm) 0.19 (s, 9H).

^{13}C NMR (101 MHz, Chloroform-d) δ_C (ppm) 87.0, 61.6, -0.2.

$\tilde{\nu}_{max}$ (ATR): 2961, 2900, 2125, 1720, 1409, 1251, 863, 839, 759, 700, 625.

The obtained data is in accordance with literature.[7]

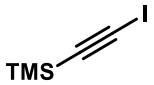

R_f (95:5 heptane/EtOAc, UV, $KMnO_4$ stain) 0.66.

^{1}H NMR (400 MHz, Chloroform-d) δ_H (ppm) 0.18 (s, 9H).

^{13}C NMR (101 MHz, Chloroform-d) δ_C (ppm) 104.3, 20.7, 0.1.

$\tilde{\nu}_{max}$ (ATR): 2959, 2898, 2096, 1409, 1250, 837, 758, 743, 732, 701, 620.

The obtained data is in accordance with literature.[8]

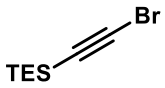

R_f (heptane, UV, $KMnO_4$ stain) 0.70.

^{1}H NMR (400 MHz, Chloroform-d) δ_H (ppm) 0.99 (t, J = 7.9 Hz, 9H), 0.61 (q, J = 7.9 Hz, 6H).

^{13}C NMR (101 MHz, Chloroform-d) δ_C (ppm) 84.7, 61.8, 7.5, 4.4.

$\tilde{\nu}_{max}$ (ATR): 2956, 2919, 2875, 2123, 1738, 1458, 1415, 1236, 1006, 975, 809, 727, 694.

The obtained data is in accordance with literature.[9]

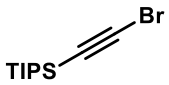

R_f (heptane/EtOAc, UV, $KMnO_4$ stain) 0.86.

^{1}H NMR (400 MHz, Chloroform-d) δ_H (ppm) 1.07 (m, 21H).

^{13}C NMR (101 MHz, Chloroform-d) δ_C (ppm) 83.5, 61.9, 18.6, 11.5.

$\tilde{\nu}_{max}$ (ATR): 2943, 2892, 2866, 2120, 1462, 1384, 1357, 1247, 1072, 1017, 996, 919, 882, 802, 675, 660, 577, 509, 467.

The obtained data is in accordance with literature.[7]

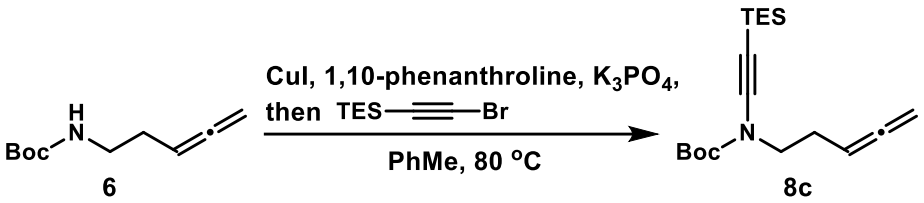

A Schlenk tube was charged with anhydrous K_3PO_4 (279 mg, 1.31 mmol, 4.8 equiv.) and flame-dried extensively under high vacuum. The Schlenk tube was refilled with argon and evacuated three times. CuI (10.4 mg, 54.6 µmol, 20 mol%) and 1,10-phenanthroline (20.0 mg, 111 µmol, 41 mol%) were transferred to the Schlenk tube followed by evacuation and argon refill three times. **6** (50.1 mg, 0.273 mmol, 1.0 equiv.) was dissolved in PhMe (2 x 0.2 mL) and added at r.t. The suspension was heated to 80 °C and after 3 min, TES acetylene bromide (76.5 mg, 0.349 mmol, 1.3 equiv.) dissolved in PhMe (0.25 mL) was added dropwise over 5 min. The suspension was cooled to r.t. after a total of 48 h followed by filtration over silica with EtOAc to obtain a clear yellow solution that was concentrated *in vacuo*. The crude material was purified by AFCC (heptane to 8:2 heptane/EtOAc) to obtain **8c** as a clear yellow oil (61.7 mg, 70%).

R_f (6:1 heptane/EtOAc, UV, $KMnO_4$ stain) 0.62.

^{1}H NMR (400 MHz, Chloroform-d) δ_H (ppm) 5.10 (p, *J* = 6.8 Hz, 1H), 4.70 (dt, *J* = 6.8, 3.1 Hz, 2H), 3.49 (t, *J* = 7.3 Hz, 2H), 2.40 – 2.32 (m, 2H), 1.49 (s, 9H), 1.00 (t, *J* = 7.9 Hz, 9H), 0.60 (q, *J* = 7.9 Hz, 6H).

^{13}C NMR (101 MHz, Chloroform-d) δ_C (ppm) 209.2, 154.2, 97.3, 86.4, 82.4, 75.4, 69.3, 48.4, 28.1, 26.8, 7.7, 4.8.

$\tilde{\nu}_{max}$ (ATR): 2980, 2954, 2936, 2912, 2875, 2175, 1958, 1724, 1457, 1416, 1369, 1291, 1256, 1160, 1017, 973, 884, 857, 764, 725.

HRMS (ESI): Calc. for $C_{18}H_{32}O_2NSi^+$ 322.2197; found 322.2192.

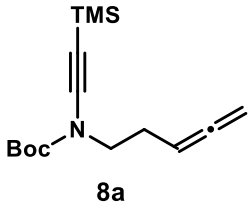

R_f (6:1 heptane/EtOAc, $KMnO_4$ stain) 0.57.

^{1}H NMR (400 MHz, Chloroform-d) δ_H (ppm) 5.10 (p, J = 6.6 Hz, 1H), 4.71 (dt, *J* = 6.6, 3.3 Hz, 2H), 3.47 (t, *J* = 7.4 Hz, 2H), 2.38 – 2.31 (m, 2H), 1.49 (s, 9H), 0.17 (s, 9H).

^{13}C NMR (101 MHz, Chloroform-d) δ_C (ppm) 209.2, 154.2, 96.5, 86.4, 82.5, 75.5, 72.0, 48.3, 28.1, 26.8, 0.4.

$\tilde{\nu}_{max}$ (ATR): 2979, 2960, 2177, 1958, 1724, 1477, 1456, 1369, 1291, 1249, 1160, 888, 842, 760.

HRMS (ESI): Calc. for $C_{15}H_{26}O_2NSi^+$ 280.1727; found 280.1720.

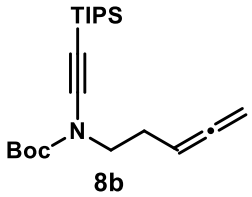

8b

R_f (6:1 heptane/EtOAc, UV, $KMnO_4$ stain) 0.65.

^{1}H NMR (400 MHz, Chloroform-d) δ_H (ppm) 5.10 (p, *J* = 6.8 Hz, 1H), 4.69 (dt, *J* = 6.8, 3.3 Hz, 2H), 3.50 (t, *J* = 7.2 Hz, 2H), 2.41 - 2.33 (m, 2H), 1.48 (s, 9H), 1.08 – 1.07 (m, 21H).

^{13}C NMR (101 MHz, Chloroform-d) δ_C (ppm) 209.3, 154.3, 97.7, 86.4, 82.4, 75.4, 68.1, 48.5, 28.3, 26.8, 18.8, 11.6.

$\tilde{\nu}_{max}$ (ATR): 2942, 2865, 2175, 1958, 1725, 1462, 1369, 1290, 1257, 1160, 995, 883, 857, 764, 702, 675, 576.

HRMS (ESI): Calc. for $C_{21}H_{38}O_2NSi^+$ 364.2666; found 364.2659.

Optimization of ynamide synthesis

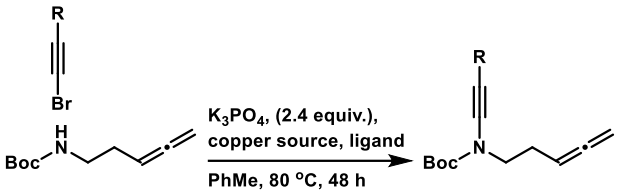

Table 1 – ynamide synthesis optimization.

Entry	R	Copper source (20 mol%)	Ligand (40 mol%)	Yield
1[a]	TMS	$CuSO_4 \cdot 5H_2O$	1	nr
2[b]	TMS	$CuSO_4 \cdot 5H_2O$	1	nr
3[b,c]	TMS	$CuSO_4 \cdot 5H_2O$	1	nr
4[b,d,f]	TMS	$CuSO_4 \cdot 5H_2O$	1	nr
5[b]	TMS	CuI	1	nr
6[b]	TMS	CuI	2 (25 equiv.)	nr
7[b]	TMS	CuI	3	nr
8[b]	TMS	CuI	4 (25 mol%)	<1
9[b]	TMS	CuI	5	<1
10[a]	TIPS	$CuSO_4 \cdot 5H_2O$	1	27
11[b]	TIPS	$CuSO_4 \cdot 5H_2O$	1	63
12[b]	TIPS	CuI	1	57
13[b,e]	TIPS	CuI	1	61
14[b,f]	TIPS	CuI	1	59
15[b]	TES	CuI	1	51
16[b,g]	TES	CuI	1	45
17[b,h]	TES	CuI	1	70
18[b,f,h]	TES	CuI	1	37

a) Flame-dried K_3PO_4 from Lancaster Synthesis. b) New anhydrous flame-dried K_3PO_4 from Acros Organics. c) Iodine instead of bromine. d) Reflux for 72 h. e) 2x1 equiv. of TIPS-alkyne with 24 h interval. f) 40 mol% copper source + 80 mol% ligand-**1**. g) Reflux. h) 4.8 equiv. K_3PO_4.

Ligands

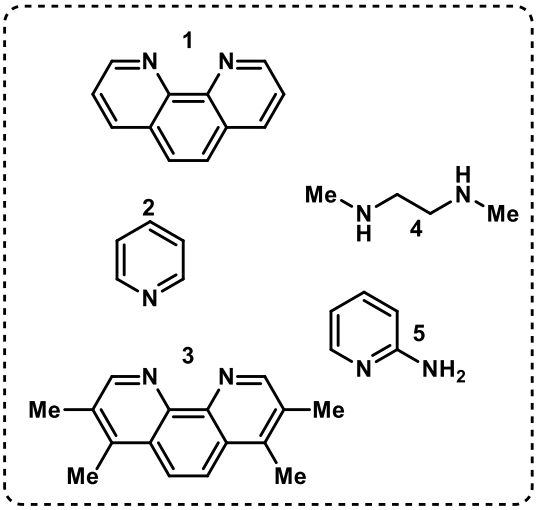

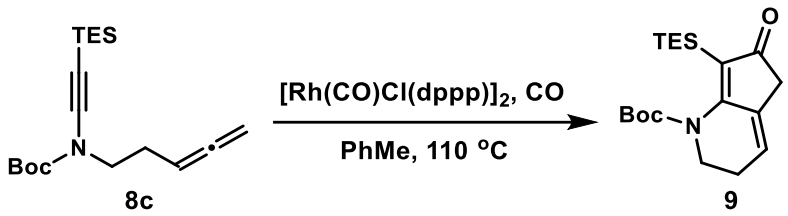

A dry 2 L three-necked flask was charged with $[Rh(CO)Cl(dppp)]_2$ (562 mg, 0.485 mmol, 2.5 moL%) followed by addition of PhMe (900 mL) which was then heated to 110 °C and then purged with CO (10% CO mixed with 90% argon). **8c** (6.191 g, 19.3 mmol, 1 equiv.) was dissolved in PhMe (60 mL) and added dropwise over 4 h with a syringe pump. The reaction was kept under a constant flow of CO during the course of the reaction. After 13 h post addition of **8c**, the reaction mixture was cooled to r.t. and then concentrated directly. The crude material was purified by AFCC (heptane to 7:3 heptane/EtOAc) to isolate **9** (4.473 g, 66%) and recovered starting material (240 mg, 4%).

The reaction may also be performed in a two-chamber system for safe handling of CO gas. The procedure employing the two-chamber system is described below.

To a dry 2 L two-chamber system, COgen (3.51 g, 14.5 mmol, 2.0 equiv.), $PdCl_2(cod)$ (206 mg, 0.721 mmol, 10 mol%), $TTBP{\cdot}HBF_4$ (207 mg, 0.713 mmol, 10 mol%) and PhMe (350 mL) are charged to chamber A. $[Rh(CO)Cl(dppp)]_2$ (208 mg, 0.18 mmol, 2.5 moL%), **8c** (2.318 g, 7.21 mmol, 1.0 equiv.) and PhMe (350 mL) are charged to chamber B. Lastly, *N*,*N*-dicyclohexylmethylamine (6.2 mL, 28.9 mmol, 4.0 equiv.) is charged to chamber A and the entire system is sealed using screw caps and Teflon® coated silicon seals. Before heating the reaction mixture, it is recommended to cover the setup using a blast shield. The two-chamber system is then heated to 110 °C in an oil bath and stirred for 16 h. Upon completion, the Teflon® coated silicon seal in chamber A is pierced using a thin cannula for a controlled release of excess CO gas while keeping the sash of the fume hood as closed as possible. The purification of the reaction mixture follows the same procedure as stated above to yield the product (1.489 g, 59%).

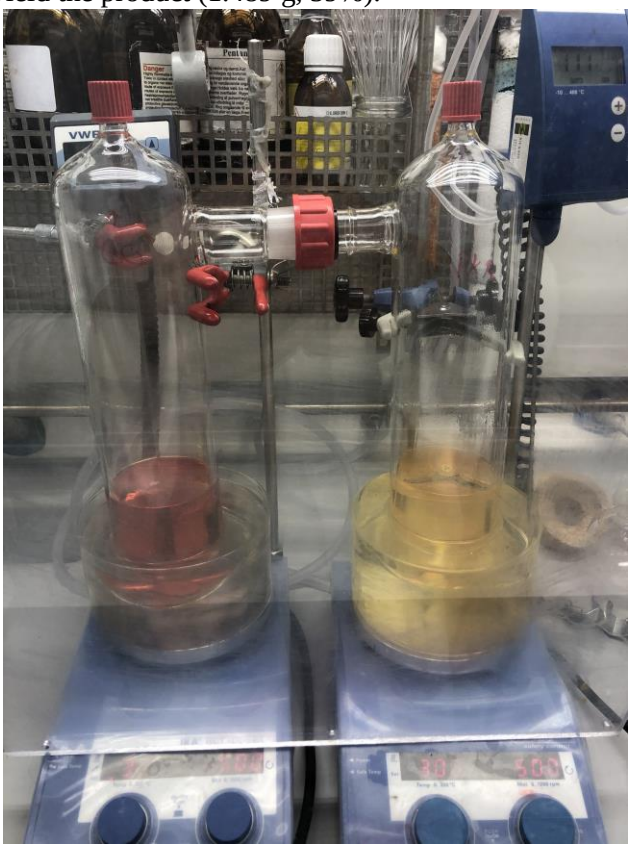

R_f (2:1 heptane/EtOAc, UV, $KMnO_4$ stain) 0.40.

^{1}H NMR (400 MHz, Chloroform-d) δ_H (ppm) 5.93 (tt, *J* = 4.2, 1.3 Hz, 1H), 3.84 (t, *J* = 5.9 Hz, 2H), 2.93 (q, *J* = 1.3 Hz, 2H), 2.31 (m, 2H), 1.53 (s, 9H), 0.92 (t, *J* = 7.8 Hz, 9H), 0.79 (m, 6H).

^{13}C NMR (101 MHz, Chloroform-d) δ_C (ppm) 207.2, 168.8, 152.3, 135.3, 131.8, 121.0, 82.1, 44.8, 38.7, 28.4, 25.1, 7.9, 3.2.

$\tilde{\nu}_{max}$ (ATR): 3457, 3029, 2970, 2949, 2873, 1738, 1721, 1687, 1546, 1456, 1402, 1366, 1279, 1227, 1217, 1156, 1130.

HRMS (ESI): Calc. for $C_{19}H_{32}O_3NSi^+$ 350.2146; found 350.2148.

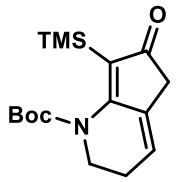

R_f (2:1 heptane/EtOAc, UV, $KMnO_4$ stain) 0.32.

^{1}H NMR (400 MHz, Chloroform-d) δ_H (ppm) 5.95 (tt, *J* = 4.4, 1.4 Hz, 1H), 3.86 (t, *J* = 5.9 Hz, 2H), 2.92 (q, *J* = 1.4 Hz, 2H), 2.34 – 2.29 (m, 2H), 1.53 (s, 9H), 0.20 (s, 9H).

^{13}C NMR (101 MHz, Chloroform-d) δ_C (ppm) 206.9, 167.6, 152.3, 135.2, 132.9, 121.3, 82.3, 44.6, 38.7, 28.5, 25.1, -0.9.

$\tilde{\nu}_{max}$ (ATR): 2918, 1717, 1686, 1552, 1458, 1402, 1390, 1366, 1333, 1226, 1156, 1131, 1019, 844, 771, 552.

HRMS (ESI): Calc. for $C_{16}H_{26}O_3NSi^+$ 308.1676; found 308.1690.

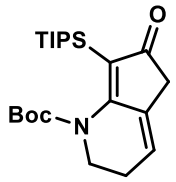

R_f (6:1 heptane/EtOAc, UV, $KMnO_4$ stain) 0.15.

^{1}H NMR (400 MHz, Chloroform-d) δ_H (ppm) 5.91 (tt, *J* = 4.3, 1.3 Hz, 1H), 3.81 (t, *J* = 5.2 Hz, 2H), 2.95 (q, *J* = 1.3 Hz, 2H), 2.31 (m, 2H), 1.50 (s, 9H), 1.48 (q, *J* = 7.5 Hz, 3H), 1.08 (d, *J* = 7.5 Hz, 18H).

^{13}C NMR (101 MHz, Chloroform-d) δ_C (ppm) 207.6, 170.1, 152.8, 135.6, 134.2, 121.0, 81.8, 45.4, 38.7, 28.3, 25.1, 19.8, 12.2.

$\tilde{\nu}_{max}$ (ATR): 2942, 2864, 1718, 1688, 1543, 1459, 1402, 1387, 1366, 1332, 1277, 1223, 1203, 1155, 1126, 1020, 884.

HRMS (ESI): Calc. for $C_{22}H_{38}O_3NSi^+$ 392.2615; found 392.2622.

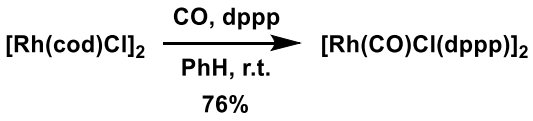

A (808.8 mg, 1.64, 1 equiv.) was dissolved in benzene (25 mL) and was put under a CO atmosphere (10% CO, 90% argon) at r.t. followed by addition of 1,3-Bis(diphenylphosphino)propane (dppp) (1355 mg, 3.29 mmol, 2.0 equiv.) dissolved in benzene (17 mL). After 5 min, the reaction mixture turns clear yellow from orange and after 1 h, the reaction mixture is completely heterogeneous and composed of yellowish solids. The reaction mixture was filtered and the collected solids were washed with heptane (3 x 30 mL). The collected solids were dried overnight at high vacuum to afford the product as light yellow solids (1.447 g, 76%).

$\tilde{\nu}_{max}$ (ATR): 3053, 1952, 1478, 1434, 1402, 1309, 1236, 1173, 1097, 946.

Melting Point: mp = 146-151 ºC.

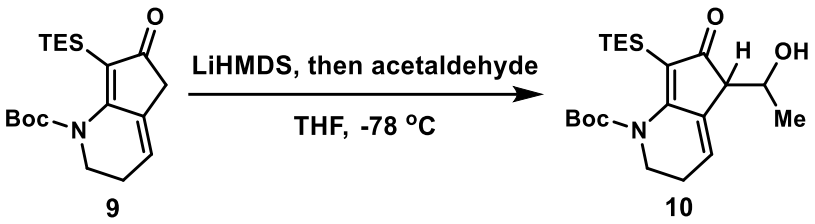

9 10

LiHMDS (1.0 M, 17.5 mL, 17.5 mmol, 1.2 equiv.) was added to a flask containing THF (280 mL) at -78 ◦C. **9** (5.093 g, 14.6 mmol, 1.0 equiv.) dissolved in THF (18 mL) was added dropwise at -78 °C and stirred for 30 min to yield a deep red solution. A stock solution of acetaldehyde (5.34 M, 4.1 mL, 21.9 mmol, 1.5 equiv.) in THF was added dropwise at -78 °C and the mixture was stirred for 1 h to obtain an orange solution. The reaction was quenched by the addition of sat. aq. NH_4Cl (100 mL) at -78 °C and the mixture was allowed to warm to r.t. slowly. At r.t., the mixture was further diluted with sat. aq. NH_4Cl (100 mL) and water (200 mL). The mixture was extracted with EtOAc (3 x 200 mL) and the combined organics were dried over Na_2SO_4, filtered through a plug of sand and celite and concentrated *in vacuo*. The crude material was purified by AFCC (heptane to 55:45 heptane/EtOAc) to isolate a mixture of diastereoisomers (4.436 g, 74%, 60:40 *syn*/*anti*) as yellow crystals. Note, to separate the two diastereoisomers, it is recommended to employ the following gradient: CH_2Cl_2 to 92:8 CH_2Cl_2/acetone.

Data for *Syn* aldol product

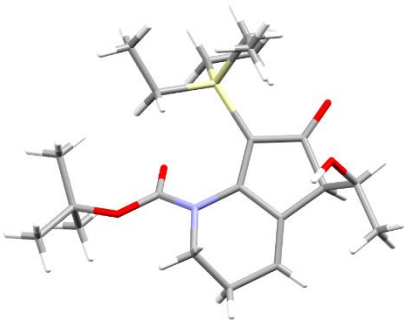

R_f (1:1 heptane/EtOAc, UV, $KMnO_4$ stain) 0.50.

^{1}H NMR (400 MHz, Chloroform-d) δ_H (ppm) 5.96 (t, *J* = 4.0 Hz, 1H), 4.12-3.95 (m, 2H). 3.67 (m, 1H), 3.55 (d, *J* = 10.0 Hz, 1H), 3.14 (d, *J* = 4.2 Hz, 1H), 2.44-2.26 (m, 2H), 1.53 (s, 9H), 1.09 (d, *J* = 6.4 Hz, 3H), 0.92 (t, *J* = 7.7 Hz, 9H), 0.81 – 0.75 (m, 6H).

^{13}C NMR (101 MHz, Chloroform-d) δ_C (ppm) 211.0, 170.0, 152.0, 137.0, 130.9, 121.9, 82.4, 69.0, 52.4, 44.7, 28.4, 25.0, 18.8, 7.8, 3.2.

$\tilde{\nu}_{max}$ (ATR): 3442, 2952, 2874, 1718, 1669, 1539, 1457, 1392, 1366, 1349, 1334, 1274, 1223, 1155, 1134, 1074, 731.

Single crystals were obtained by vapor diffusion of heptane into a heptane/EtOAc solution containing *syn*-**10** at 5 °C.

Data for *Anti* aldol product

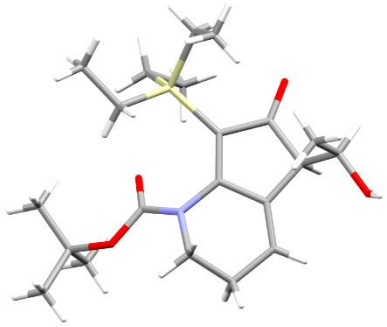

R_f (1:1 heptane/EtOAc, UV, $KMnO_4$ stain) 0.44.

^{1}H NMR (400 MHz, Chloroform-d) δ_H (ppm) 6.12 (t, *J* = 4.2 Hz, 1H), 4.08 – 3.99 (m, 1H), 3.92 (pd, *J* = 6.1, 1.7 Hz, 1H), 2.81 (dd, *J* = 7.8, 1.0 Hz, 1H), 2.44-2.28 (m, 2H), 1.53 (s, 9H), 1.26 (d, *J* = 6.1 Hz, 3H), 0.91 (t, *J* = 7.7 Hz, 9H), 0.84 – 0.70 (m, 6H).

^{13}C NMR (101 MHz, Chloroform-d) δ_C (ppm) 210.2, 169.8, 152.1, 136.0, 129.6, 123.9, 82.5, 68.7, 53.6, 44.5, 28.4, 25.1, 21.0, 7.9, 3.2.

$\tilde{\nu}_{max}$ (ATR): 3424, 2953, 2874, 1719, 1682, 1543, 1457, 1392, 1366, 1347, 1333, 1276, 1225, 1155, 1136, 1065, 729.

Single crystals were obtained by vapor diffusion of heptane into a heptane/EtOAc solution containing *anti*-**10** at 5 °C.

HRMS is reported for a mixture of the diastereoisomers.

HRMS (ESI): Calc. for $C_{21}H_{36}O_4NSi^+$ 394.2408; found 394.2410.

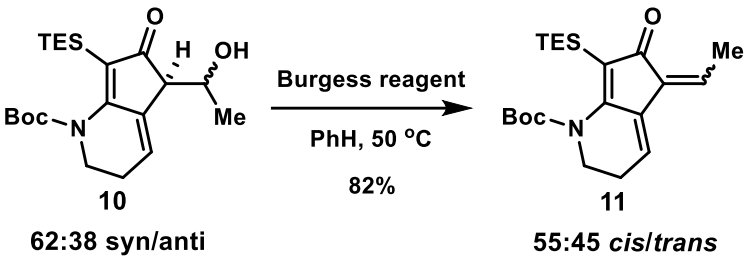

10 (1967 mg, 5.0 mmol, 1 equiv.) was dissolved in PhH (110 mL) followed by addition of Burgess reagent (1784 mg, 7.49 mmol, 1.5 equiv.) at r.t. and then it was heated to 50 °C. After 1 h, full conversion was obtained and the reaction mixture was allowed to cool to r.t. The reaction mixture was poured over brine (150 mL) and then further diluted with Et_2O (150 mL). The mixture was extracted (3 x 150 mL) with Et_2O and the combined organics were dried over Na_2SO_4, filtered through sand and celite and concentrated *in vacuo*. The crude material was purified by AFCC (heptane to heptane/EtOAc 2:1) to isolate **11** as a mixture of *cis*/*trans* (55:45 ratio) (1544 mg, 82%) as an orange oil. The two isomers may be separated by the gradient stated above.

Data for *cis*-***11***:

R_f (2:1 heptane/EtOAc, UV, $KMnO_4$ stain) 0.61.

^{1}H NMR (400 MHz, Chloroform-d) δ_H (ppm) 6.30 (q, *J* = 7.5 Hz, 1H), 6.10 (t, *J* = 4.8 Hz, 1H), 3.83 (bs, 2H), 2.37 (q, *J* = 4.8 Hz, 2H), 2.29 (d, *J* = 7.5 Hz, 3H), 1.52 (s, 9H), 0.94 (t, *J* = 7.4 Hz, 9H), 0.82 (m, 6H).

^{13}C NMR (101 MHz, Chloroform-d) δ_C (ppm) 198.8, 164.4, 152.3, 134.9, 131.7, 130.1, 129.1, 115.6, 82.1, 44.6, 28.5, 24.8, 14.0, 7.9, 3.3

$\tilde{\nu}_{max}$ (ATR): 2950, 1717, 1687, 1543, 1391, 1366, 1221, 1154, 1118, 1006, 718.

HRMS (ESI): Calc. for $C_{21}H_{34}O_3NSi^+$ 376.2302; found 376.2300.

Data for *trans*-**11**:

R_f (2:1 heptane/EtOAc, UV, $KMnO_4$ stain) 0.54.

^{1}H NMR (400 MHz, Chloroform-d) δ_H (ppm) 6.67 (q, *J* = 7.5 Hz, 1H), 6.38 (t, *J* = 4.8 Hz, 1H), 3.84 (bs, 2H), 2.44 (q, *J* = 4.8 Hz, 2H), 2.02 (d, *J* = 7.5 Hz, 3H), 1.53 (s, 9H), 0.92 (t, *J* = 7.3 Hz, 9H), 0.81 (q, *J* = 7.3 Hz, 6H.

^{13}C NMR (101 MHz, Chloroform-d) δ_C (ppm) 197.1, 165.9, 152.2, 134.6, 131.3, 128.7, 128.5, 122.2, 82.2, 44.2, 28.4, 25.4, 14.3, 7.9, 3.3.

$\tilde{\nu}_{max}$ (ATR): 2952, 2874, 1717, 1689, 1658, 1638, 1542, 1457, 1391, 1367, 1329, 1279, 1223, 1155, 1106, 1065, 1019, 737.

HRMS (ESI): Calc. for $C_{21}H_{34}O_3NSi^+$ 376.2302; found 376.2300.

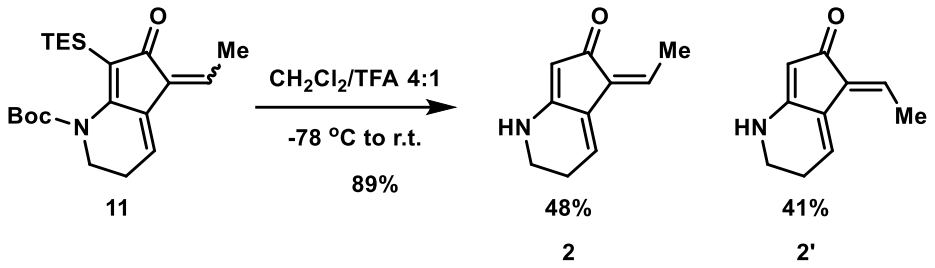

11 (1544 mg) was dissolved in CH_2Cl_2 (60 mL) and then cooled to -78 °C followed by dropwise addition of TFA (15 mL) resulting in a yellow solution. The reaction mixture was then allowed to warm to r.t. slowly over 20 min. After 2 h at r.t., the reaction mixture was diluted with PhMe (60 mL) and then concentrated *in vacuo*. The material was redissolved in 1:1 1-butanol/EtOAc (20 mL) and poured over sat. aq. $NaHCO_3$ (100 mL). The water was extracted (5 x 20 mL) with 1:1 1-butanol/EtOAc and the combined organics were dried over Na_2SO_4, filtered through sand and celite and concentrated *in vacuo*. The crude material was purified by AFCC (CH_2Cl_2 to 8:2 CH_2Cl_2/*i*PrOH) to isolate **2** (317.3 mg, 48%) as light yellow crystals and **2'** (269.6 mg, 41%) as light yellow crystals.

Data for streptazone B_1 (**2**):

R_f (9:1 CH_2Cl_2/*i*PrOH, UV, $KMnO_4$ stain) 0.54.

^{1}H NMR (400 MHz, Chloroform-d) δ_H (ppm) 6.21 (q, *J* = 7.5 Hz, 1H), 6.14 (td, *J* = 4.4, 1.1 Hz, 2H), 5.28 (s, 1H), 5.03 (bs, 1H), 3.41 (td, *J* = 6.7, 2.1 Hz, 2H), 2.50 (td, *J* = 6.7, 4.8, 2H), 2.31 (d, *J* = 7.5 Hz, 3H).

^{13}C NMR (101 MHz, Chloroform-d) δ_C (ppm) 193.3, 162.7, 132.2, 131.0, 126.3, 115.8, 103.7, 39.8, 23.6, 13.5.

$\tilde{\nu}_{max}$ (ATR): 3147, 3105, 2940, 2904, 1663, 1636, 1562, 1489, 1454, 1409, 1335, 1289, 1235, 1156, 1091, 982.

HRMS (ESI): Calc. for $C_{10}H_{12}ON^+$ 162.0913; found 162.0926.

Data for streptazone B_2 (**2'**):

R_f (9:1 CH_2Cl_2/*i*PrOH, UV, $KMnO_4$ stain) 0.36.

^{1}H NMR (400 MHz, Chloroform-d) δ_H (ppm) 6.54 (q, *J* = 7.5 Hz, 1H), 6.40 (td, *J* = 4.6, 1.0 Hz, 1H), 5.23 (d, *J* = 1.2 Hz, 1H), 3.44 (td, *J* = 6.7, 2.2 Hz, 2H), 2.57 (td, *J* = 6.7, 4.5 Hz, 2H), 2.02 (d, *J* = 7.5 Hz, 3H).

^{13}C NMR (101 MHz, Chloroform-d) δ_C (ppm) 191.3, 164.4, 132.4, 131.4, 125.3, 122.5, 100.2, 39.3, 24.3, 14.3.

$\tilde{\nu}_{max}$ (ATR): 3215, 2933, 1662, 1640, 1574, 1486, 1456, 1353, 1331, 1296, 1239, 1177, 1007, 797.

HRMS (ESI): Calc. for $C_{10}H_{12}ON^+$ 162.0913; found 162.0930.

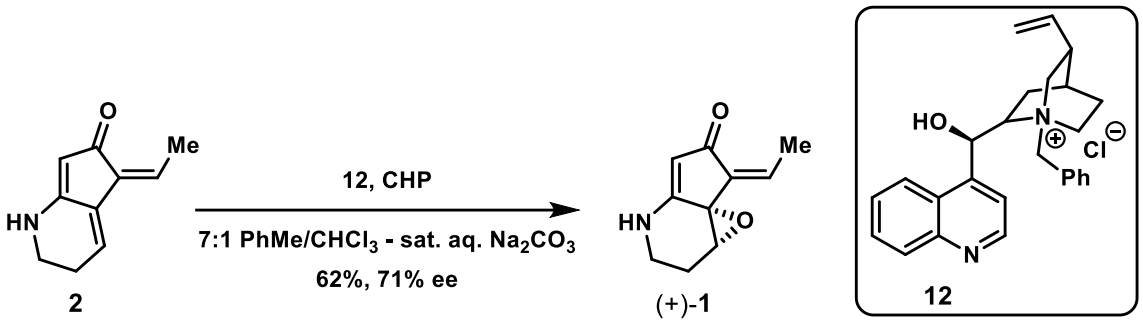

2 (49.8 mg, 0.309 mmol, 1 equiv.) and **12** (26.9 mg, 0.0626 mmol, 20 mol%) was charged to a flask followed by addition of 7:1 PhMe/$CHCl_3$ (3.32 mL) and sat. aq. Na_2CO_3 (3.32 mL) and lastly CHP (80%, 571 µL, 3.09 mmol, 10 equiv.) at r.t. After 17 h at r.t., the reaction mixture was diluted with brine (30 mL) and extracted with CH_2Cl_2 (4 x 20 mL). The combined organics were dried over Na_2SO_4, filtered through sand and celite and concentrated *in vacuo*. The crude material was purified by AFCC (CH_2Cl_2 to 88:12 CH_2Cl_2/*i*PrOH) to isolate streptazone A (**1**) as a light yellowish crystalline material (33.9 mg, 62%, 72% ee). The sample was enantioenriched to >99% ee by slow evaporation at r.t. from a homogeneous CH_2Cl_2 solution.

Data for streptazone A (**1**):

R_f (9:1 EtOAc/MeOH, UV, $KMnO_4$ stain) 0.42.

^{1}H NMR (400 MHz, Chloroform-d) δ_H (ppm) 5.78 (qd, *J* = 7.4, 0.8 Hz, 1H), 5.36 (s, 1H), 5.22 (bs, 1H), 3.89 (d, *J* = 2.8 Hz, 1H), 3.52 (td, *J* = 12.5, 3.8 Hz, 1H), 3.14 (dtt, *J* = 12.5, 5.7, 1.3 Hz, 1H), 2.32 (m, 1H), 2.24 (d, *J* = 7.4 Hz, 3H), 2.10 (ddd, *J* = 14.6, 12.5, 5.7 Hz, 1H).

^{13}C NMR (101 MHz, Chloroform-d) δ_C (ppm) 192.0, 165.0, 130.9, 129.1, 105.9, 59.1, 58.2, 36.7, 25.1, 13.3.

$\tilde{\nu}_{max}$ (ATR): 3216, 2949, 1686, 1651, 1588, 1437, 1336, 1198, 1170, 983, 846.

HRMS (ESI): Calc. for $C_{10}H_{12}O_2N^+$ 178.0863; found 178.0867.

$[\alpha]_D^{26.9}$: +66.9° (c = 0.175 g/100 mL, MeOH), [lit. +118°, 22 °C, c = 0.34, MeOH)[5].

UPCC: IB, gradient CO_2/MeOH, 3.0 mL·min^{-1}; $t_{natural\ (+)}$ = 4.776; $t_{unnatural\ (-)}$ = 4.881.

Single crystals were obtained by dissolving **1** in CH_2Cl_2 which was then allowed to evaporate slowly o/n at r.t. to obtain crystals suitable for X-ray diffraction.

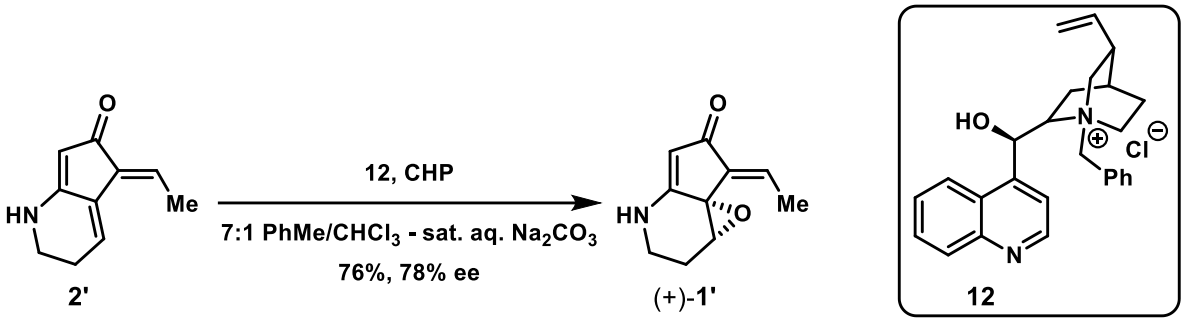

2' (50.2 mg, 0.311 mmol, 1 equiv.) and **12** (27.2 mg, 0.0633 mmol, 20 mol%) was charged to a flask followed by addition of 7:1 PhMe/$CHCl_3$ (3.73 mL) and sat. aq. Na_2CO_3 (3.73 mL) and lastly cumene hydroperoxide (80%, 574 μL, 3.11 mmol, 10 equiv.) at r.t. After 17 h, full conversion was obtained. The reaction mixture was diluted with brine (30 mL) and extracted with CH_2Cl_2 (4 x 20 mL). The combined organics were dried over Na_2SO_4, filtered through sand and celite and concentrated *in vacuo*. The crude material was purified by AFCC (CH_2Cl_2 to 3:1 CH_2Cl_2/*i*PrOH) to isolate **1'** as a light orange crystalline material (41.8 mg, 76%, 78% ee). We decided to define **1'** as streptazone A_2 based on the geometric relationship between streptazone B_1 (**2**) and streptazone B_2 (**2'**) following the original isolation study.[10] The sample was enantioenriched to >99% ee by slow evaporation at r.t. from a homogeneous CH_2Cl_2 solution.

Data for streptazone A_2 (**1**'):

R_f (9:1 EtOAc/MeOH, UV, $KMnO_4$ stain) 0.28.

^{1}H NMR (400 MHz, Chloroform-d) δ_H (ppm) 6.57 (q, *J* = 7.5 Hz, 1H), 5.36 (s, 1H), 5.35 (bs, 1H), 4.24 (d, *J* = 3.0 Hz, 1H), 3.54 (td, *J* = 12.5, 3.8 Hz, 1H), 3.16 (dtt, *J* = 12.6, 5.7, 0.9 Hz, 1H), 2.37 (m, 1H), 2.17 (ddd, *J* = 14.6, 12.6, 5.7 Hz, 1H), 1.80 (d, *J* = 7.5 Hz, 3H).

^{13}C NMR (101 MHz, Chloroform-d) δ_C (ppm) 189.86, 166.20, 131.56, 128.39, 103.56, 59.67, 57.91, 36.82, 25.46, 12.41.

$\tilde{\nu}_{max}$ (ATR): 3197, 2920, 1693, 1654, 1583, 1487, 1454, 1351, 1296, 1240, 1195, 1005, 902.

HRMS (ESI): Calc. for $C_{10}H_{12}O_2N^+$ 178.0863; found 178.0863.

$[\alpha]_D^{24.8}$: +54.8° (c = 0.155 g/100 mL, MeOH).

UPCC: IB, gradient CO_2/MeOH, 3.0 mL·min^{-1}; $t_{(-)}$ = 4.839; $t_{(+)}$ = 4.904.

Single crystals were obtained by dissolving **1'** in CH_2Cl_2 which was then allowed to evaporate slowly o/n at r.t. to obtain crystals suitable for X-ray diffraction.

Optimization of asymmetric epoxidation.

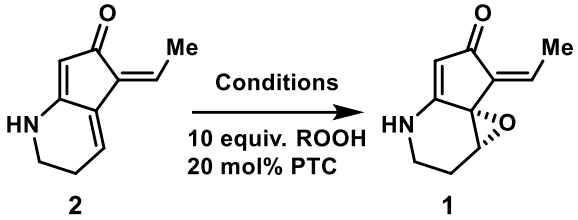

Table 2 – optimization of regio- and enantioselective epoxidation.

Entry	PTC/ROOH	Solvent	T (°C)/ Time	Yield (%) (**2**/**1**)	ee (%)
1	**12**/CHP	CH_2Cl_2/sat. aq. K_2CO_3	r.t./24 h	0/47	72
2	**PTC1**/CHP	CH_2Cl_2/sat. aq. K_2CO_3	r.t./24	0/47	54
3	**PTC2**/CHP	CH_2Cl_2/sat. aq. K_2CO_3	r.t./24	26/23	4
4	**12**/CHP	7:1 (PhMe/$CHCl_3$)/sat. aq. K_2CO_3	r.t./24 h	0/32	75
5	**12**/CHP	7:1 (PhMe/$CHCl_3$)/sat. aq. Cs_2CO_3	r.t./24 h	0/3	69
6	**12**/CHP	7:1 (PhMe/$CHCl_3$)/sat. aq. Cs_2CO_3	0 °C/24 h	0/22	67
7	**12**/TBHP	7:1 (PhMe/$CHCl_3$)/sat. aq. K_2CO_3	r.t./24 h	0/27	78
8	**PTC3**/CHP	7:1 (PhMe/$CHCl_3$)/sat. aq. K_2CO_3	r.t./24 h	6/26	32
9	**12**/H_2O_2	7:1 (PhMe/$CHCl_3$)/sat. aq. K_2CO_3	r.t./24 h	64/4*	26
10	**12**/CHP	7:1 (PhMe/$CHCl_3$)/sat. aq. Na_2CO_3	r.t./17 h	0/56	76
11[a]	**12**/CHP	7:1 (PhMe/$CHCl_3$)/sat. aq. Na_2CO_3	r.t./17 h	0/63	59
12[b]	**12**/CHP	7:1 (PhMe/$CHCl_3$)/sat. aq. Na_2CO_3	r.t./17 h	0/58	80
13[b,c]	**12**/CHP	7:1 (PhMe/$CHCl_3$)/sat. aq. Na_2CO_3	r.t./17 h	0/65	80

*__2__ isomerized to __2__' using hydrogen peroxide. a) 4 x higher concentration of __2__. b) conducted with __2'__. c) conducted with (S)-diastereoisomer.

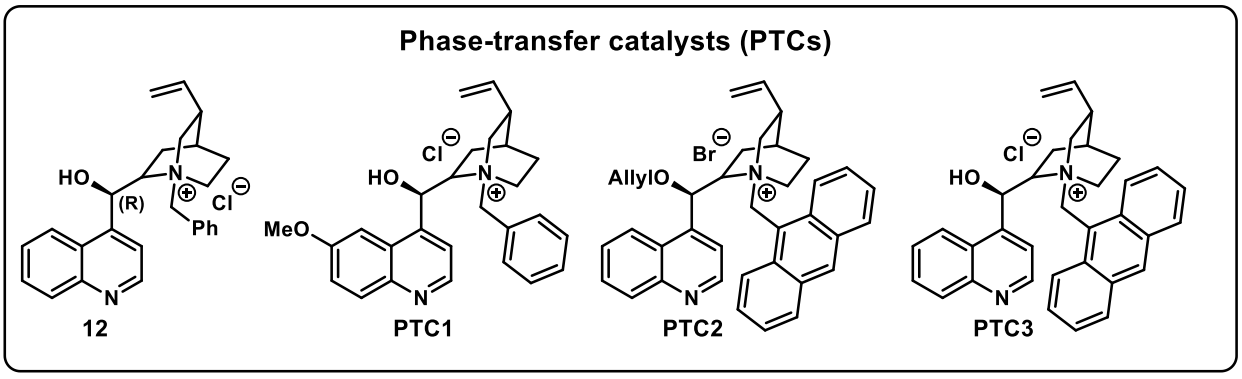

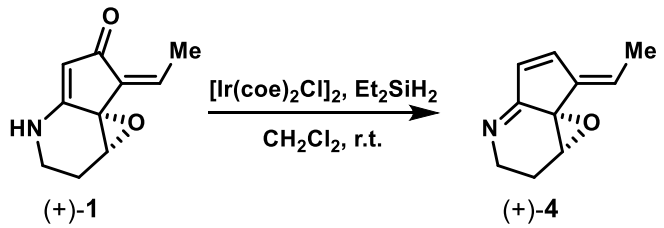

(+)-**1** (+)-**4**

(+)-**1** (15.7 mg, 0.0886 mmol, 1 equiv.) was dissolved in CH_2Cl_2 (2.6 mL) followed by addition of Et_2SiH_2 (23 µL, 0.18 mmol, 2 equiv.) and then dropwise addition of stock iridium (9.3 mM in CH_2Cl_2, 95 µL, 0.88 µmol, 1 mol%) at r.t. Gas development was observed after addition of iridium catalyst. After 6 h at r.t., TLC indicated significant conversion to (+)-**4**. The reaction mixture was directly subjected to purification by AFCC (CH_2Cl_2 to 7:3 CH_2Cl_2/*i*PrOH) to isolate (+)-**4** (4.7 mg, 33%) and remaining starting material (6.7 mg, 43%) and isolate an impure sample of dihydroabikoviromycin (0.8 mg, <6%).

Data for abikoviromycin (**4**):

R_f (9:1 CH_2Cl_2/*i*PrOH, UV, $KMnO_4$ stain) 0.80.

^{1}H NMR (400 MHz, Chloroform-d) δ_H (ppm) 7.41 (dt, *J* = 6.3, 1.2 Hz, 1H), 6.52 (dm, *J* = 6.2 Hz, 1H), 5.49 (qt, *J* = 7.4, 1.4 Hz, 1H), 3.91 (m, 1H), 3.80 (ddt, *J* = 15.5, 5.7, 1.5 Hz, 1H), 3.72 – 3.63 (m, 1H), 2.17 (dddd, *J* = 14.8, 5.5, 2.4, 1.4 Hz, 1H), 1.88 (d, *J* = 7.3 Hz, 3H), 1.60 (ddd, *J* = 14.8, 12.4, 5.6, Hz, 1H).

^{13}C NMR (101 MHz, Chloroform-d) δ_C (ppm) 172.2, 142.4, 136.8, 133.1, 119.6, 59.7, 54.7, 44.8, 22.01, 14.2.

$\tilde{\nu}_{max}$ (ATR): 3279, 2939, 2863, 1649, 1447, 1428, 977, 911, 781.

HRMS (ESI): Calc. for $C_{10}H_{12}ON^+$ 162.0913; found 162.0922.

$[\alpha]_D^{25.2}$: +80° (c = 0.025 g/100 mL, 0.1 M aq. NaOH), [lit. +67.5°, 20 °C, c = 0.025, 0.1 M aq. NaOH)[6].

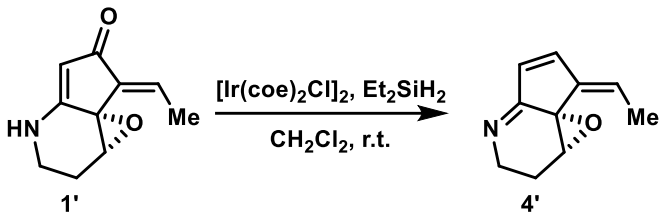

1' 4'

1' (19.7 mg, 0.111 mmol, 1 equiv.) was dissolved in CH_2Cl_2 (3.3 mL) followed by addition of Et_2SiH_2 (29 µL, 0.222 mmol, 2 equiv.) and then dropwise addition of stock iridium (6.7 mM in CH_2Cl_2, 165 µL, 1.11 µmol, 1 mol%) at r.t. After 3 h, the reaction mixture was directly subjected to purification by AFCC (CH_2Cl_2 to 7:3 CH_2Cl_2/*i*PrOH) to obtain **4'** (7.4 mg, 41%), reisolation of starting material (2.7 mg, 14%) and *trans*-dihydroabikoviromycin (1.4 mg, 8%).

R_f (9:1 CH_2Cl_2/*i*PrOH, UV, $KMnO_4$ stain) 0.72.

^{1}H NMR (400 MHz, Chloroform-d) δ_H (ppm) 7.06 (d, *J* = 6.0 Hz, 1H), 6.37 (d, *J* = 6.1 Hz, 1H), 5.83 (q, *J* = 7.6 Hz, 1H), 4.24 (t, *J* = 2.0 Hz, 1H), 3.78 (ddt, *J* = 15.4, 5.6, 1.5 Hz, 1H), 3.69 – 3.60 (m, 1H), 2.20 (dddd, *J* = 14.8, 5.4, 2.5, 1.4 Hz, 1H), 1.77 (d, *J* = 7.5 Hz, 3H), 1.64 (ddd, *J* = 14.7, 12.7, 5.7 Hz, 1H).

^{13}C NMR (101 MHz, Chloroform-d) δ_C (ppm) 172.5, 148.6, 136.9, 131.3, 125.4, 59.0, 55.7, 44.2, 22.2, 12.9.

$\tilde{\nu}_{max}$ (ATR): 3280, 2939, 2864, 1647, 1536, 1429, 967, 909, 844, 779.

HRMS (ESI): Calc. for $C_{10}H_{12}ON^+$ 162.0913; found 162.0918.

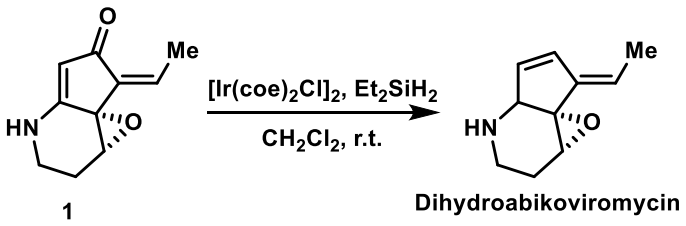

1 Dihydroabikoviromycin

1 (10.6 mg, 0.0598 mmol, 1 equiv.) was dissolved in CH_2Cl_2 (1.6 mL) followed by addition of Et_2SiH_2 (62 µL, 0.478 mmol, 8 equiv.) and then stock iridum (11.4 mM in CH_2Cl_2, 53 µL, 0.60 µmol, 1 mol%) at r.t. The reaction mixture was heated to reflux and stirred for a total of 6 h and then directly subjected to purification by AFCC (CH_2Cl_2 to 7:3 CH_2Cl_2/*i*PrOH) to isolate **4** (2.1 mg, 22%) and dihydroabikoviromycin (2.7 mg, 28%).

R_f (9:1 CH_2Cl_2/*i*PrOH, UV, $KMnO_4$ stain) 0.33.

^{1}H NMR (400 MHz, Chloroform-d) δ_H (ppm) 6.65 (ddd, *J* = 6.4, 1.8, 1.0 Hz, 1H), 6.07 (m, 1H), 5.12 (q, *J* = 7.2 Hz, 1H), 3.92 (bs, 1H), 3.17 (bs, 1H), 2.88 (ddt, *J* = 13.3, 6.4, 1.0 Hz, 1H), 2.69 (ddd, *J* = 13.2, 12.1, 4.0 Hz, 1H), 2.04 (ddt, *J* = 15.2, 4.1, 1.3 Hz, 1H), 1.86 – 1.79 (m, 1H), 1.77 (d, *J* = 7.2 Hz, 3H), 1.29 (s, 1H).

^{13}C NMR (101 MHz, Chloroform-d) δ_C (ppm) 140.5, 134.9, 131.6, 114.9, 64.6, 63.4, 59.4, 40.0, 26.6, 14.2.

$\tilde{\nu}_{max}$ (ATR): 3279, 3062, 2928, 1642, 1550, 1450, 1425, 1376, 1351, 1320, 1247, 1222, 1100, 1075, 1066, 1018, 957, 897, 885, 793, 737, 683, 661, 622, 587.

HRMS (ESI): Calc. for $C_{10}H_{14}ON^+$ 164.1070; found 164.1082.

$[\alpha]_D^{25.1}$: +260° (c = 0.005 g/100 mL, MeOH), [lit. +276°, 22 °C, c = 1, MeOH)[6].

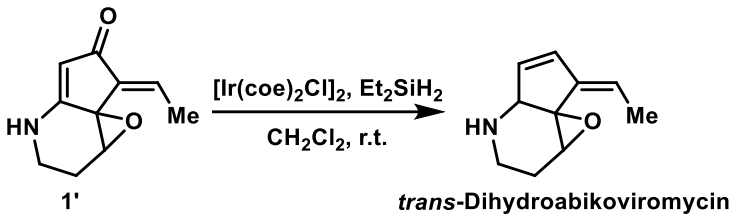

1'

trans-Dihydroabikoviromycin

1' (20.1 mg, 0.113 mmol, 1 equiv.) was dissolved in CH_2Cl_2 (3.3 mL) followed by addition of Et_2SiH_2 (29.5 µL, 0.228 mmol, 2 equiv.) and then dropwise addition of stock iridium (7.8 mM in CH_2Cl_2, 145 µL, 1.13 µmol, 1 mol%) at r.t. After 24 h, the reaction mixture was directly subjected to purification by AFCC (CH_2Cl_2 to 7:3 CH_2Cl_2/*i*PrOH) to obtain **4'** (1.0 mg, <5%) and *trans*-dihydroabikoviromycin (9.1 mg, 49%).

R_f (9:1 CH_2Cl_2/*i*PrOH, UV, $KMnO_4$ stain) 0.22.

^{1}H NMR (400 MHz, Chloroform-d) δ_H (ppm) 6.27 (dd, *J* = 6.2, 1.6 Hz, 1H), 5.88 – 5.84 (m, 1H), 5.57 (q, *J* = 7.5 Hz, 1H), 3.93 (s, 1H), 3.60 (bs, 1H), 2.86 (ddt, *J* = 13.3, 6.4, 1.0 Hz, 1H), 2.64 (ddd, *J* = 13.2, 12.1, 4.0 Hz, 1H), 2.10 – 2.05 (m, 1H), 1.84 (dddd, *J* = 14.9, 12.1, 6.4, 2.4 Hz, 1H), 1.71 (d, *J* = 7.5 Hz, 3H).

^{13}C NMR (101 MHz, Chloroform-d) δ_C (ppm) 140.0, 137.3, 132.3, 120.8, 65.8, 64.3, 56.4, 39.3, 26.3, 11.7.

$\tilde{\nu}_{max}$ (ATR): 3286, 3054, 2990, 2932, 2912, 2857, 1694, 1655, 1583, 1452, 1425, 1295, 1109, 1015, 945, 911, 899, 884, 837, 778.

HRMS (ESI): Calc. for $C_{10}H_{14}ON^+$ 164.1070; found 164.1082.

Evaluation of reductive conditions.

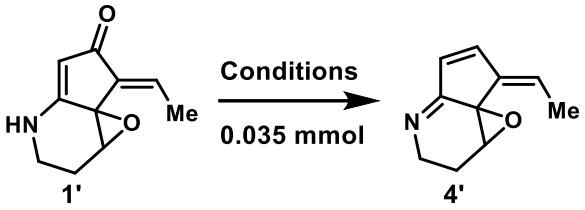

Table 3 – full evaluation of reductive conditions.

Entry	Conditions	Result
1	Tf_2O then $Pd(OAc)_2$, TPP, Et_3N, HCO_2H	Decomposition
2	Tf_2O then $Pd(acac)_2$, Bu_3P, Bu_3N, HCO_2H	**1'** recovered
3	Tf_2O then $Pd(PPh_3)_4$, LiCl, Bu_3SnH	Decomposition
4	Tf_2O then Et_3SiH, 2-Fluoropyridine	Decomposition
5	Tf_2O then L-selectride	Decomposition
7	Comin's reagent, $CeCl_3$	**1'** recovered
8	Schwartz reagent	**1'** recovered
9	$Zn(OAc)_2$, $(EtO)_3SiH$	**1'** recovered
10	$LiAlH(O\textit{t}Bu)_3$, CuBr	**1'** recovered
11	Stryker's reagent, $PhMe_2SiH$	**1'** recovered
12	$NaBH_4$, $CeCl_3$	**1'** recovered
13	$[Ir(coe)_2Cl]_2$, Et_2SiH_2	**1'** recovered + **4'**

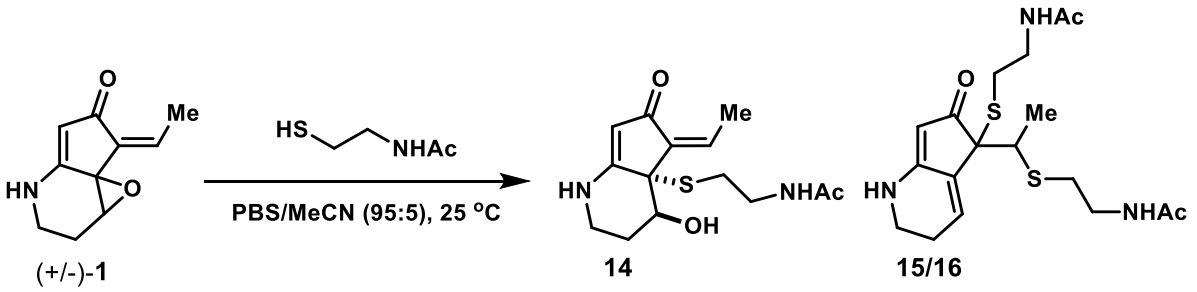

The PBS buffer was prepared by dissolving 1 PBS tablet (P4417, *Sigma-Aldrich*) in 19 mL MQ water and 1 mL MeCN to yield a 0.1 M PBS buffer. (+/-)-**1** (25.0 mg, 0.141 mmol, 1 equiv.) was mixed with PBS buffer (2.822 mL) and sonicated in a falcon tube (15 mL) until a homogeneous solution was obtained. Then, *N*-acetylcysteamine (95%, 45 µL, 0.423 mmol, 3.0 equiv.) was added at r.t. After 24 h, the reaction mixture was directly subjected to purification by MPLC (Luna® 5 µm PFP (2), 100 Å, LC column 100 x 212 mm AX) (flow: 20 mL/min, A: MQ water, B: MeCN, method: start 5% B, isocratic 5 min, then increase to 13% B over 10 min, then isocratic 10 min). **14** elutes at 14:00 min (12.3% B), the minor diastereoisomer elutes at 21:05 min (13% B), the major diastereoisomer elutes at 23:55 min (13% B). Residual starting material elutes at 21:58 (13% B). **14**-**16** were lyophilized to obtain the pure compounds as light orange puffy solids, **14** (18.7 mg, 45%), **15** (4.0 mg, 7%) and **16** (8.1 mg, 14%).

Data for **14**:

^{1}H NMR (400 MHz, Deuterium oxide-d_2) δ_H 6.18 (q, *J* = 7.5 Hz, 1H), 5.44 (s, 1H), 4.38 (dd, *J* = 4.9, 2.4 Hz, 1H), 3.71 (ddd, *J* = 13.5, 8.7, 4.5 Hz, 1H), 3.44 (ddd, *J* = 14.0, 8.6, 6.3 Hz, 1H), 3.34 – 3.20 (m, 2H), 2.66 – 2.43 (m, 3H), 2.18 (d, *J* = 7.5 Hz, 3H), 2.05 – 1.97 (m, 1H), 1.96 (s, 3H).

^{13}C NMR (101 MHz, Deuterium oxide-d_2) δ_C (ppm) 194.1, 174.3, 174.0, 135.6, 131.7, 104.2, 66.8, 55.4, 38.5, 36.6, 28.7, 25.5, 21.8, 13.0.

HRMS (ESI): Calc. for $C_{14}H_{21}O_3N_2S^+$ 297.1267; found 297.1278.

Data for **15**:

^{1}H NMR (400 MHz, Deuterium oxide-d_2) δ_H (ppm) 6.65 (td, *J* = 4.3, 1.3 Hz, 1H), 5.26 (d, *J* = 1.3 Hz, 1H), 3.52 – 3.34 (m, 4H), 3.20 (td, *J* = 6.6, 2.1 Hz, 2H), 3.16 (q, *J* = 6.8 Hz, 1H), 2.81 (t, *J* = 6.5 Hz, 2H), 2.57 – 2.51 (m, 2H), 2.44 (td, *J* = 6.6, 2.1 Hz, 2H), 1.99 (s, 3H), 1.95 (s, 3H), 1.16 (d, *J* = 6.8 Hz, 3H).

^{13}C NMR (101 MHz, Deuterium oxide-d_2) δ_C (ppm) 198.3, 174.1, 173.9, 168.7, 132.8, 130.4, 98.9, 61.8, 46.1, 38.8, 38.7, 38.2, 31.4, 28.5, 22.7, 21.8, 21.7, 17.6.

HRMS (ESI): Calc. for $C_{18}H_{28}O_3N_3S_2^+$ 398.1567; found 398.1580.

Data for **16**:

^{1}H NMR (400 MHz, Deuterium oxide-d_2) δ_H (ppm) 6.54 (td, *J* = 4.3, 1.3 Hz, 1H), 5.24 (d, *J* = 1.2 Hz, 1H), 3.51 – 3.13 (m, 8H), 2.67 (td, *J* = 6.6, 2.2 Hz, 2H), 2.53 (ddd, *J* = 8.6, 6.1, 4.2 Hz, 2H), 2.47 (t, *J* = 6.6 Hz, 2H), 1.96 (s, 3H), 1.94 (s, 3H), 1.48 (d, *J* = 7.0 Hz, 3H).

^{13}C NMR (101 MHz, Deuterium oxide-d_2) δ_C (ppm) 199.0, 174.0, 173.9, 168.4, 132.9, 130.3, 98.6, 60.9, 44.2, 38.7, 38.6, 38.2, 30.9, 28.6, 22.8, 21.8, 21.7, 17.5.

HRMS (ESI): Calc. for $C_{18}H_{28}O_3N_3S_2^+$ 398.1567; found 398.1573.

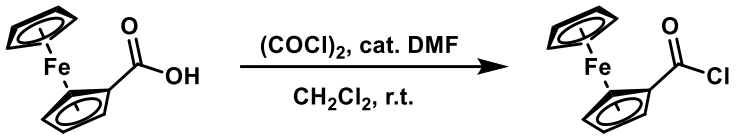

Ferrocene-CO_2H (515 mg, 2.24 mmol, 1 equiv.) was charged to a flask followed by addition of CH_2Cl_2 (15 mL), DMF (2 drops) and then oxalyl chloride (1.5 mL) at r.t. resulting in the generation of bubbles and a color change from orange to dark red. The reaction mixture was stirred for 19 h at r.t. and then concentrated directly *in vacuo*. To the resulting black crude material, hexane (20 mL) and CH_2Cl_2 (4 mL) and the mixture was heated to reflux using a heat gun. The resulting red solution was collected in a new flask and concentrated by nitrogen gas flow to yield the product (433 mg, 78%) as red crystals.

^{1}H NMR (400 MHz, Chloroform-d) δ_H (ppm) 4.92 (t, *J* = 2.0 Hz, 2H), 4.64 (t, *J* = 2.0 Hz, 2H), 4.34 (s, 5H).

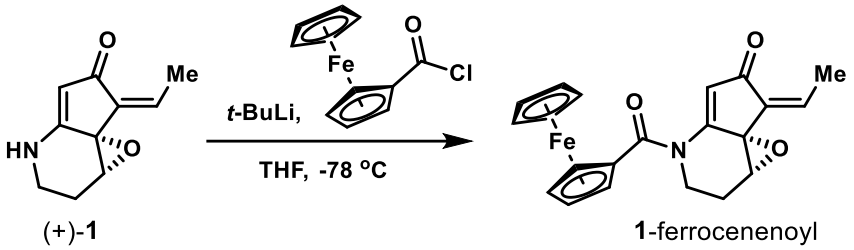

(+)-**1** (5.6 mg, 0.032 mmol, 1 equiv.) was dissolved in THF (1 mL) and cooled to -78 °C, followed by addition of *tert*-buyllithium (1.7 M in pentane, 22 µL, 0.037 mmol, 1.2 equiv.) at -78 °C to yield a yellow solution. Immediately after *tert*-butylithium addition, stock ferrocene-CO_2Cl (0.083 M in THF, 500 µL) was added at -78 °C. The reaction mixture was stirred at -78 °C for 30 min to obtain full conversion. The reaction was quenched by the addition of sat. aq. NH_4Cl (0.5 mL) at -78 °C. The mixture was heated to r.t. and poured over EtOAc (15 mL) and additional sat. aq. NH_4Cl (20 mL) was added. The mixture was extracted (3 x 15 mL) with EtOAc and the combined organics were dried over Na_2SO_4, filtered through sand and celite and concentrated *in vacuo*. The crude material was purified by AFCC (CH_2Cl_2 to 95:5 CH_2Cl_2/acetone, then isocratic 95:5 CH_2Cl_2/acetone) to isolate the product (4.7 mg, 38%) as an orange solid.

Data for (+)-**1**-ferrocenenoyl:

R_f (EtOAc, UV, $KMnO_4$ stain) 0.81.

^{1}H NMR (400 MHz, Chloroform-d) δ_H (ppm) 6.65 (s, 1H), 5.95 (q, *J* = 7.4 Hz, 1H), 4.80 (dt, *J* = 2.5, 1.3 Hz, 2H), 4.69 (dt, *J* = 2.5, 1.2 Hz, 2H), 4.47 (dtt, *J* = 6.4, 2.5, 1.3 Hz, 2H), 4.24 (s, 5H), 4.15 (ddd, *J* = 12.5, 4.9, 1.6 Hz, 2H), 3.88 (d, *J* = 2.9 Hz, 1H), 3.79 (td, *J* = 12.7, 3.5 Hz, 1H), 2.38 (dtd, *J* = 14.9, 3.4, 2.2 Hz, 1H), 2.28 (d, *J* = 7.4 Hz, 3H), 2.13 (ddd, *J* = 14.9, 12.9, 5.1 Hz, 1H).

^{13}C NMR (101 MHz, Chloroform-d) δ_C (ppm) 193.5, 174.0, 157.3, 132.2, 129.4, 120.3, 75.6, 72.8, 71.4, 71.1, 70.7, 70.1, 60.9, 57.8, 41.6, 25.7, 13.70.

HRMS (ESI): Calc. for $C_{21}H_{19}O_3NFeNa^+$ 412.0607; found 412.0617.

$[\boldsymbol{\alpha}]_{\boldsymbol{D}}^{\mathbf{24.1}}$: +67.7 (c = 0.155 g/100 mL, EtOAc).

Single crystals were obtained by dissolving (+)-**1**-ferrocenenoyl (1.6 mg) in CH_2Cl_2 and adding heptane to yield a homogeneous 2:1 solution of CH_2Cl_2/heptane. This sample was allowed to evaporate slowly o/n at r.t. to obtain crystals suitable for X-ray diffraction.

^{1}HNMR data comparison of natural[10] streptazone B_1 and synthetic streptazone B_1 in methanol-d4 recalibrated to methanol-d4 peak (3.310 ppm).

Natural	*J* (Hz)	**Synthetic**	*J* (Hz)	**|Δδ|**
6.31	td (4.5, 1.3)	6.32	t (4.5)	0.01
6.25	q (7.5)	6.26	q (7.5)	0.01
5.17	bs	5.18	bs	0.01
3.36	t (7.0)	3.37	t (7.0)	0.01
2.47	td (7.0, 4.5)	2.48	td (7.0, 4.4)	0.01
2.22	d (7.5)	2.23	d (7.5)	0.01

^{13}CNMR data comparison of natural[10] streptazone B_1 and synthetic streptazone B_1 in methanol-d4 recalibrated to methanol-d4 peak (49.0 ppm).

Natural	*J* (Hz)	**Synthetic**	*J* (Hz)	**|Δδ|**
195.1	s	195.4	s	0.3
165.7	s	165.2	s	0.5
132.4	s	132.5	s	0.1
132.3	s	132.3	s	0
126.7	d	126.7	s	0
119.2	d	119.1	s	0.1
102.4	d	102.4	s	0
39.9	t	39.9	s	0
24.0	t	24.1	s	0.1
13.6	q	13.5	s	0.1

^{1}HNMR data comparison of natural[10] streptazone B_2 and synthetic streptazone B_2 in methanol-d4 recalibrated to methanol-d4 peak (3.310 ppm).

Natural	*J* (Hz)	**Synthetic**	*J* (Hz)	**|Δδ|**
6.58	tm (4.5)	6.60	t (4.5)	0.02
6.38	q (7.5)	6.39	q (7.6)	0.01
5.13	d (1.0)	5.15	d (1.0)	0.02
3.39	t (7.5)	3.41	t (7.0)	0.02
2.55	td (7.5, 4.5)	2.57	td (6.9, 4.5)	0.02
2.03	d (7.5)	2.04	d (7.5)	0.01

^{13}CNMR data comparison of natural[10] streptazone B_2 and synthetic streptazone B_2 in methanol-d4 recalibrated to methanol-d4 peak (49.0 ppm).

Natural	*J* (Hz)	**Synthetic**	*J* (Hz)	**|Δδ|**
193.4	s	193.4	s	0
167.5	s	167.5	s	0
133.7	s	133.7	s	0
131.4	s	131.4	s	0
126.2	d	126.1	s	0.1
125.8	d	125.8	s	0
99.0	d	99.0	s	0
39.5	t	39.5	s	0
24.7	t	24.7	s	0
14.3	q	14.3	s	0

^{1}HNMR data comparison of natural[10] streptazone A and synthetic streptazone A in acetone-d6 recalibrated to acetone-d6 peak (2.05 ppm).

Natural	*J* (Hz)	**Synthetic**	*J* (Hz)	**|Δδ|**
7.32	bs	7.27	bs	0.05
5.69	qd (7.3, 0.7)	5.70	qd (7.3, 0.8)	0.01
5.18	s	5.18	s	0
3.95	d (2.7)	3.96	d (2.9)	0.01
3.35	ddd (12.3, 12.3, 4.0)	3.35	td (12.6, 4.0)	0
3.18	dddm (12.3, 5.5, 5.5)	3.22-3.16	m	0.01
2.28	dm (15.0)	2.28	dddd (14.7, 4.3, 2.9, 1.6)	0
2.15	d (7.3)	2.16	d (7.3)	0.01
2.13-2.06	m	2.14-2.08	m	-

^{13}CNMR data comparison of natural[10] streptazone A and synthetic streptazone A in acetone-d6 recalibrated to acetone-d6 peak (29.84 ppm). We suspect that the reported chemical shifts in the isolation paper was not calibrated to acetone-d6 and thereby demonstrating a consistent shift between 0.7-0.9 ppm relative to our synthetic sample. Note also, in the case of signal 25.5, 36.7, 59.4, 105.1, 132.7, and 165.8, we observed a small signal shifted downfield. We currently lack an explanation for this effect in acetone-d6, however, this is not observed in chloroform-d.

Natural	*J* (Hz)	**Synthetic**	*J* (Hz)	**|Δδ|**
191.7	s	190.9	s	0.8
166.6	s	165.8	s	0.8
133.4	s	132.7	s	0.7
128.2	d	127.5	s	0.7
105.9	d	105.1	s	0.8
60.1	s	59.4	s	0.7
59.6	d	58.9	s	0.7
37.6	t	36.7	s	0.9
26.2	t	25.5	s	0.7
13.6	q	12.9	s	0.7

^{1}HNMR data comparison of natural[11] abikoviromycin and synthetic abikoviromycin in chloroform-d recalibrated to chloroform-d peak (7.26 ppm).

Natural	*J* (Hz)	**Synthetic**	*J* (Hz)	**|Δδ|**
7.43	d (6.5)	7.41	dt (6.3, 1.2)	0.02
6.53	d (6.5)	6.52	dm (6.2)	0.01
5.50	q (7.0)	5.49	qt (7.4, 1.4)	0.01
3.92	s	3.91	m	0.01
3.81	dd (15, 5.5)	3.80	ddt (15.5, 5.7, 1.5)	0.01
3.69	dt (15, 5.5)	3.72-3.63	m	0.02
2.19	m	2.17	dddd (14.8, 5.5, 2.4, 1.4)	0.02
1.90	d (7.0)	1.88	d (7.3)	0.02
1.62	m	1.60	ddd (14.8, 12.4, 5.6)	0.02

^{13}CNMR data comparison of natural[11] abikoviromycin and synthetic abikoviromycin in chloroform-d recalibrated to chloroform-d peak (77.16 ppm).

Natural	*J* (Hz)	**Synthetic**	*J* (Hz)	**|Δδ|**
172.1	-	172.2	-	0.1
142.3	-	142.4	-	0.1
136.5	-	136.8	-	0.3
132.8	-	133.1	-	0.3
119.5	-	119.6	-	0.1
59.5	-	59.7	-	0.2
54.5	-	54.7	-	0.2
44.5	-	44.8	-	0.3
21.8	-	22.0	-	0.2
14.0	-	14.2	-	0.2

[1]HNMR data comparison of natural[12] dihydroabikoviromycin and synthetic dihydroabikoviromycin in chloroform-d recalibrated to chloroform-d peak (7.26 ppm). The chemical shifts were not reported in standard format in the isolation studies, hence an overlay of the isolated dihydroabikoviromycin (natural) is compared to the synthetic sample.

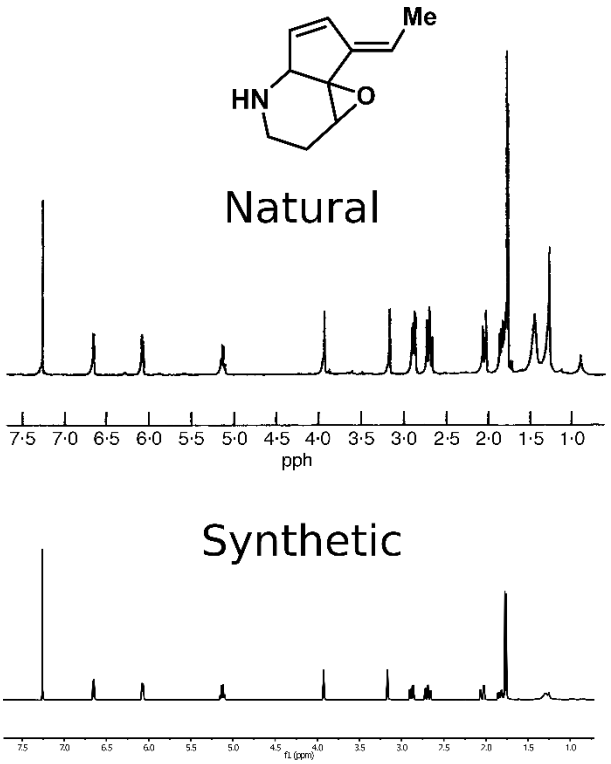

[13]CNMR data comparison of natural[12] dihydroabikoviromycin and synthetic dihydroabikoviromycin in chloroform-d recalibrated to chloroform-d peak (77.16 ppm). Note, *J* couplings were not reported.

Natural	*J* (Hz)	**Synthetic**	*J* (Hz)	**|Δδ|**
140.4	s	140.5	-	0.1
134.8	d	134.9	-	0.1
131.4	d	131.6	-	0.2
114.7	d	114.9	-	0.2
64.5	s	64.6	-	0.1
63.2	d	63.4	-	0.2
59.3	d	59.4	-	0.1
39.9	t	40.0	-	0.1
26.4	t	26.6	-	0.2
14.0	q	14.2	-	0.2

General stabilities

Streptazone B_1/B_2 – these compounds should be stored as the solid materials in a freezer (our freezer runs at -24 °C) to prevent decomposition. The material does decompose if stored at r.t. in solution for extended time periods. This was evident as we had to prepare fresh samples for TLC analysis approximately every 3 weeks as the solution changed from clear transparent to brown with precipitation.

Streptazone A(**1**)/A_2(**1'**) – these compounds exhibited the same instabilities as streptazone B_1/B_2, however, to a much lower extent. Generally, we could employ the same sample for TLC analysis over almost 2 months before a new sample had to be prepared. In comparison to B_1/B_2, these compounds are highly acid labile as demonstrated by the heatmaps shown below where **1** decomposed completely at pH = 4 after 24 h whereas significant amount of **1'** had decomposed after the same time period. The heatmap furthermore demonstrate that **1** is stable up to pH = 10 over 48 h, whereas **1'** decomposes significantly at the same pH over 48 h.

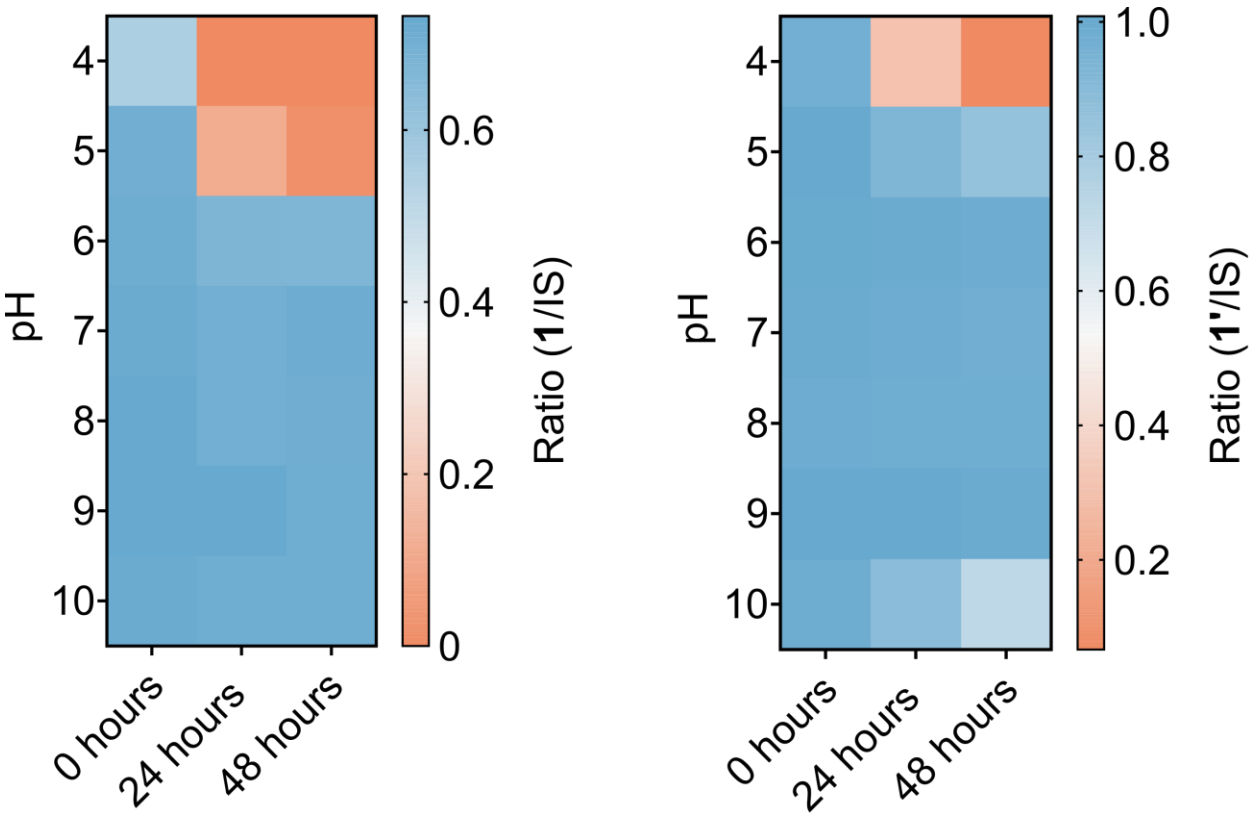

Buffer preparation:

pH 4 buffer: an ammonium formate solution was pH adjusted to 4.0 with a 0.1 M formic acid solution. This was further diluted until a concentration of 0.0111 M ammonium formate was reached.

pH 5 buffer: an ammonium formate solution was pH adjusted to 5.0 with a 0.1 M formic acid solution. This was further diluted until a concentration of 0.0111 M ammonium formate was reached.

pH 6 buffer: an ammonium bicarbonate solution was pH adjusted to 6.0 with a 0.1 M formic acid solution. This was further diluted until a concentration of 0.0111 M ammonium bicarbonate was reached.

pH 7 buffer: an ammonium bicarbonate solution was pH adjusted to 7.0 with a 0.1 M formic acid solution. This was further diluted until a concentration of 0.0111 M ammonium bicarbonate was reached.

pH 8 buffer: an ammonium bicarbonate solution was pH adjusted to 8.0 with a 0.1 M formic acid solution. This was further diluted until a concentration of 0.0111 M ammonium bicarbonate was reached.

pH 9 buffer: an ammonium bicarbonate solution was pH adjusted to 9.0 with a 0.1 M ammonium hydroxide solution. This was further diluted until a concentration of 0.0111 M ammonium bicarbonate was reached.

pH 10 buffer: a sodium tetraborate decahydrate solution was pH adjusted to 10.0 with a 0.1 M sodium hydroxide solution. This was further diluted until a concentration of 0.0111 M sodium tetraborate decahydrate was reached.

Acetanilide was employed as an internal standard (IS) for studying the stability of **1** and **1'**.

Stock solutions of acetanilide (4 mM), **1** (4 mM) and **1'** (4 mM) were prepared in MeCN. For each pH, 50 µL stock acetanilide and either **1** or **1'** were mixed. Then, the corresponding buffer solution was added (900 µL) to yield a final volume of 1000 µL and final concentration of 0.01 M buffer and 200 µM acetanilide and **1** or **1'**. The sample was immediately analyzed by analytical HPLC (this time point constitutes the 0 hours time point) and subsequently at 24 hours and 48 hours. The area under the peak was integrated and the ratio between either **1** or **1'** relative to internal standard was plotted in the heatmap.

Abikoviromycin – this particular natural product was indeed found to encompass instabilities associated with *in vacuo* concentration and prolonged storage of stock solutions at room temperature. Specifically, following its formation and isolation using CH_2Cl_2/*i*PrOH solvent system on SiO_2, the sample had to be monitored carefully during its concentration. If the sample became too concentrated, a brown solution resulted and a brown insoluble substance was formed. We found that concentrating the sample to a volume of approx. 2 mL at 0.11 mmol scale *in vacuo* at 30 °C and then further concentration by nitrogen gas flow at room temperature decreased the extent to which abikoviromycin underwent polymerization. However, even this approach induced polymerization, see pictures below. Note, generally we observed that isomerization to the opposite isomer (*cis* to *trans* and *trans* to *cis*) resulted whenever the sample was dissolved and then reconcentrated, this operation should therefore be conducted as few times as possible.

Clean and clear solution after purification (approx. 2 mL)

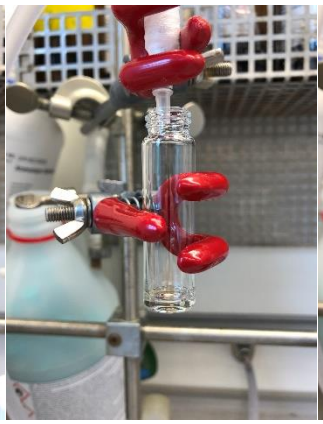

More concentrated (approx. 0.4 mL) – no color change

Fully concentrated once – a brown color results

Redissolved and concentrated 5 consecutive times – significant color change

The resulting sample in $CDCl_3$ after 5 consecutive concentrations.

UPC^2 chromatograms

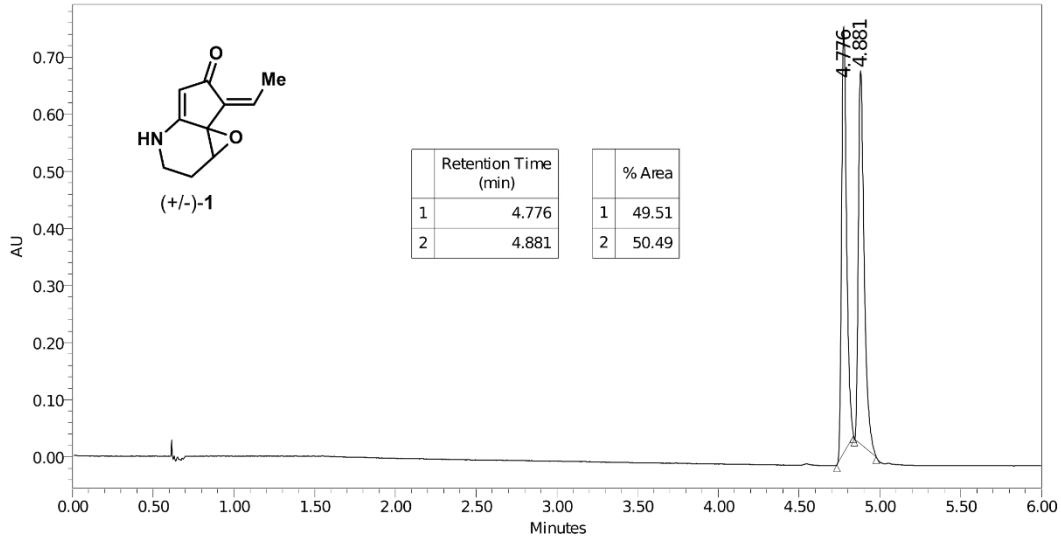

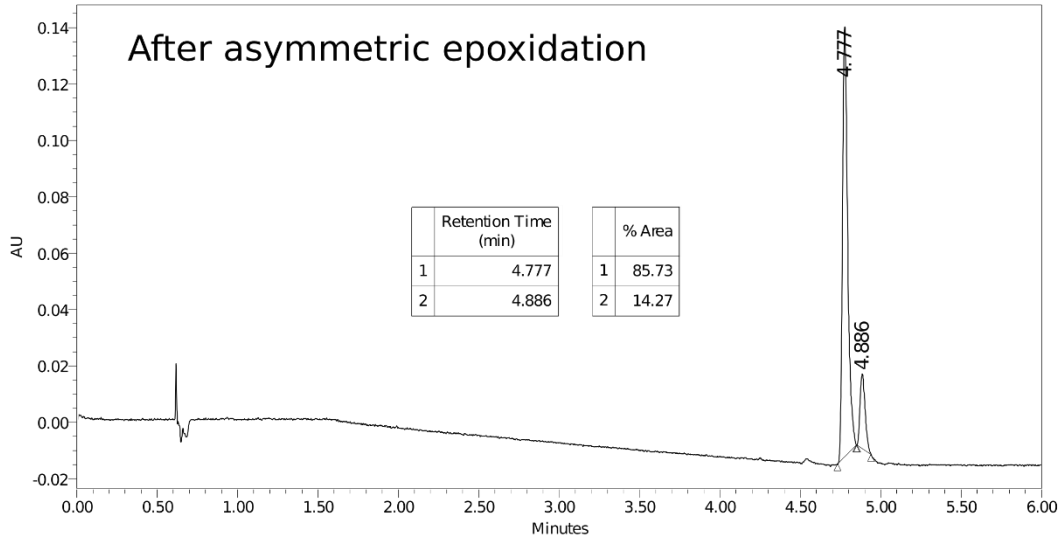

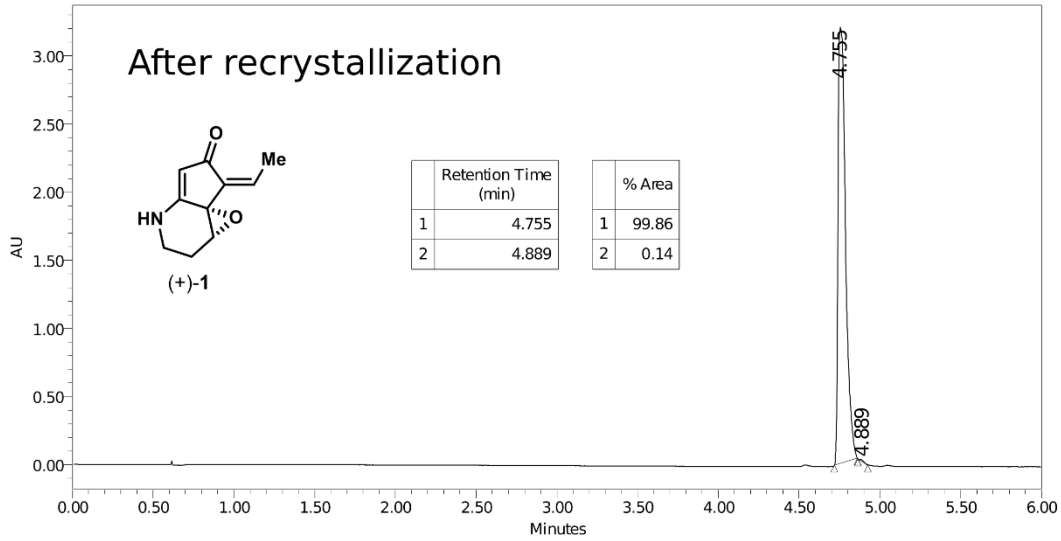

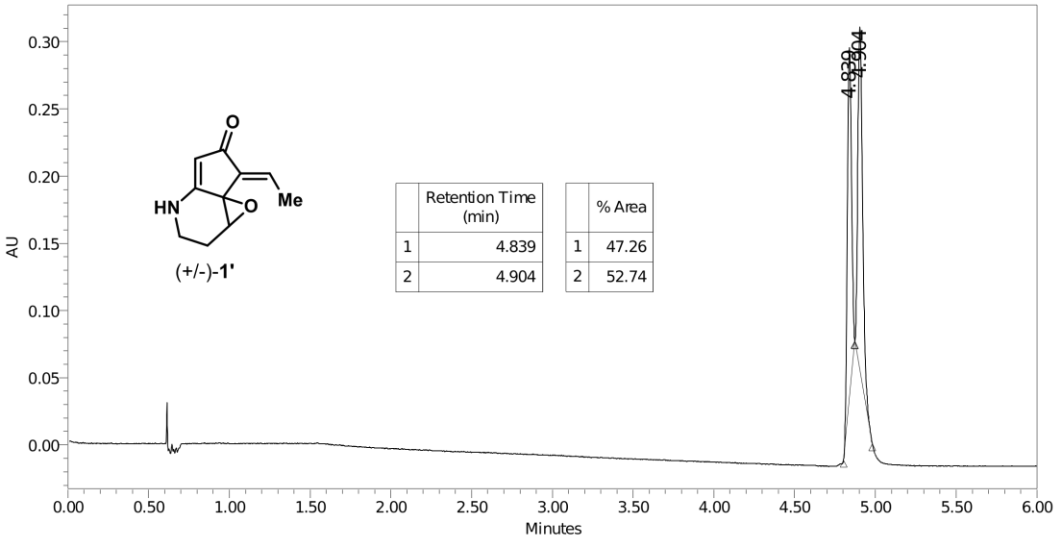
(+/-)-1'
Retention Time (min)
1 4.839
2 4.904
% Area
1 47.26
2 52.74
4.839
4.904
AU
Minutes

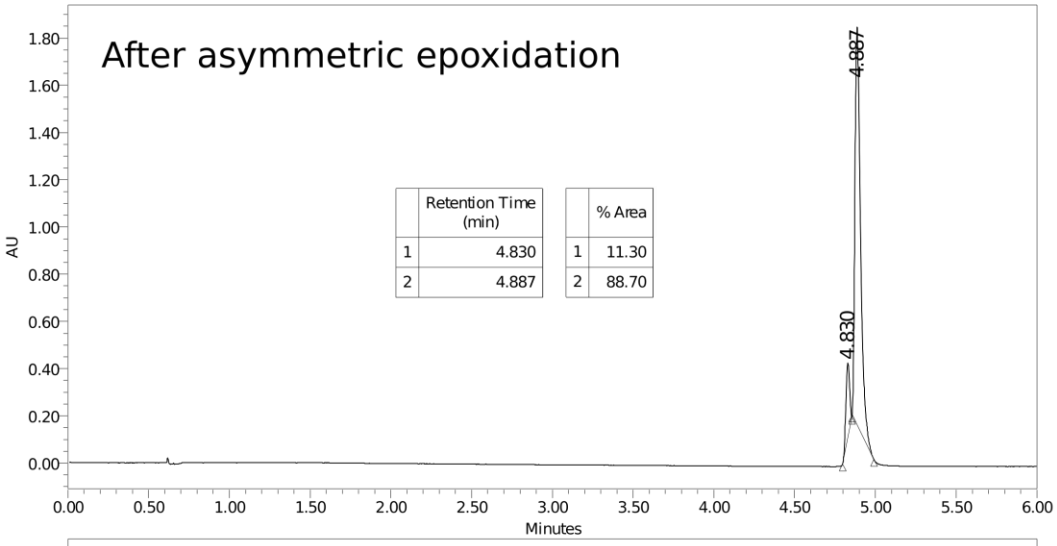
After asymmetric epoxidation
Retention Time (min)
1 4.830
2 4.887
% Area
1 11.30
2 88.70
4.887
4.830
AU
Minutes

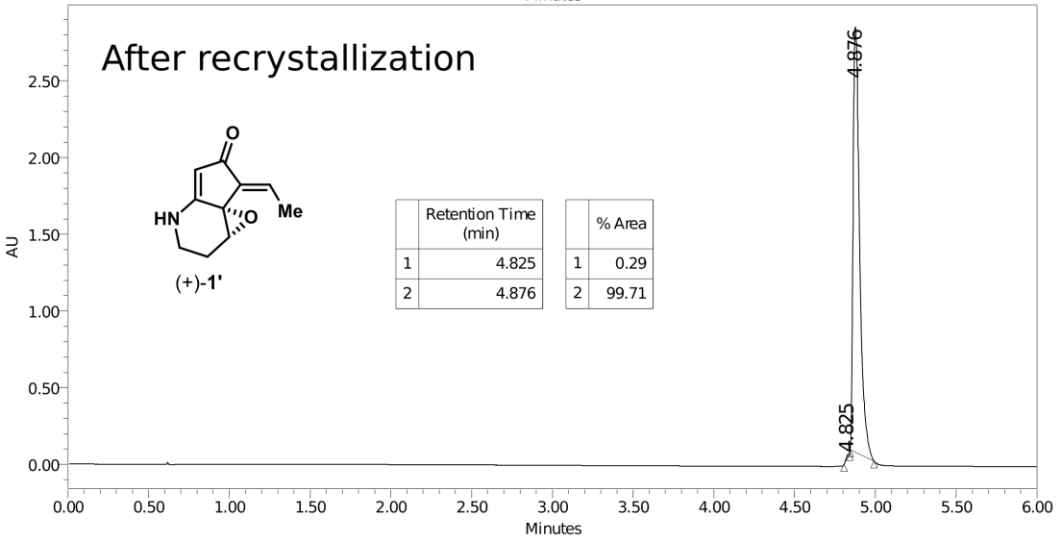
After recrystallization
(+)-1'
Retention Time (min)
1 4.825
2 4.876
% Area
1 0.29
2 99.71
4.876
4.825
AU
Minutes

Crystallographic data

Data for (+/-)-*syn*-**10** aldol product.

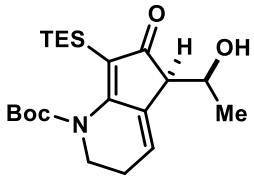

(+/-)-*syn*-**10**

Item	Value
Molecular formula	C21 H35 N O4 Si
Formula weight	393.59
Crystal system	monoclinic
Space Group	P 1 21/c 1
a (Å)	14.8757
b (Å)	14.3307
c (Å)	10.5542
α (°)	90
β (°)	100.167
γ (°)	90
Volume ($Å^3$)	2214.61
Z	4
T (K)	100
ρ ($g\ cm^{-1}$)	1.18
λ (Å)	0.71073
μ (mm^{-1})	0.131
# measured refl	42130
# unique refl	6529
R_{int}	0.0367
# parameters	252
$R(F^2)$, all refl	0.0459
$R_w(F^2)$, all refl	0.0963
Goodness of fit	1.054

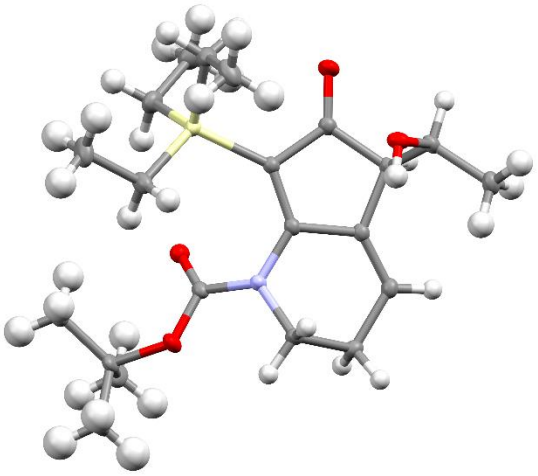

Data for (+/-)-*anti*-**10** aldol product.

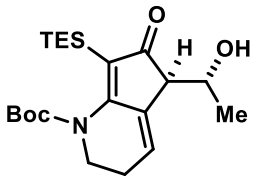

(+/-)-*anti*-**10**

Item	Value
Molecular formula	C21 H35 N O4 Si
Formula weight	393.59
Crystal system	orthorhombic
Space Group	P b c a
a (Å)	9.2476
b (Å)	16.4845
c (Å)	28.5316
α (°)	90
β (°)	90
γ (°)	90
Volume ($Å^3$)	4349.42
Z	8
T (K)	100
ρ ($g\ cm^{-1}$)	1.202
λ (Å)	0.71073
μ (mm^{-1})	0.133
# measured refl	73846
# unique refl	8987
R_{int}	0.0464
# parameters	252
$R(F^2)$, all refl	0.0584
$R_w(F^2)$, all refl	0.1139
Goodness of fit	1.072

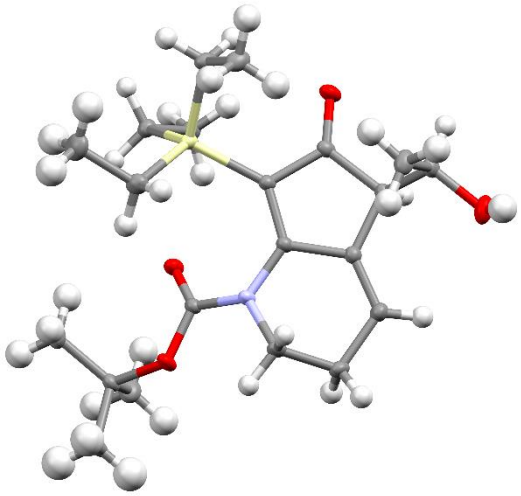

Data for racemic streptazone A (**1**).

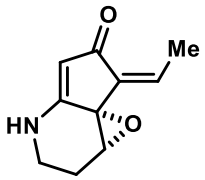

(+/-)-**1**

Item	Value
Molecular formula	C10 H11 N O2
Formula weight	177.2
Crystal system	monoclinic
Space Group	P 1 21/c 1
a (Å)	10.1937
b (Å)	10.2486
c (Å)	8.3093
α (°)	90
β (°)	97.629
γ (°)	90
Volume ($Å^3$)	860.4
Z	4
T (K)	100
ρ ($g\ cm^{-1}$)	1.368
λ (Å)	0.71073
μ (mm^{-1})	0.096
# measured refl	7344
# unique refl	1813
R_{int}	0.0581
# parameters	119
$R(F^2)$, all refl	0.0612
$R_w(F^2)$, all refl	0.1396
Goodness of fit	1.106

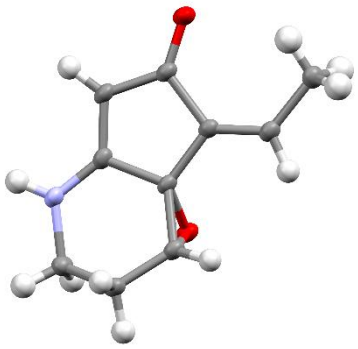

Data for racemic streptazone A_2 (**1'**).

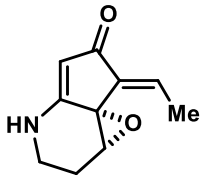

(+/-)-**1'**

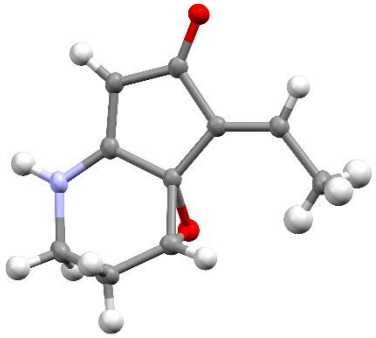

Item	Value
Molecular formula	C10 H11 N O2
Formula weight	177.2
Crystal system	monoclinic
Space Group	P 1 21/c 1
a (Å)	8.9264
b (Å)	6.5846
c (Å)	14.801
α (°)	90
β (°)	95.889
γ (°)	90
Volume ($Å^3$)	865.3
Z	4
T (K)	100
ρ ($g\ cm^{-1}$)	1.36
λ (Å)	0.71073
μ (mm^{-1})	0.095
# measured refl	23466
# unique refl	2300
R_{int}	0.052
# parameters	119
R(F^2), all refl	0.0592
R_w(F^2), all refl	0.1145
Goodness of fit	1.086

Data for (+)-**1**-ferrocenenoyl.

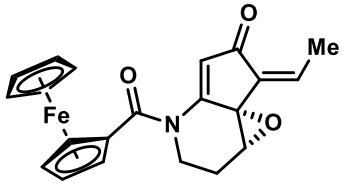

(+)-**1**-ferrocenenoyl

Item	Value
Molecular formula	C21 H19 Fe N O3
Formula weight	389.22
Crystal system	orthorhombic
Space Group	P 21 21 21
a (Å)	7.3596
b (Å)	14.0237
c (Å)	16.1154
α (°)	90
β (°)	90
γ (°)	90
Volume ($Å^3$)	1663.25
Z	4
T (K)	100
ρ ($g\ cm^{-1}$)	1.554
λ (Å)	0.71073
μ (mm^{-1})	0.928
# measured refl	16760
# unique refl	4165
R_{int}	0.0509
# parameters	236
R(F^2), all refl	0.0383
R_w(F^2), all refl	0.0755
Goodness of fit	1.024
Flack parameter	0.018(10)

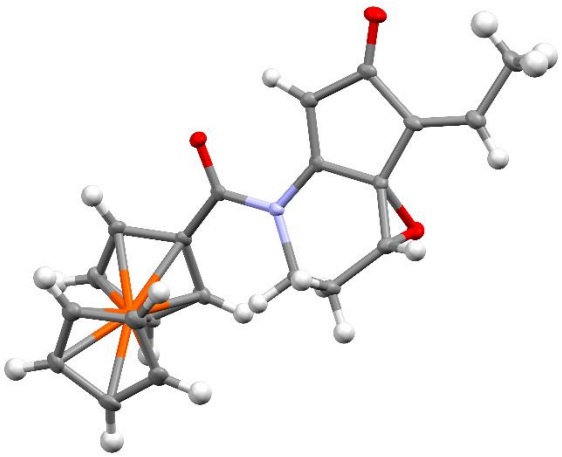

NMR Spectra

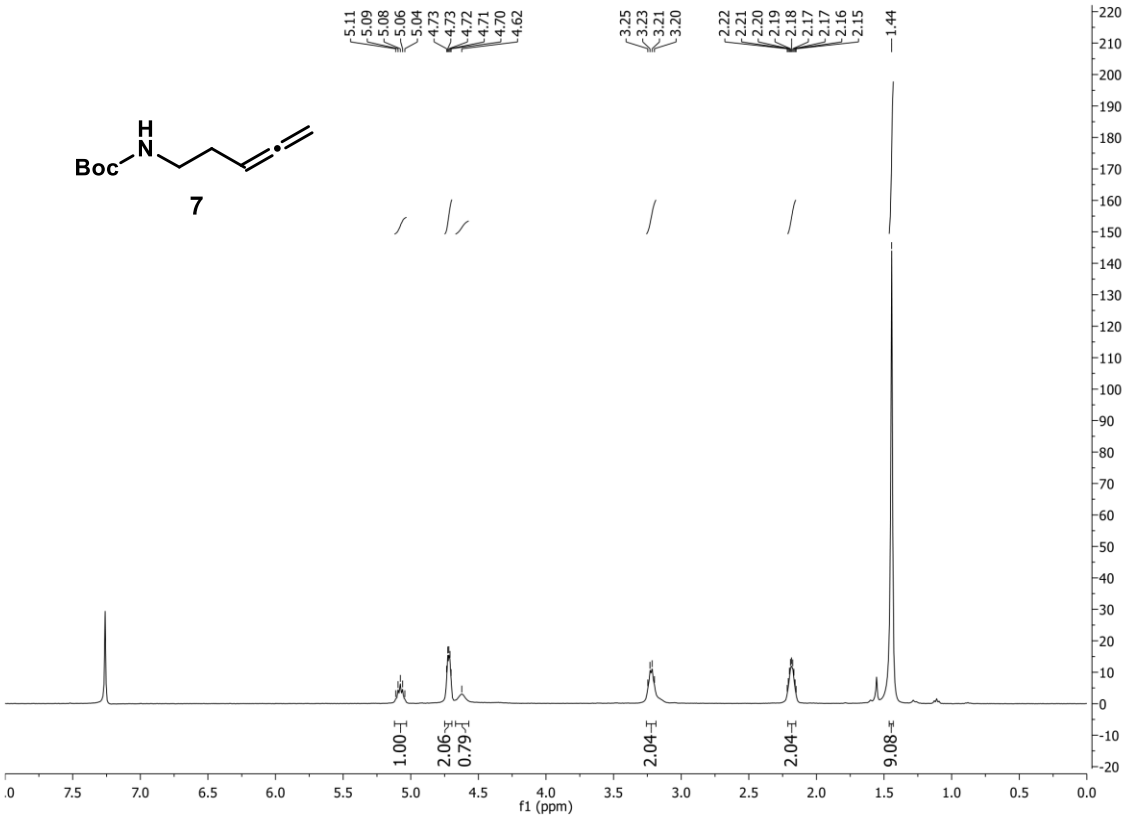
5.11
5.09
5.08
5.06
5.04
4.73
4.72
4.71
4.70
4.62
3.25
3.23
3.21
3.20
2.22
2.21
2.20
2.19
2.18
2.17
2.17
2.16
2.15
1.44
Boc
7
1.00
2.06
0.79
2.04
2.04
9.08
f1 (ppm)

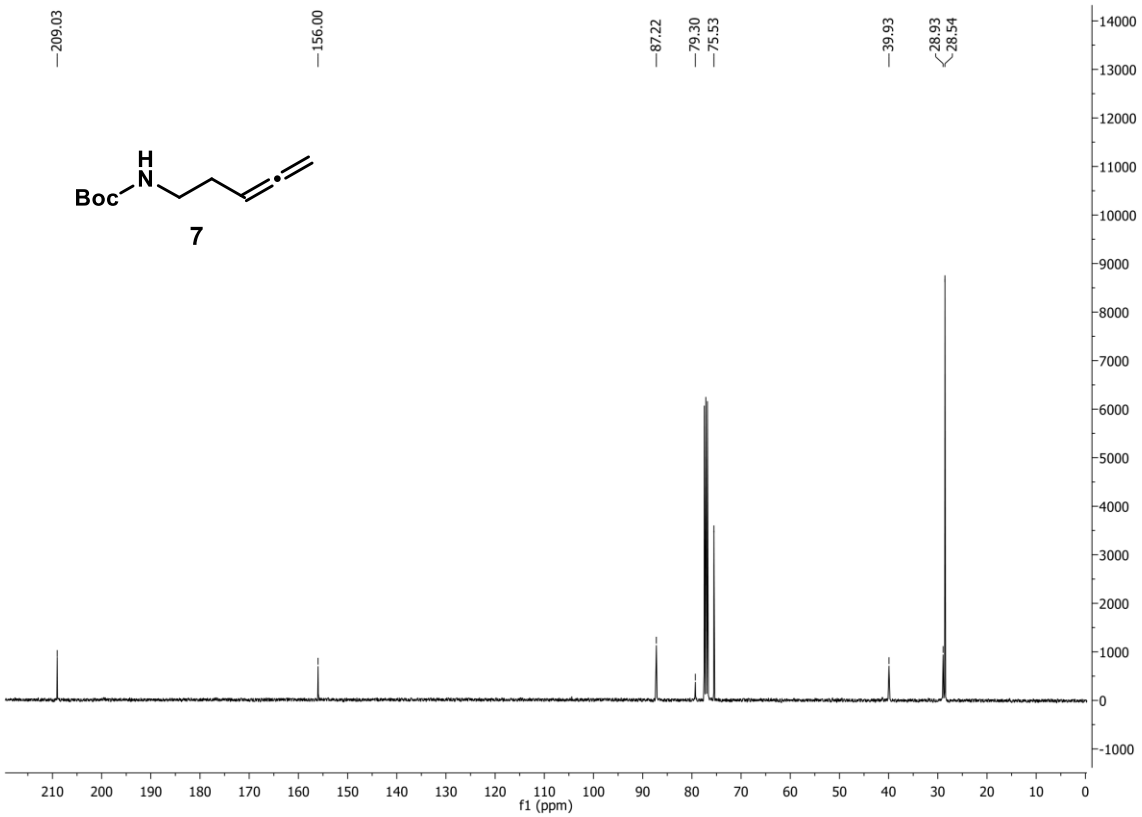
209.03
156.00
87.22
79.30
75.53
39.93
28.93
28.54
Boc
7
f1 (ppm)

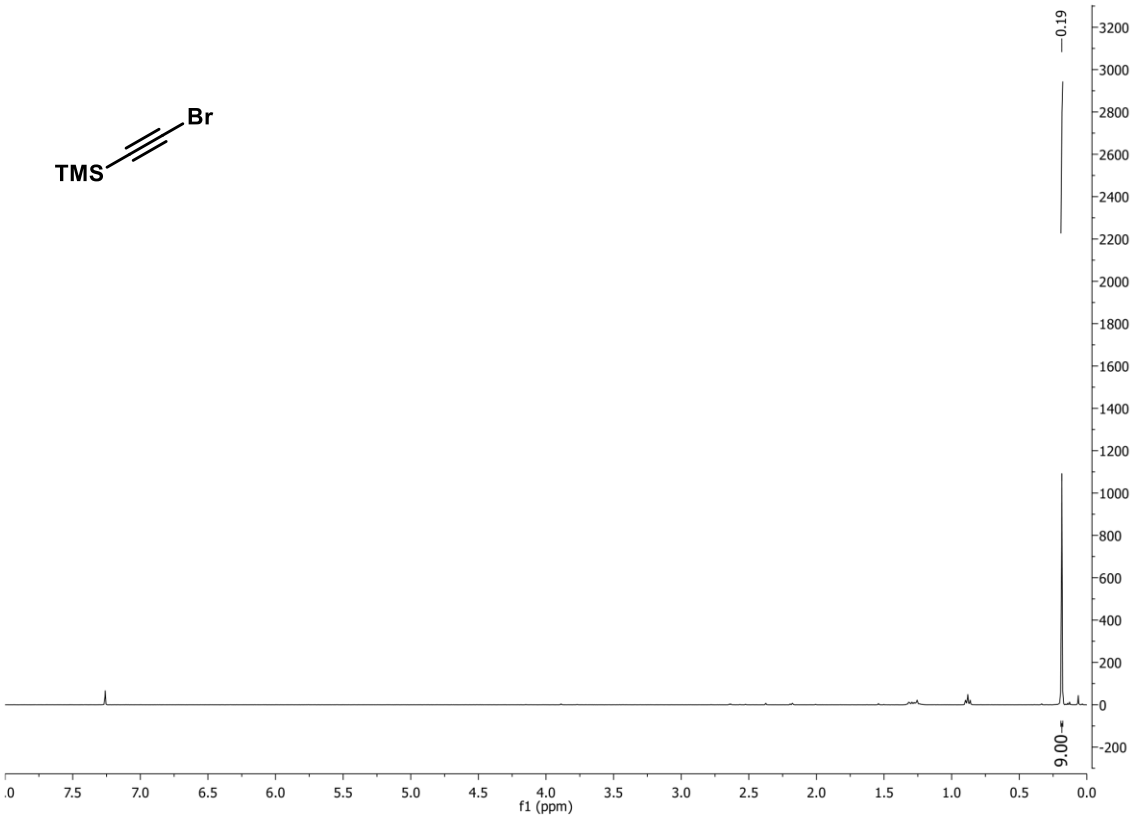
Br
TMS
0.19
9.00
f1 (ppm)

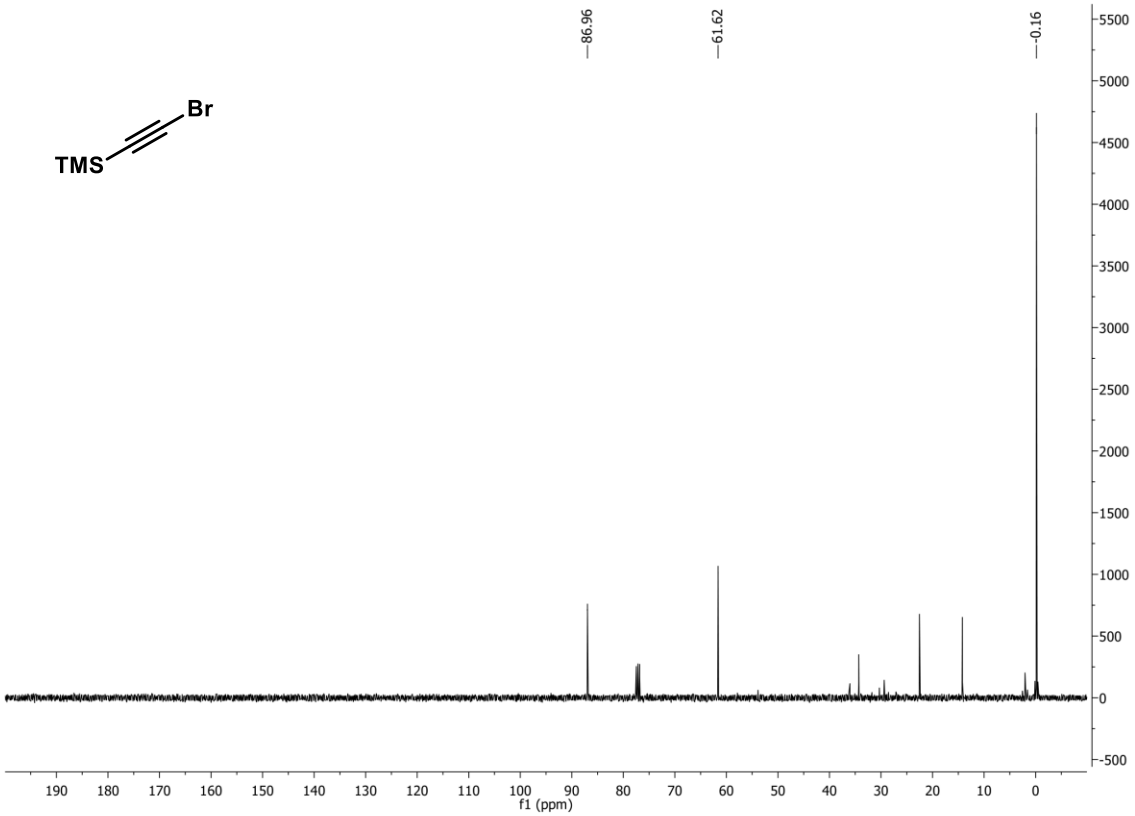
Br
TMS
86.96
61.62
0.16
f1 (ppm)

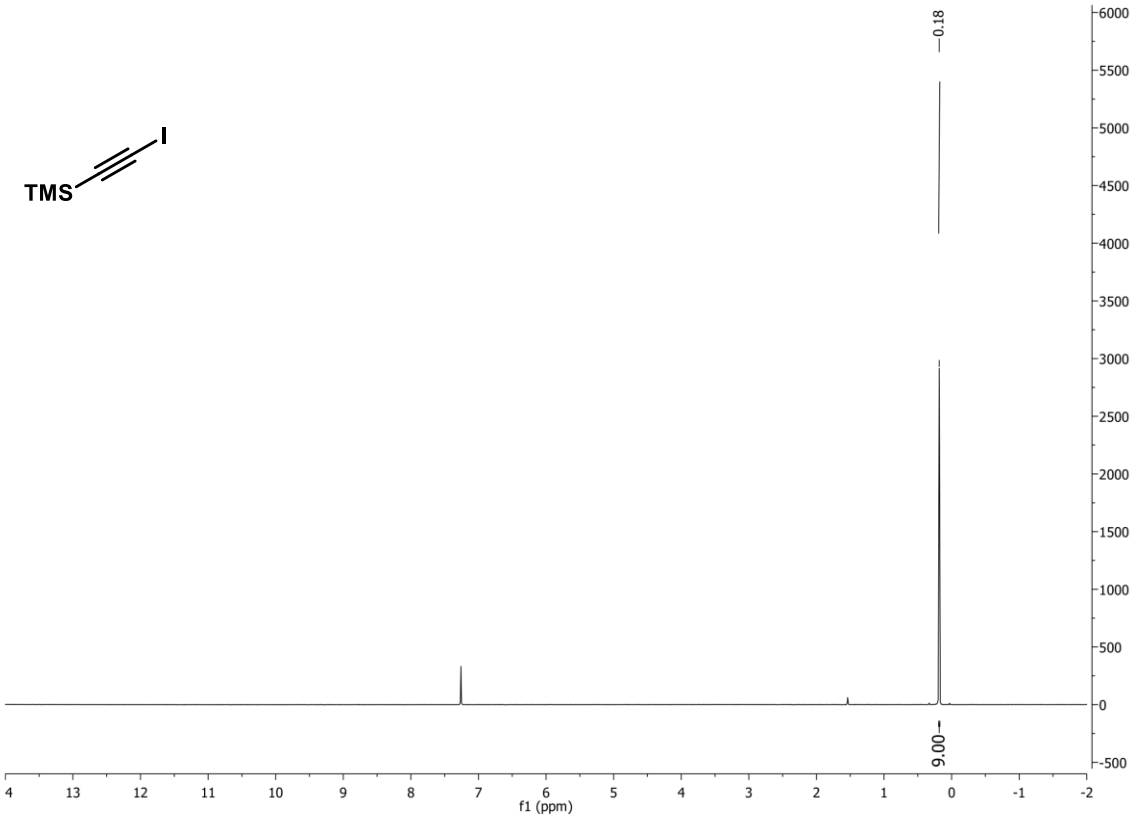
TMS
I
0.18
9.00
f1 (ppm)

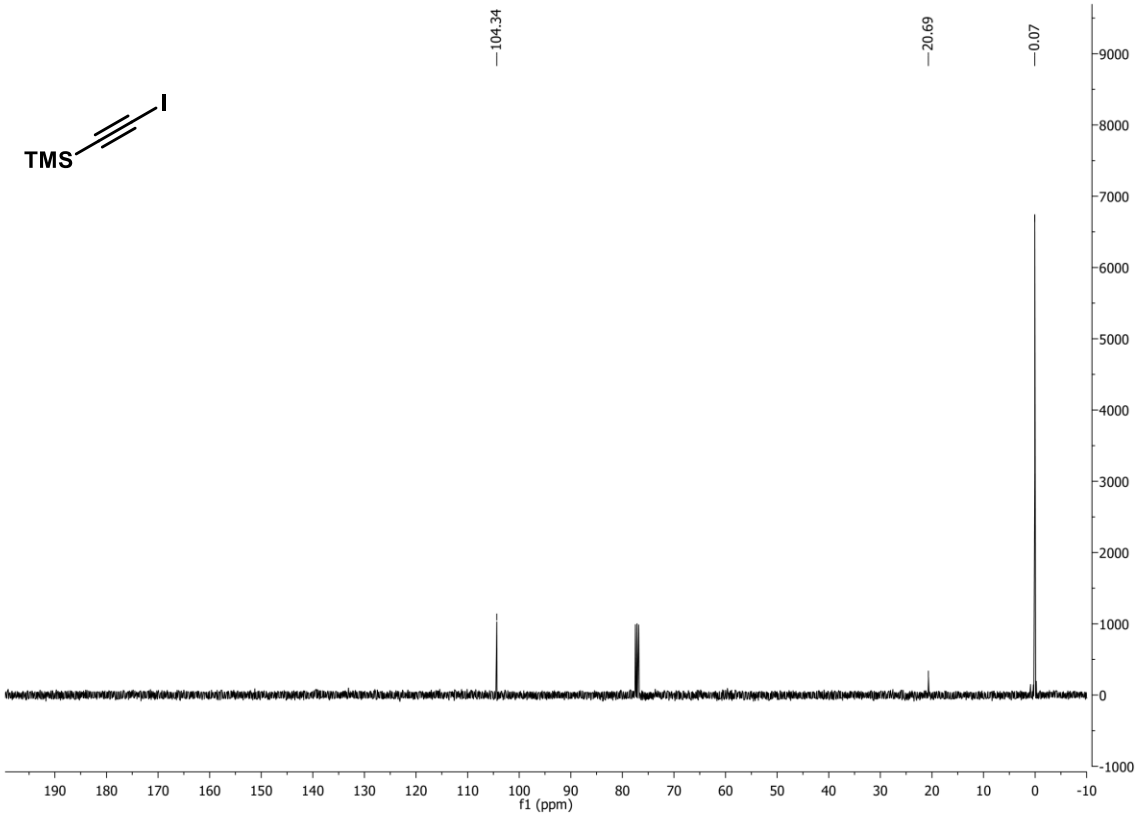
TMS
I
104.34
20.69
0.07
f1 (ppm)

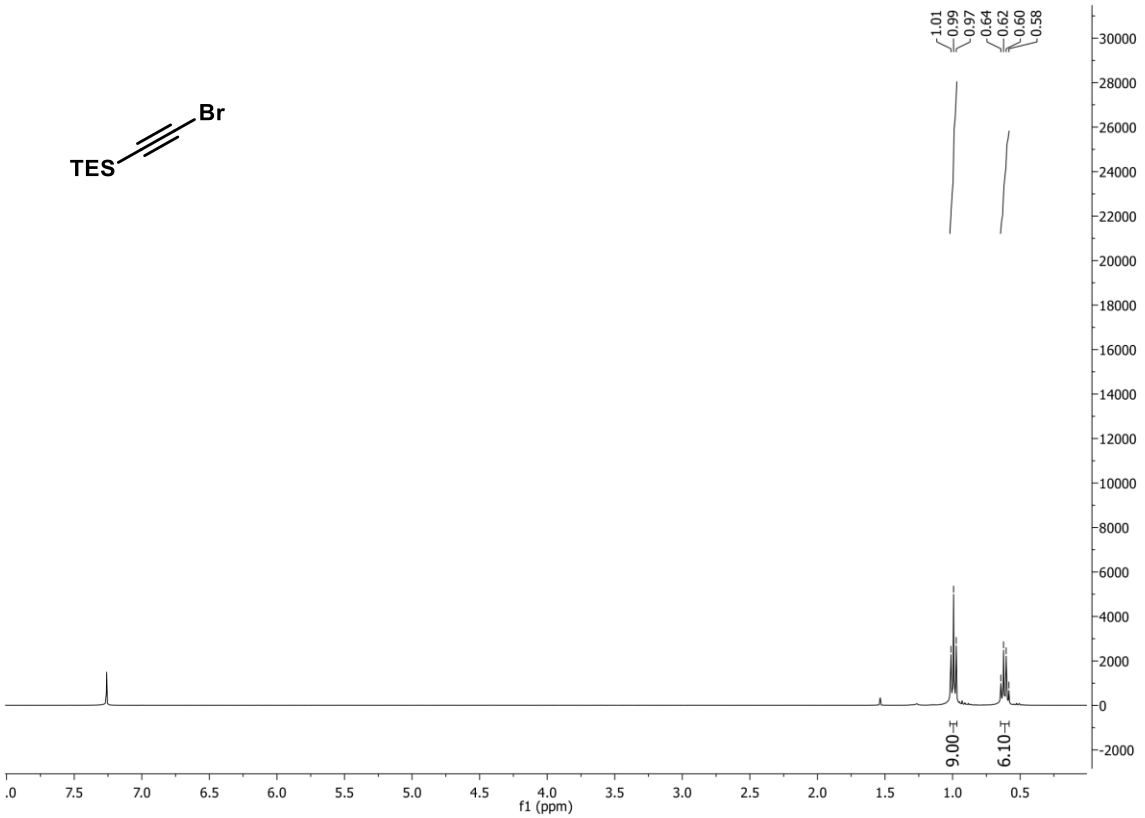
Br
TES
1.01
0.99
0.97
0.64
0.62
0.60
0.58
9.00
6.10
f1 (ppm)

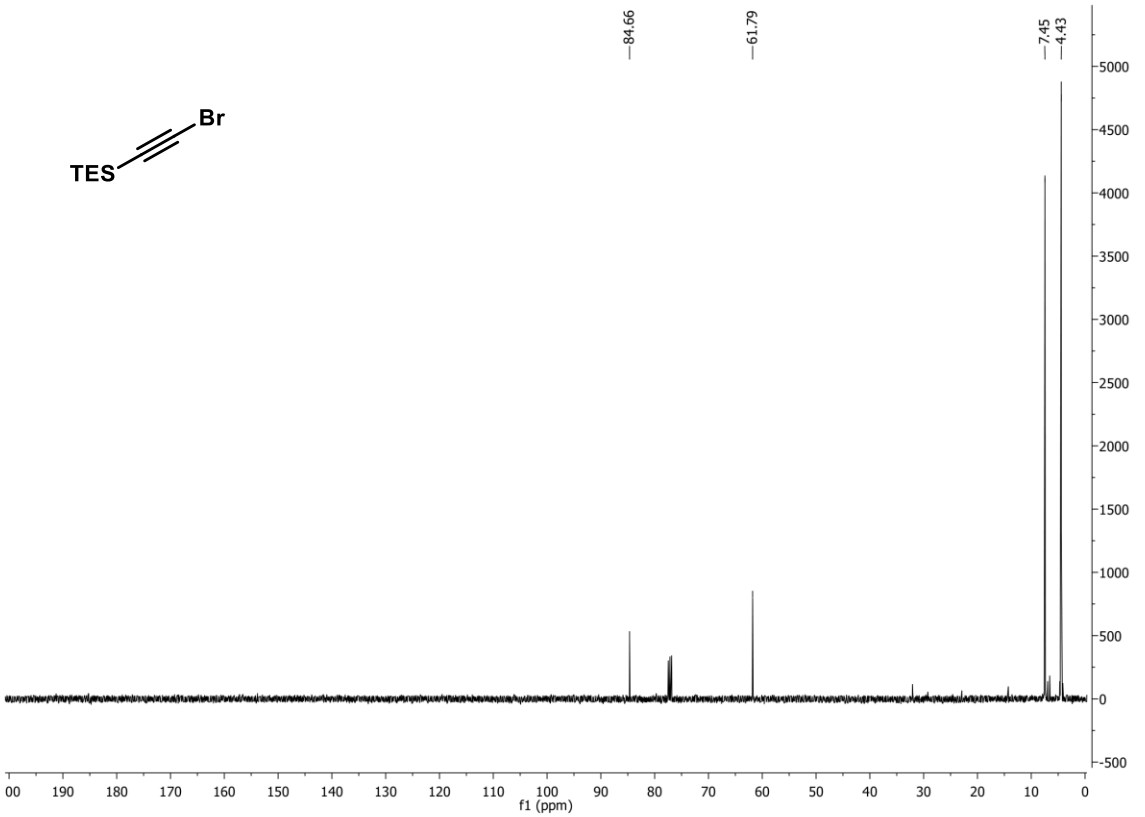
Br
TES
84.66
61.79
7.45
4.43
f1 (ppm)

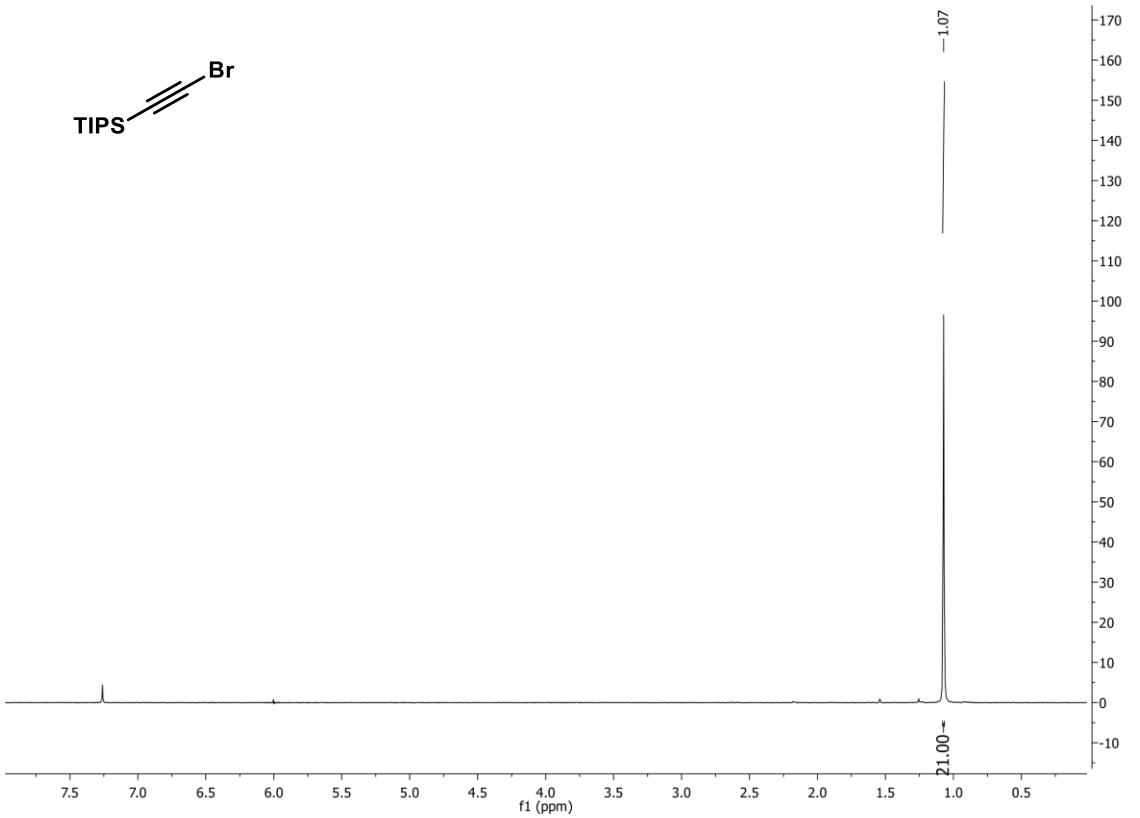
Br
TIPS
1.07
21.00
f1 (ppm)

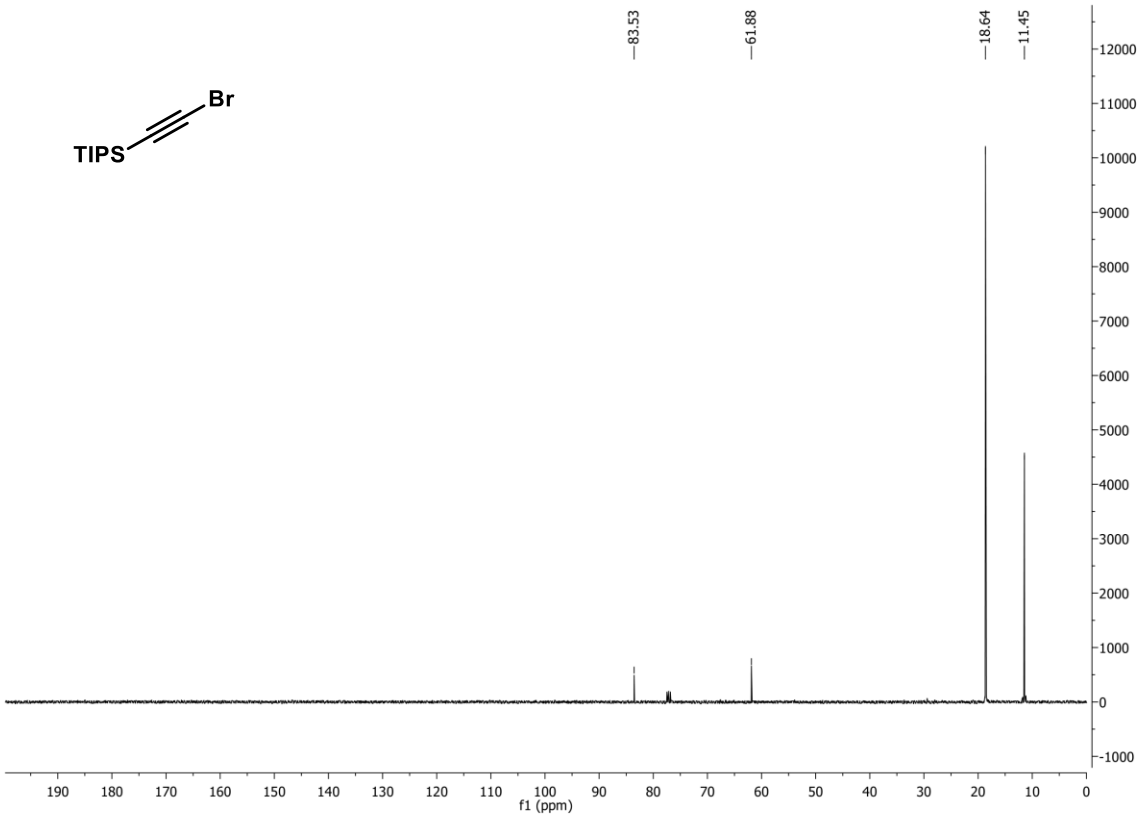
Br
TIPS
83.53
61.88
18.64
11.45
f1 (ppm)

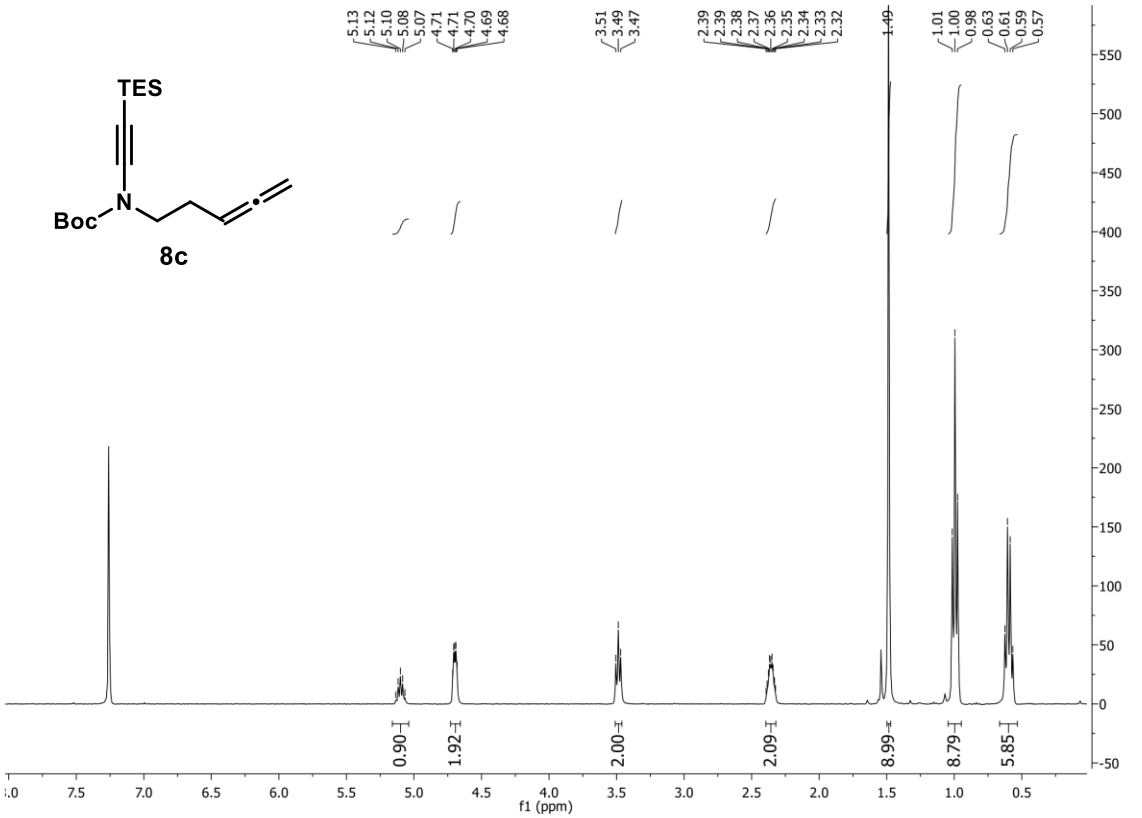
TES
N
Boc
8c
5.13
5.12
5.10
5.08
5.07
4.71
4.71
4.70
4.69
4.68
3.51
3.49
3.47
2.39
2.39
2.38
2.37
2.36
2.35
2.34
2.33
2.32
1.49
1.01
1.00
0.98
0.63
0.61
0.59
0.57
0.90
1.92
2.00
2.09
8.99
8.79
5.85
f1 (ppm)

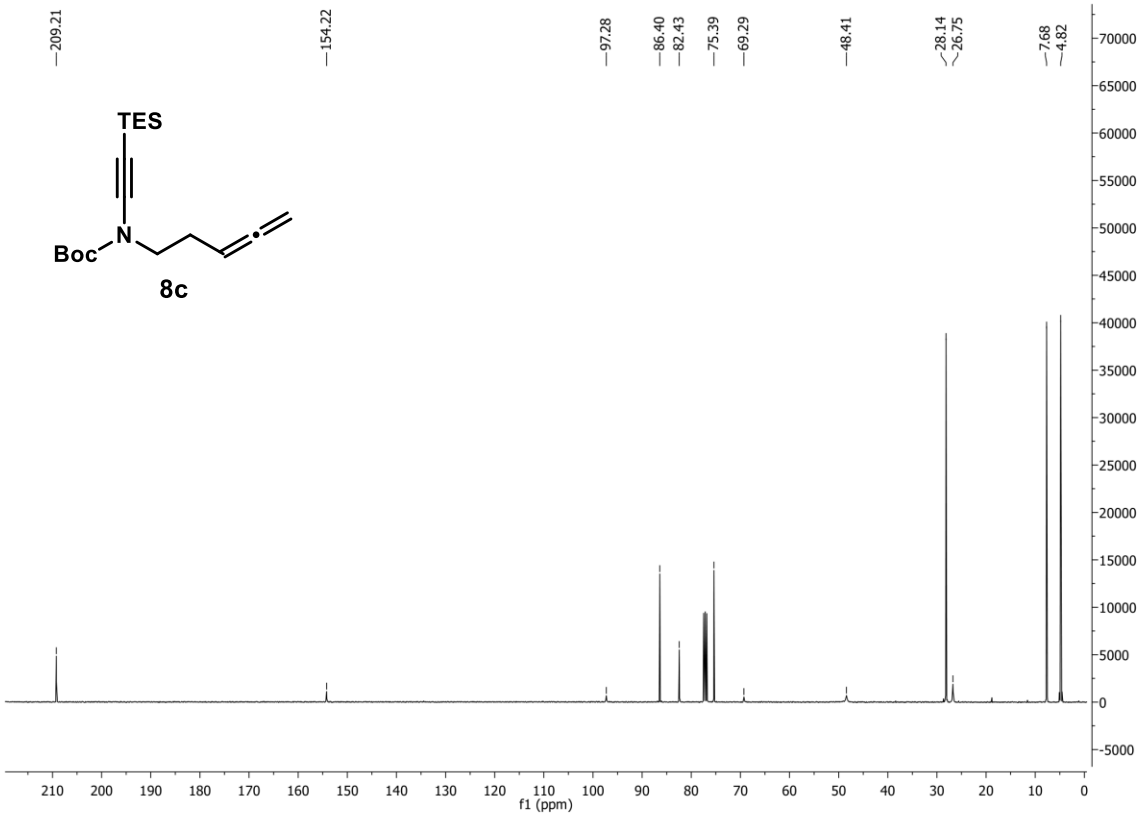
TES
N
Boc
8c
209.21
154.22
97.28
86.40
82.43
75.39
69.29
48.41
28.14
26.75
7.68
4.82
f1 (ppm)

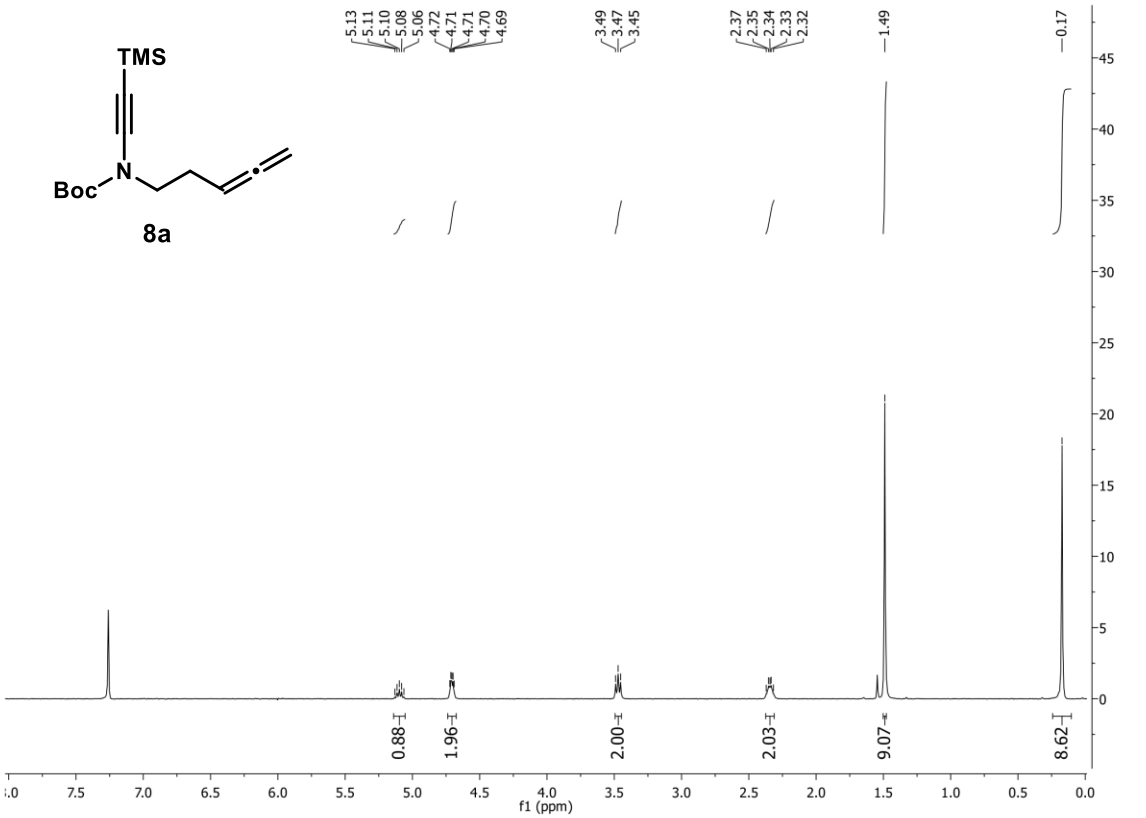
TMS
N
Boc
8a
5.13
5.11
5.10
5.08
5.06
4.72
4.71
4.71
4.70
4.69
3.49
3.47
3.45
2.37
2.35
2.34
2.33
2.32
1.49
0.17
0.88
1.96
2.00
2.03
9.07
8.62
f1 (ppm)

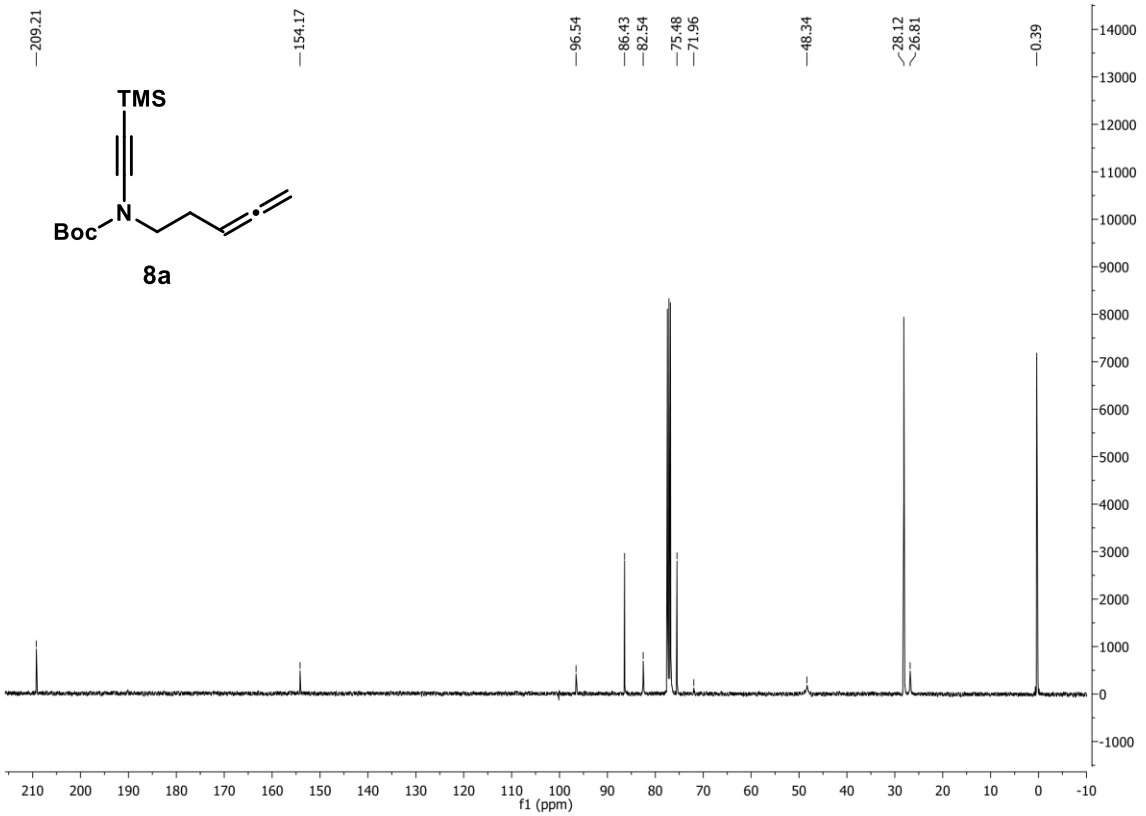
TMS
N
Boc
8a
209.21
154.17
96.54
86.43
82.54
75.48
71.96
48.34
28.12
26.81
0.39
f1 (ppm)

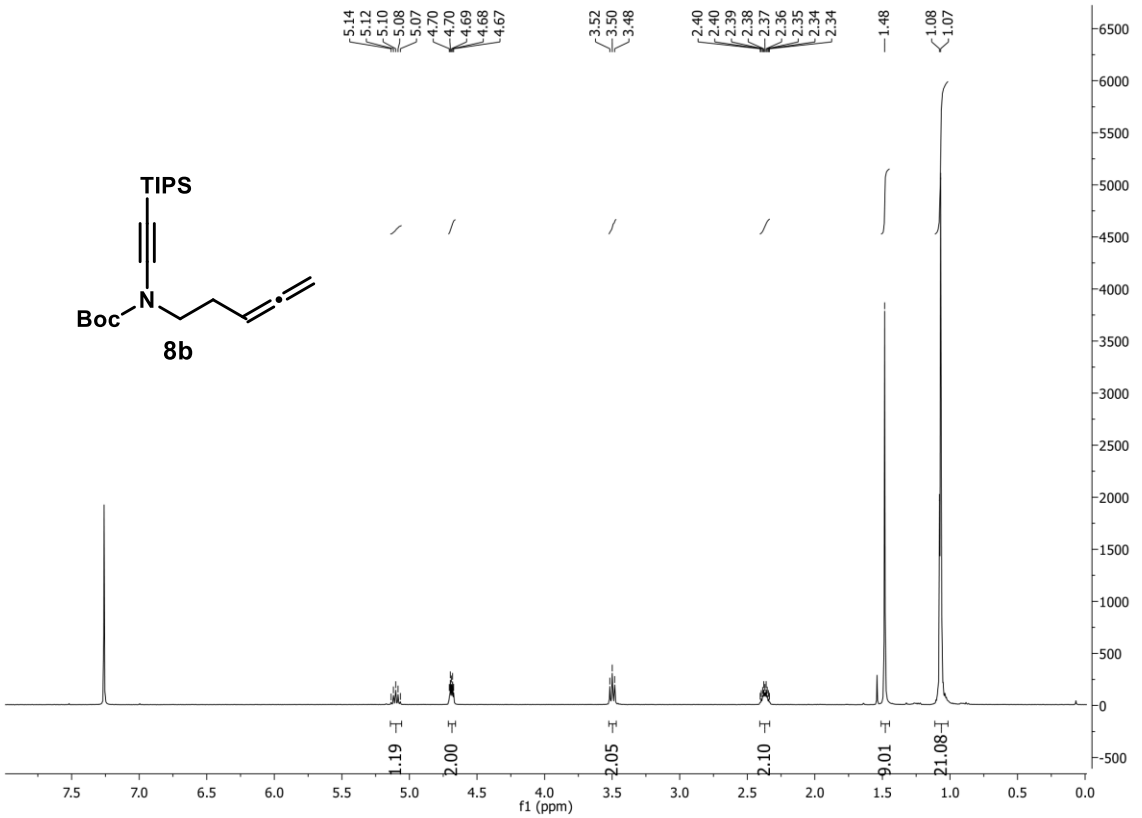
TIPS
N
Boc
8b
5.14
5.12
5.10
5.08
5.07
4.70
4.70
4.69
4.68
4.67
3.52
3.50
3.48
2.40
2.40
2.39
2.38
2.37
2.36
2.35
2.34
2.34
1.48
1.08
1.07
1.19
2.00
2.05
2.10
9.01
21.08
f1 (ppm)

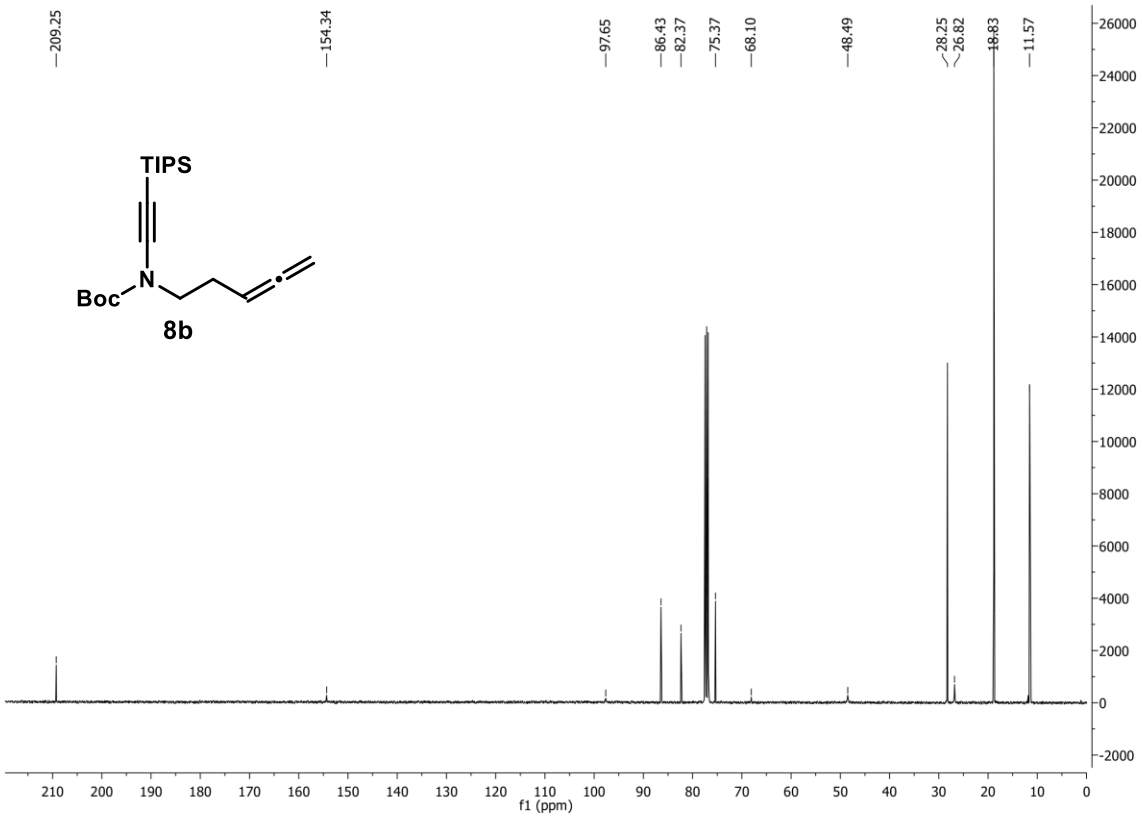
TIPS
N
Boc
8b
209.25
154.34
97.65
86.43
82.37
75.37
68.10
48.49
28.25
26.82
18.83
11.57
f1 (ppm)

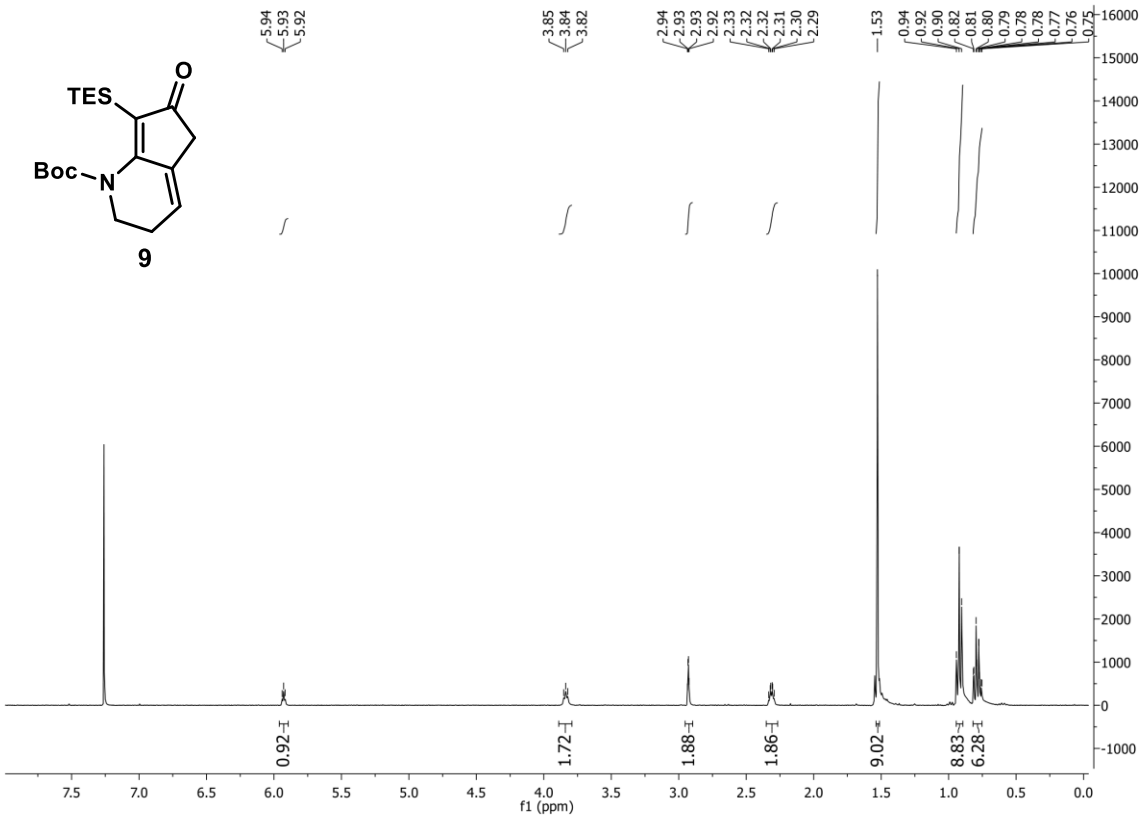
TES
O
Boc
N
9
5.94
5.93
5.92
3.85
3.84
3.82
2.94
2.93
2.93
2.92
2.33
2.32
2.32
2.31
2.30
2.29
1.53
0.94
0.92
0.90
0.82
0.81
0.80
0.79
0.78
0.78
0.77
0.76
0.75
0.92
1.72
1.88
1.86
9.02
8.83
6.28
f1 (ppm)

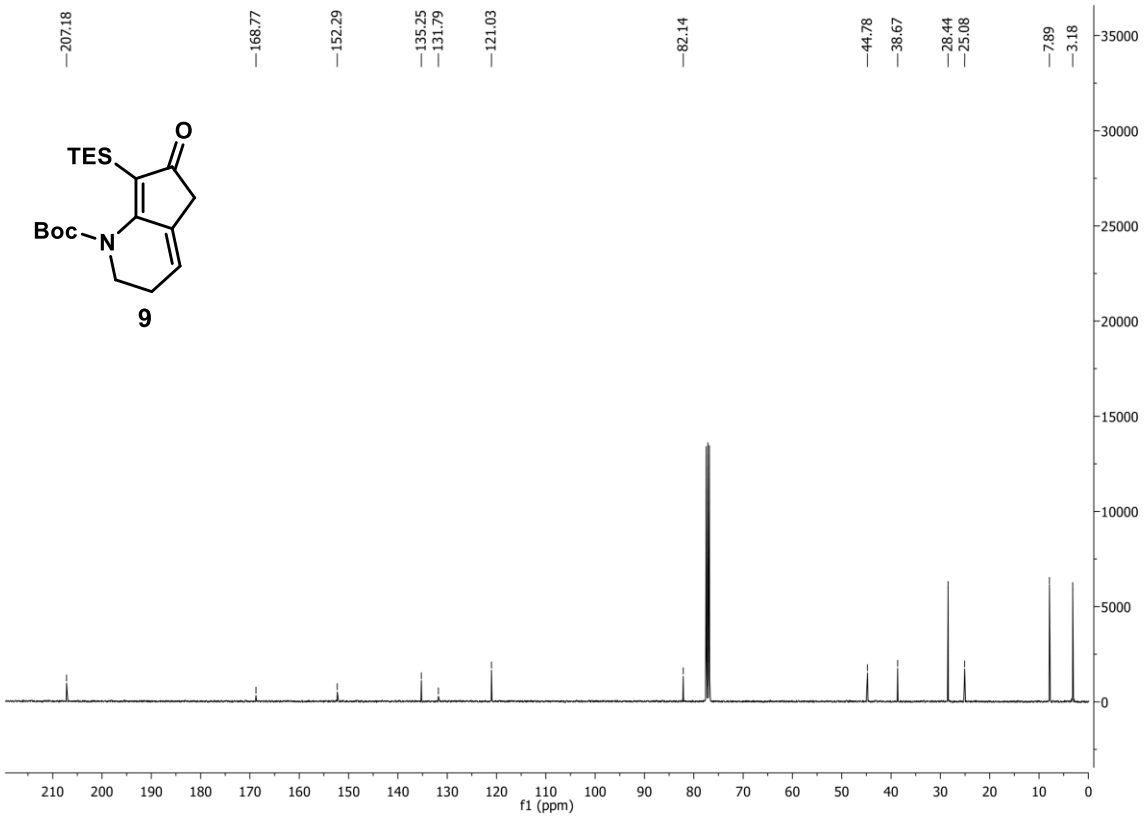
TES
O
Boc
N
9
207.18
168.77
152.29
135.25
131.79
121.03
82.14
44.78
38.67
28.44
25.08
7.89
3.18
f1 (ppm)

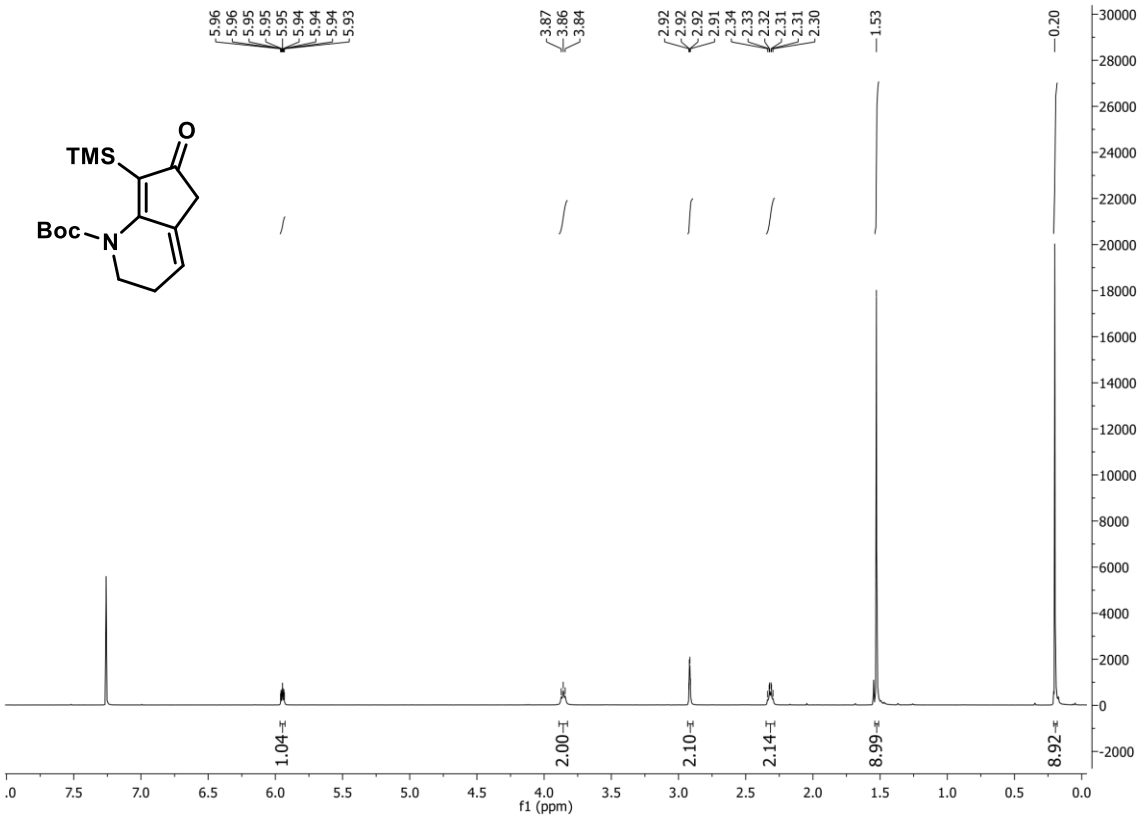
TMS
O
Boc
N
5.96
5.96
5.95
5.95
5.95
5.94
5.94
5.94
5.93
3.87
3.86
3.84
2.92
2.92
2.92
2.91
2.34
2.33
2.32
2.31
2.31
2.30
1.53
0.20
1.04
2.00
2.10
2.14
8.99
8.92
f1 (ppm)

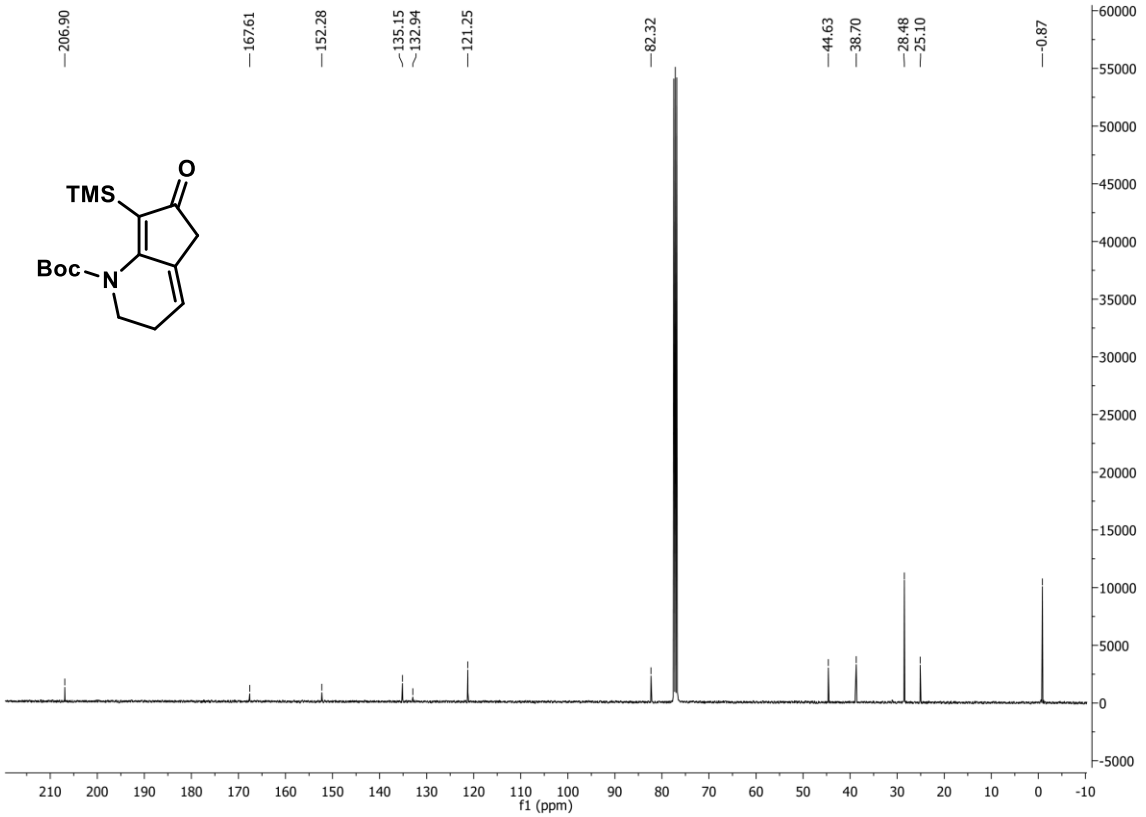
TMS
O
Boc
N
206.90
167.61
152.28
135.15
132.94
121.25
82.32
44.63
38.70
28.48
25.10
0.87
f1 (ppm)

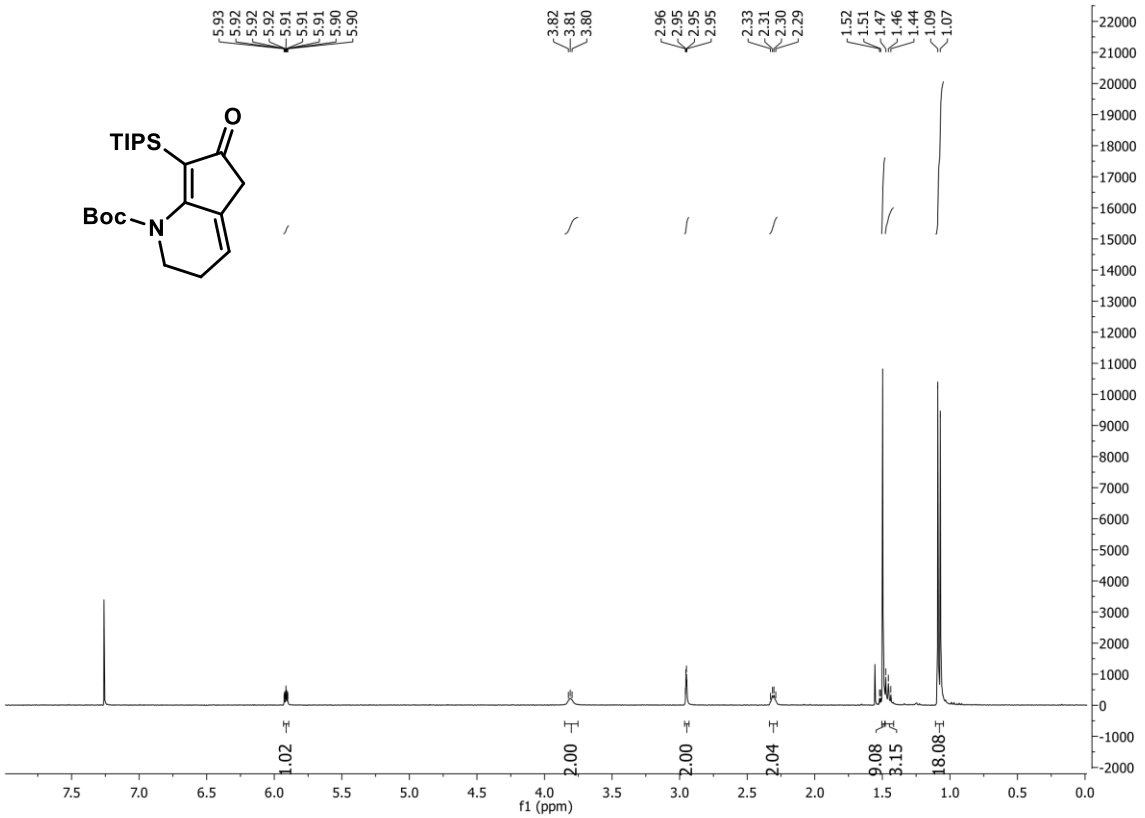
5.93
5.92
5.92
5.92
5.91
5.91
5.91
5.90
5.90
3.82
3.81
3.80
2.96
2.95
2.95
2.95
2.33
2.31
2.30
2.29
1.52
1.51
1.47
1.46
1.44
1.09
1.07
TIPS
O
Boc
N
1.02
2.00
2.00
2.04
9.08
3.15
18.08
f1 (ppm)

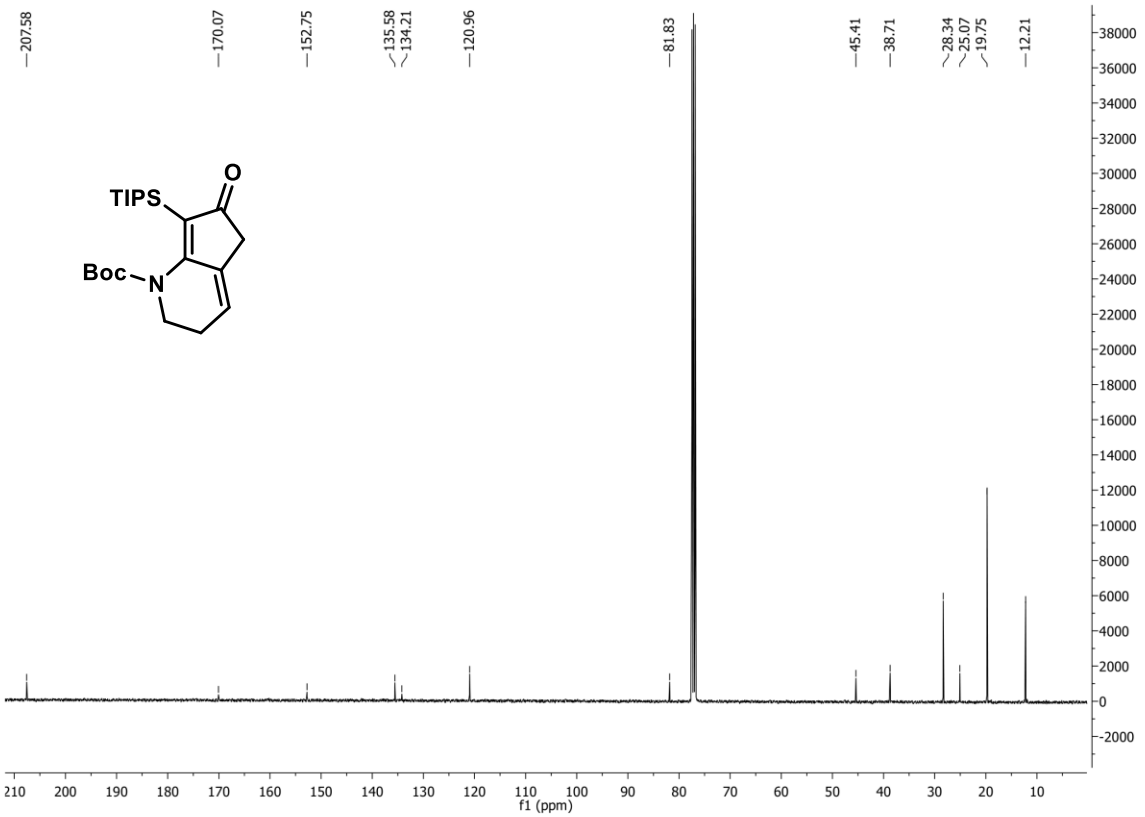
207.58
170.07
152.75
135.58
134.21
120.96
81.83
45.41
38.71
28.34
25.07
19.75
12.21
TIPS
O
Boc
N
f1 (ppm)

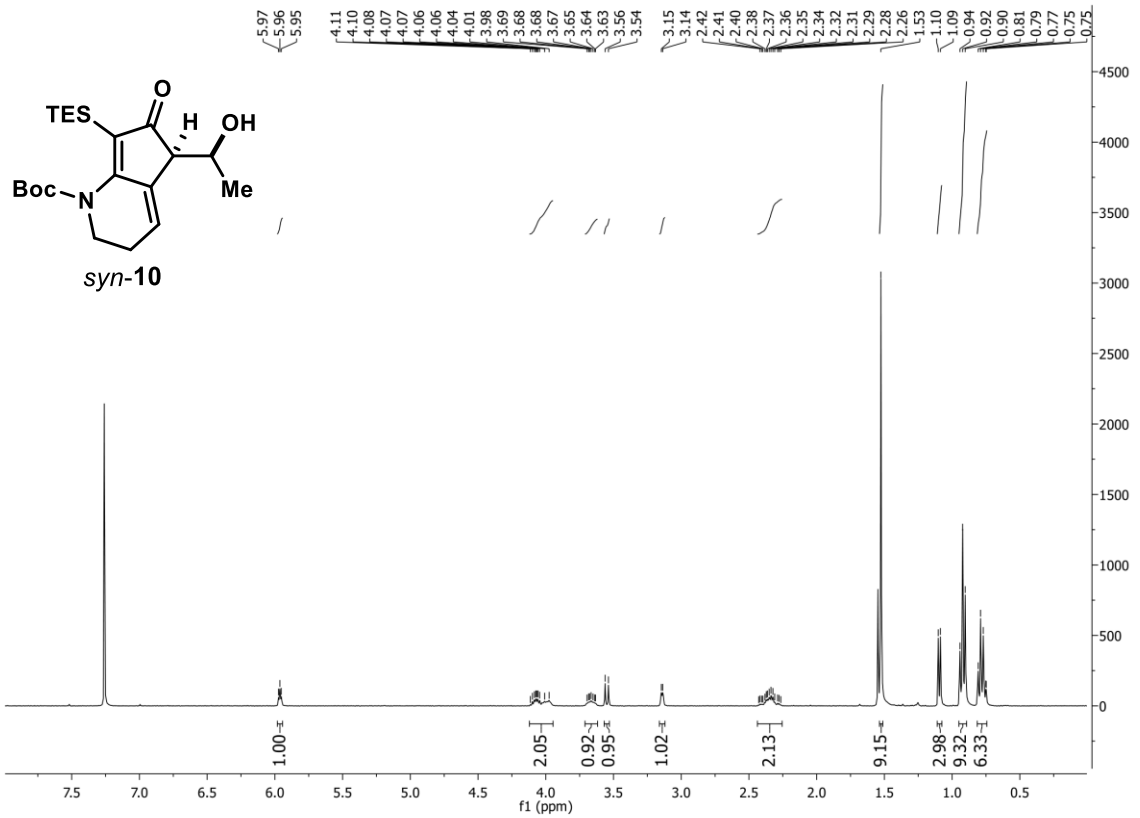
TES
O
H
OH
Boc
N
Me
syn-10
5.97 5.96 5.95 4.11 4.10 4.08 4.07 4.07 4.06 4.06 4.04 4.01 3.98 3.69 3.68 3.68 3.67 3.65 3.64 3.63 3.56 3.54 3.15 3.14 2.42 2.41 2.40 2.38 2.37 2.36 2.35 2.34 2.32 2.31 2.29 2.28 2.26 1.53 1.10 1.09 0.94 0.92 0.90 0.81 0.79 0.77 0.75 0.75
1.00 2.05 0.92 0.95 1.02 2.13 9.15 2.98 9.32 6.33
f1 (ppm)

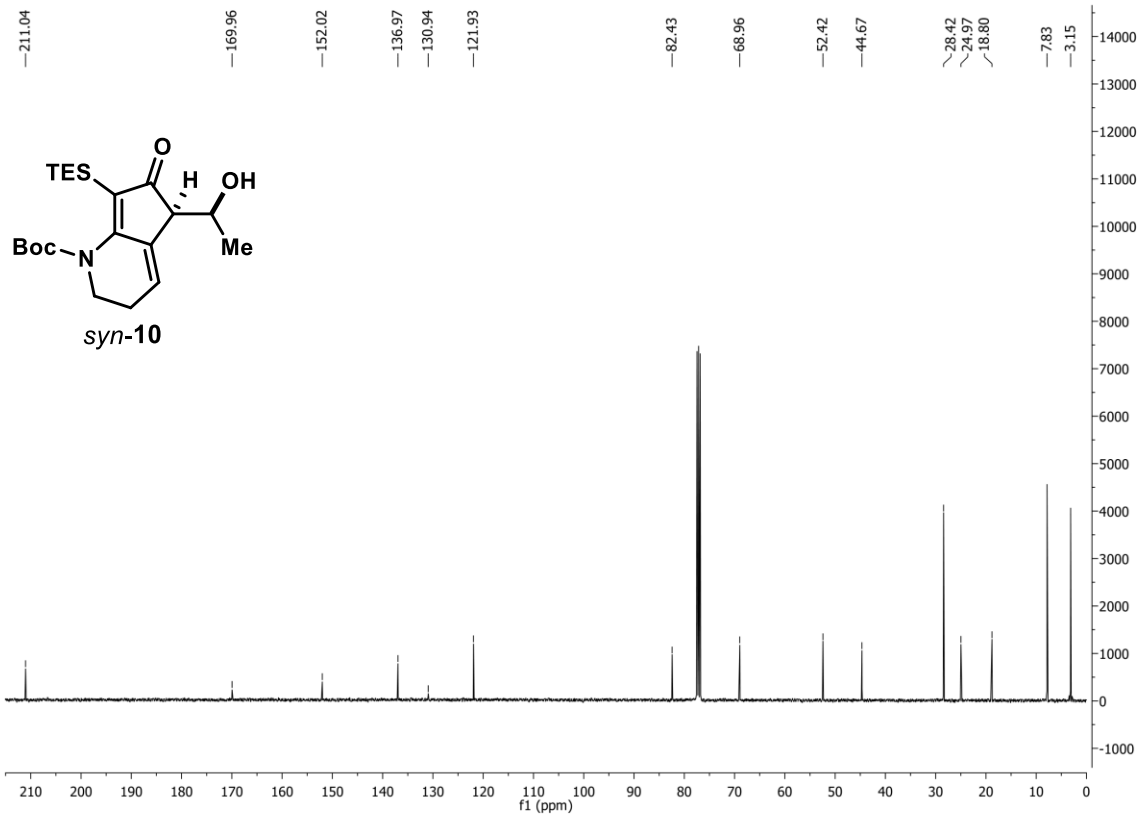
TES
O
H
OH
Boc
N
Me
syn-10
211.04 169.96 152.02 136.97 130.94 121.93 82.43 68.96 52.42 44.67 28.42 24.97 18.80 7.83 3.15
f1 (ppm)

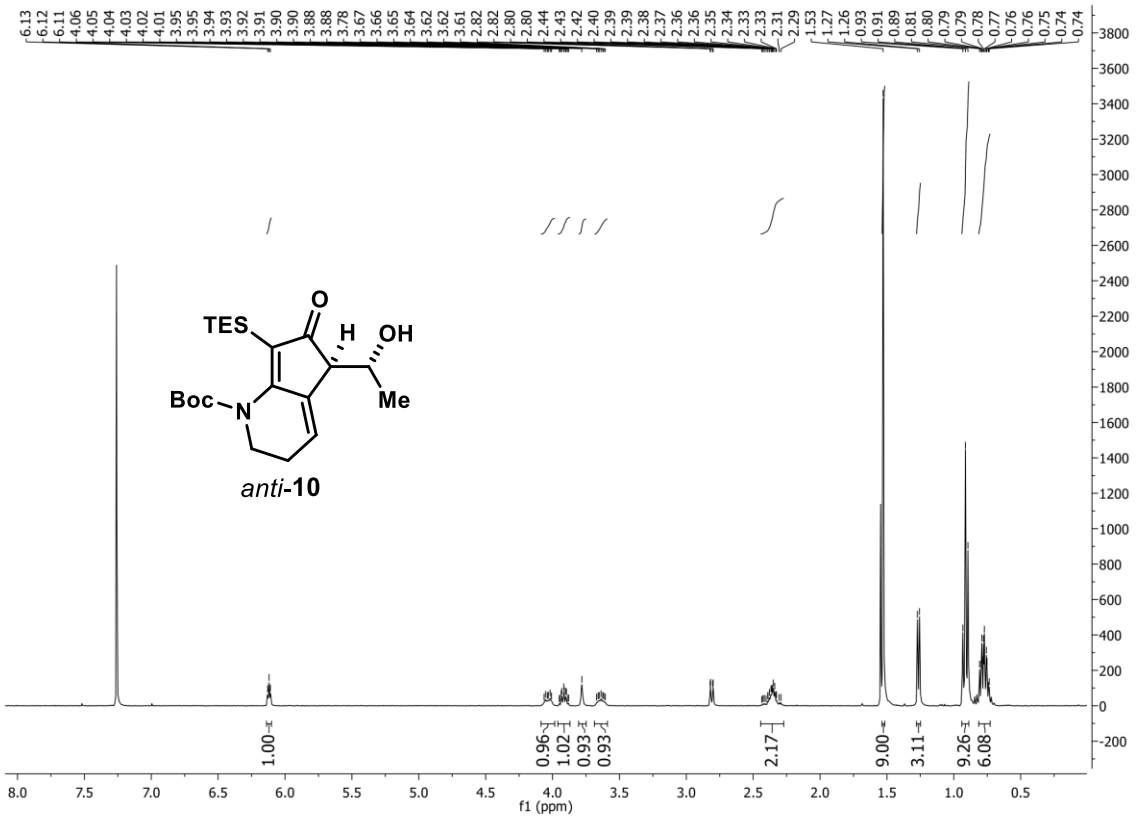
TES
O
H
OH
Boc
N
Me
anti-10
f1 (ppm)

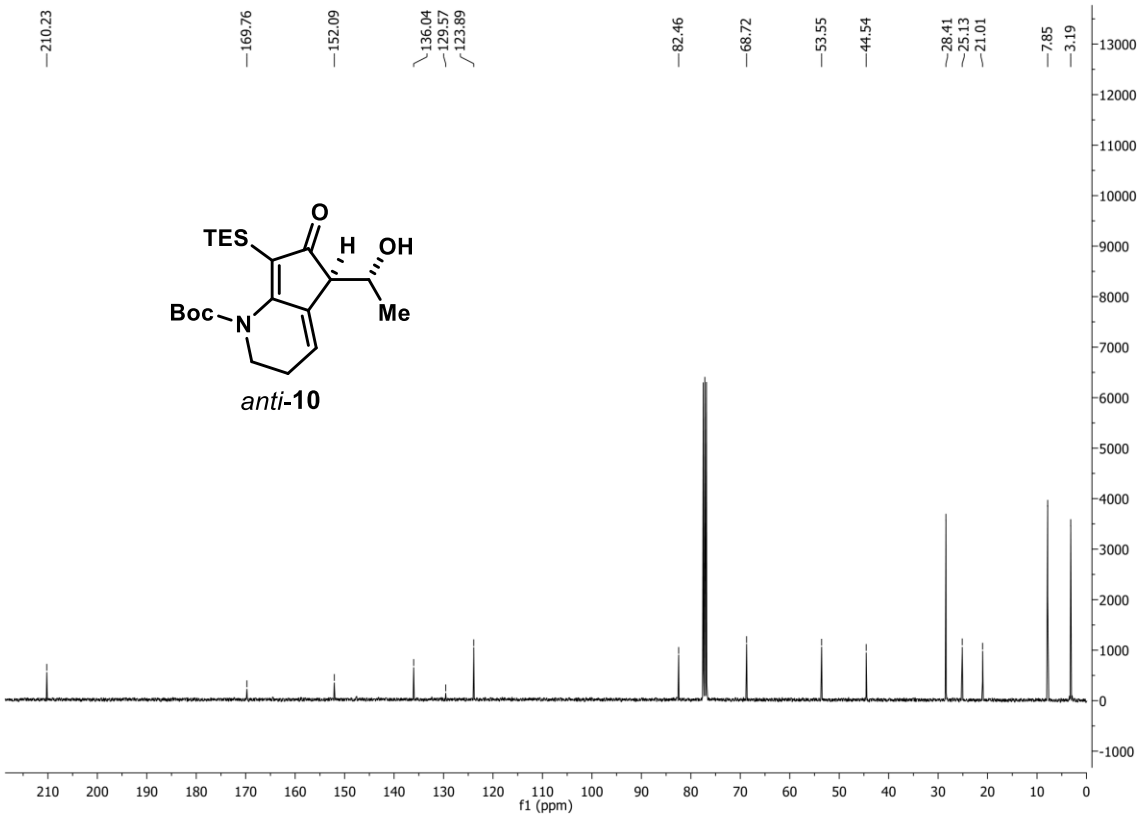
TES
O
H
OH
Boc
N
Me
anti-10
f1 (ppm)

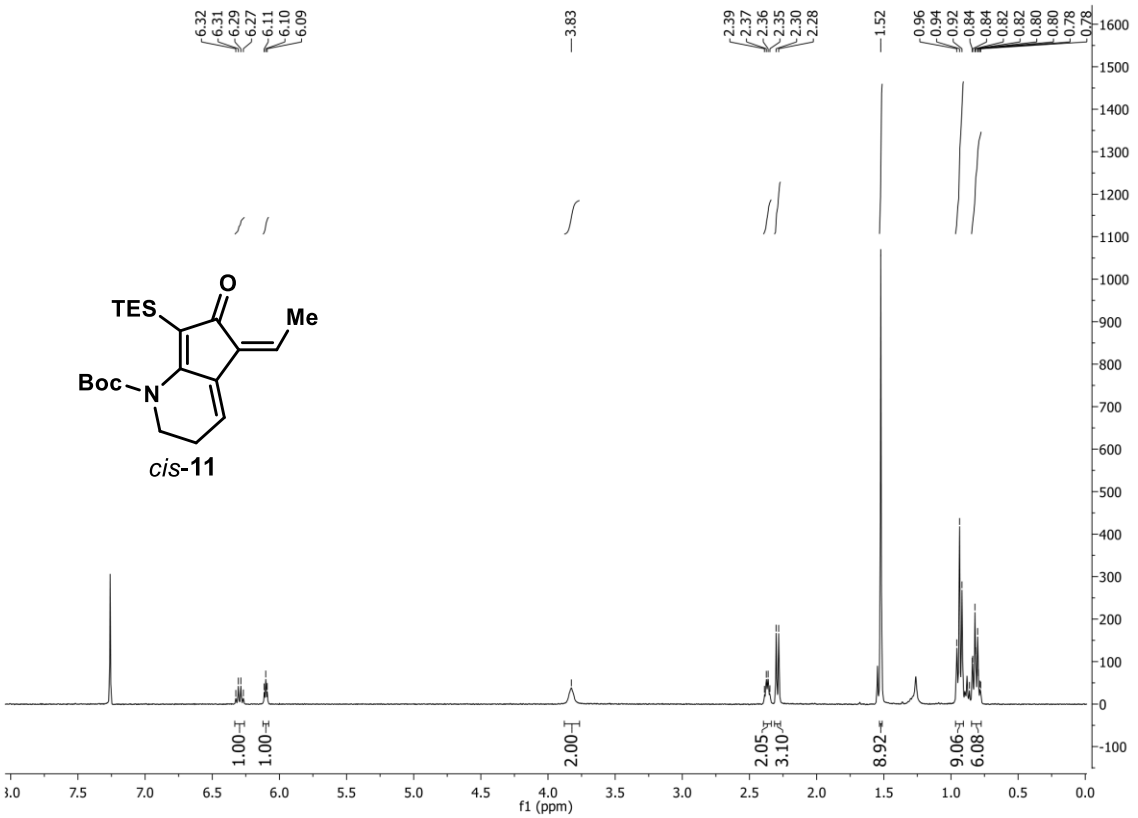
6.32
6.31
6.29
6.27
6.11
6.10
6.09
3.83
2.39
2.37
2.36
2.35
2.30
2.28
1.52
0.96
0.94
0.92
0.84
0.84
0.82
0.82
0.80
0.80
0.78
0.78
TES
O
Me
Boc
N
cis-11
1.00
1.00
2.00
2.05
3.10
8.92
9.06
6.08
f1 (ppm)

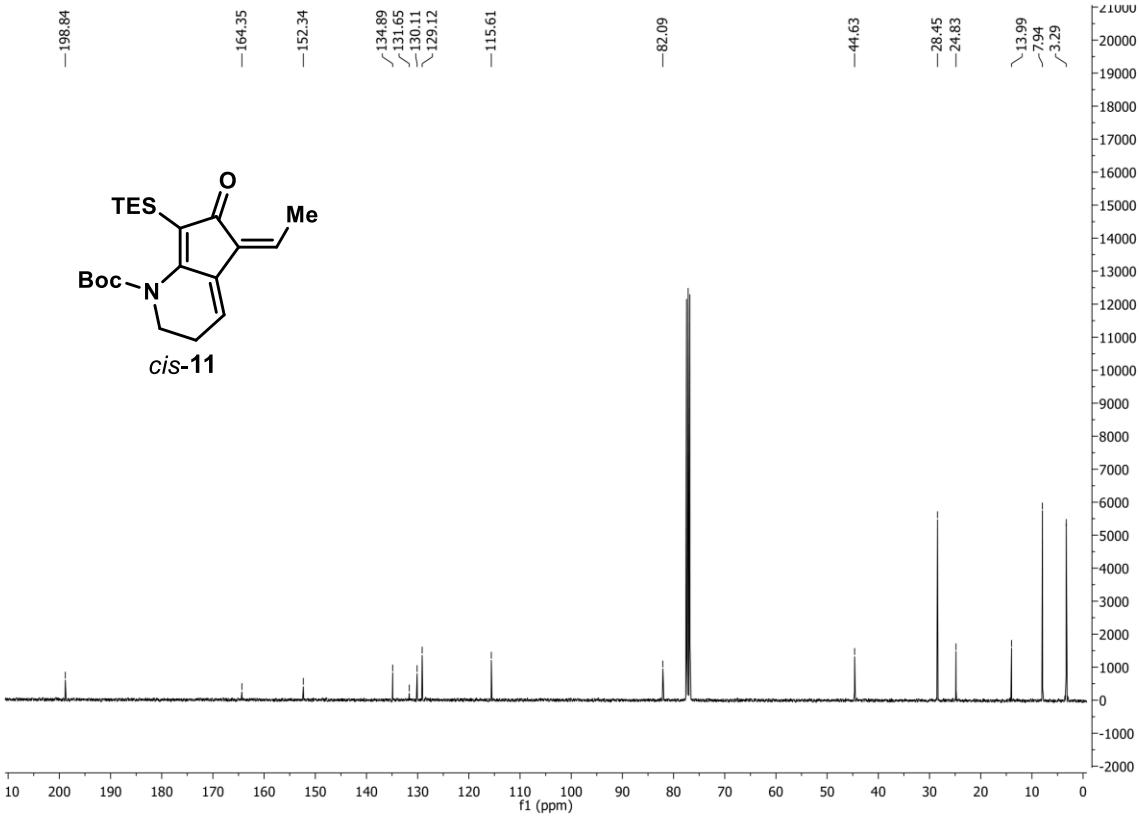
198.84
164.35
152.34
134.89
131.65
130.11
129.12
115.61
82.09
44.63
28.45
24.83
13.99
7.94
3.29
TES
O
Me
Boc
N
cis-11
f1 (ppm)

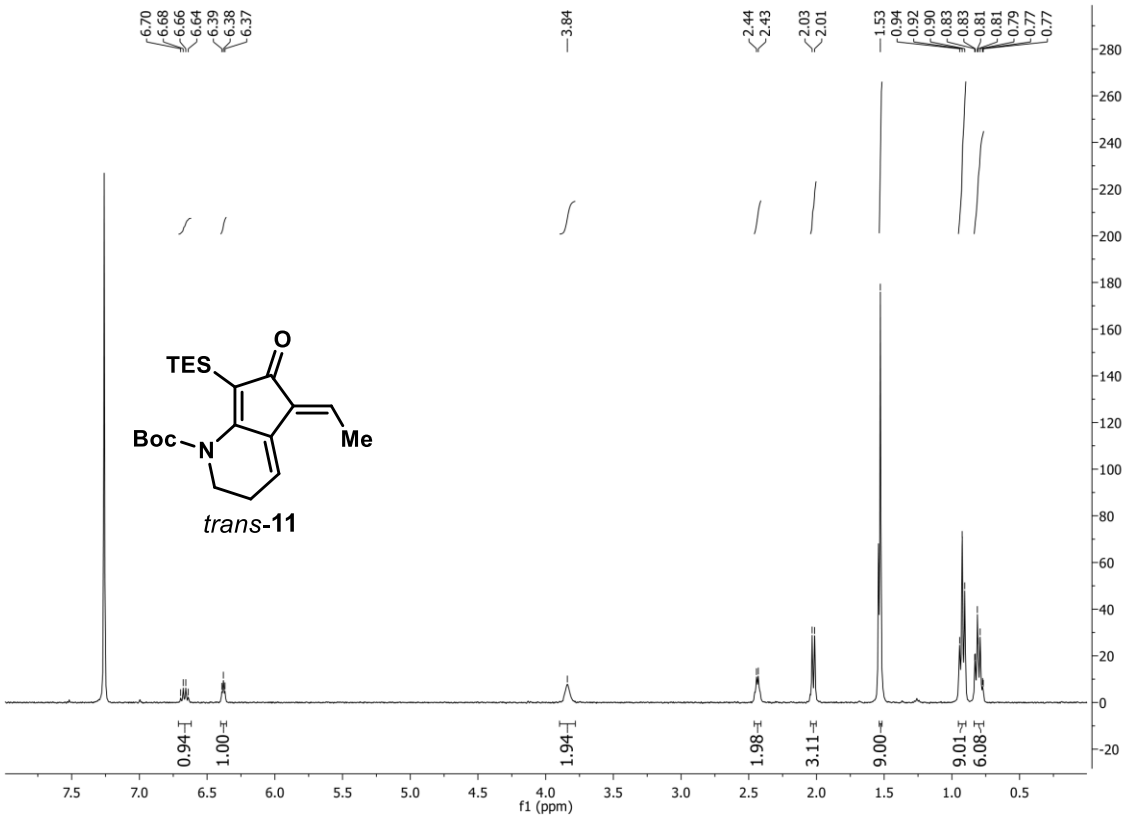
6.70
6.68
6.66
6.64
6.39
6.38
6.37
3.84
2.44
2.43
2.03
2.01
1.53
0.94
0.92
0.90
0.83
0.81
0.81
0.79
0.77
0.77
TES
O
Boc
N
Me
trans-11
0.94
1.00
1.94
1.98
3.11
9.00
9.01
6.08
f1 (ppm)

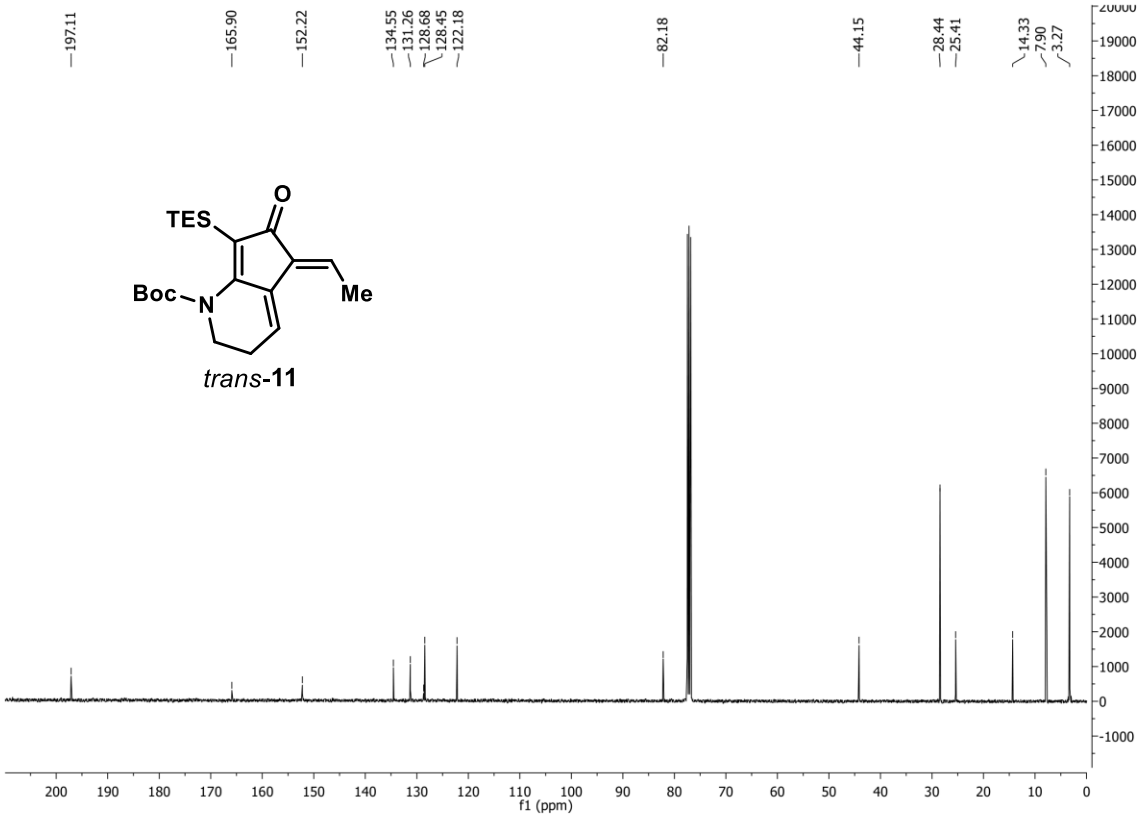
197.11
165.90
152.22
134.55
131.26
128.68
128.45
122.18
82.18
44.15
28.44
25.41
14.33
7.90
3.27
TES
O
Boc
N
Me
trans-11
f1 (ppm)

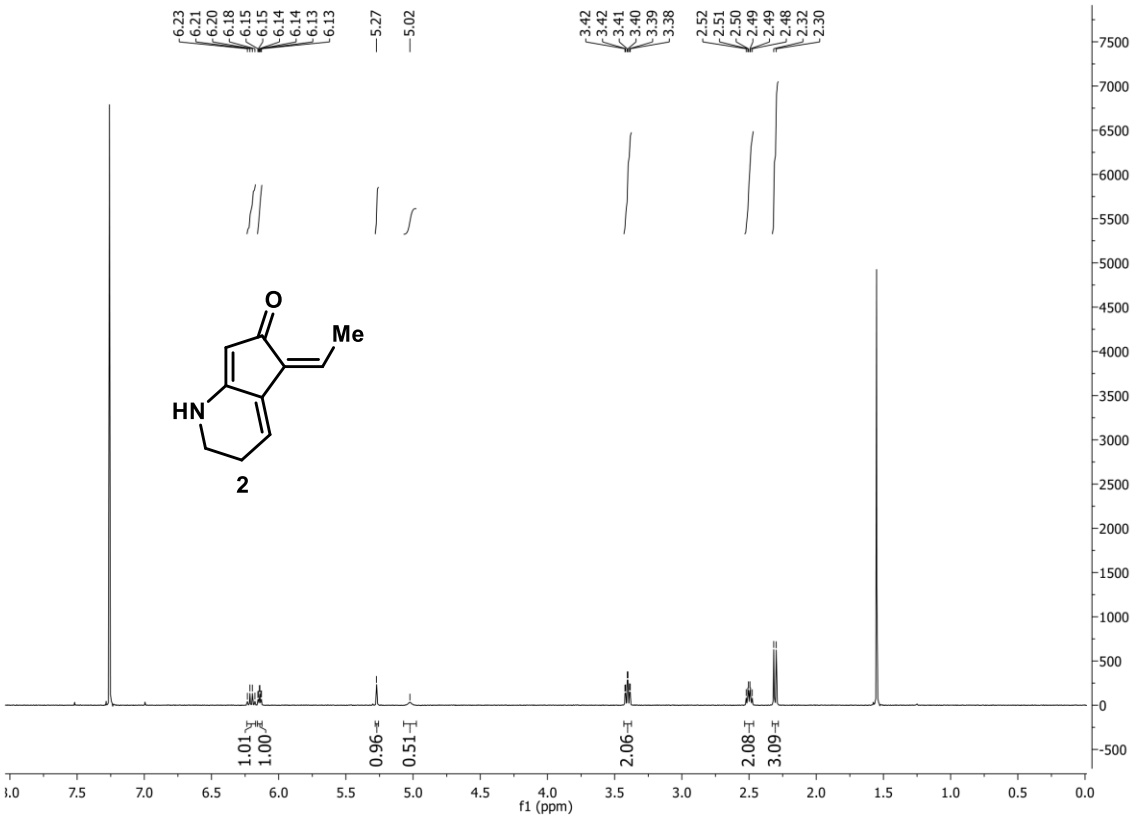
6.23
6.21
6.20
6.18
6.15
6.15
6.14
6.14
6.13
6.13
5.27
5.02
3.42
3.42
3.41
3.40
3.39
3.38
2.52
2.51
2.50
2.49
2.49
2.48
2.32
2.30
O
Me
HN
2
1.01
1.00
0.96
0.51
2.06
2.08
3.09
f1 (ppm)

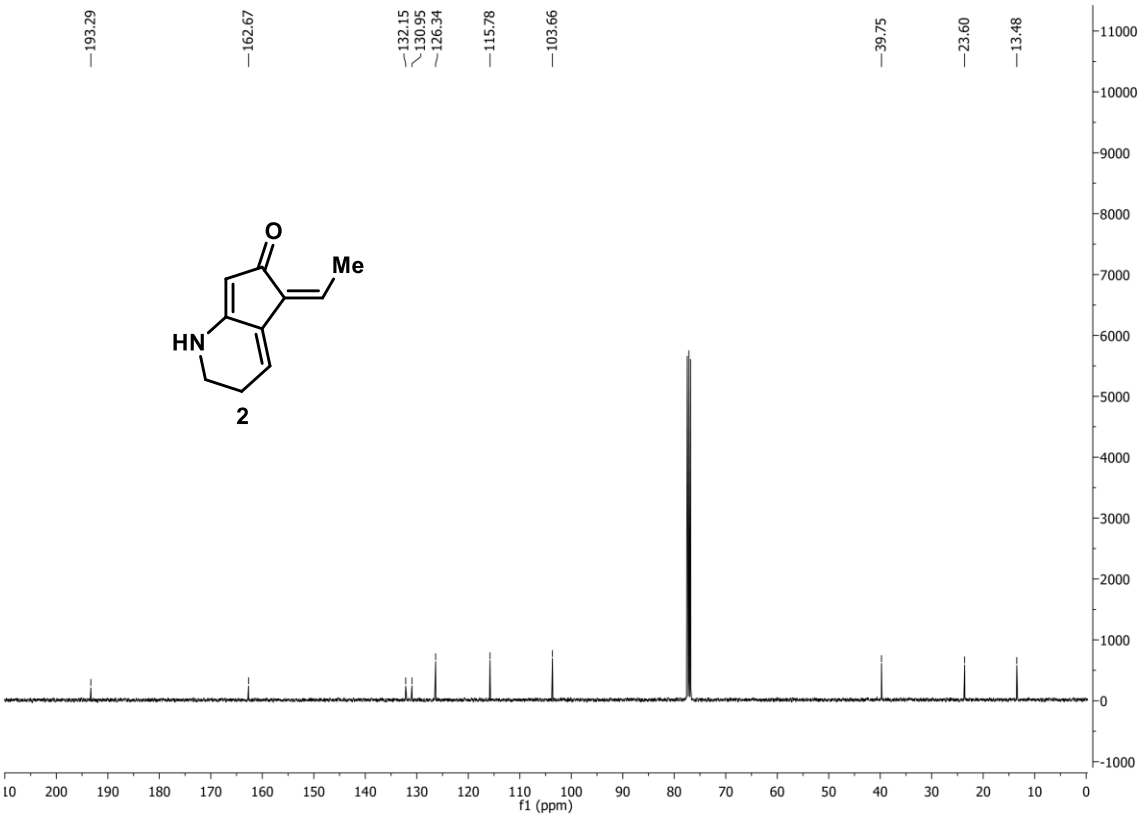
193.29
162.67
132.15
130.95
126.34
115.78
103.66
39.75
23.60
13.48
O
Me
HN
2
f1 (ppm)


6.57
6.55
6.53
6.52
6.41
6.40
6.40
6.39
6.39
5.23
5.23
3.46
3.45
3.44
3.43
3.42
3.42
2.60
2.58
2.58
2.57
2.56
2.55
2.03
2.02
O
HN
Me
2'
1.00
1.03
1.68
2.13
2.12
3.15
f1 (ppm)

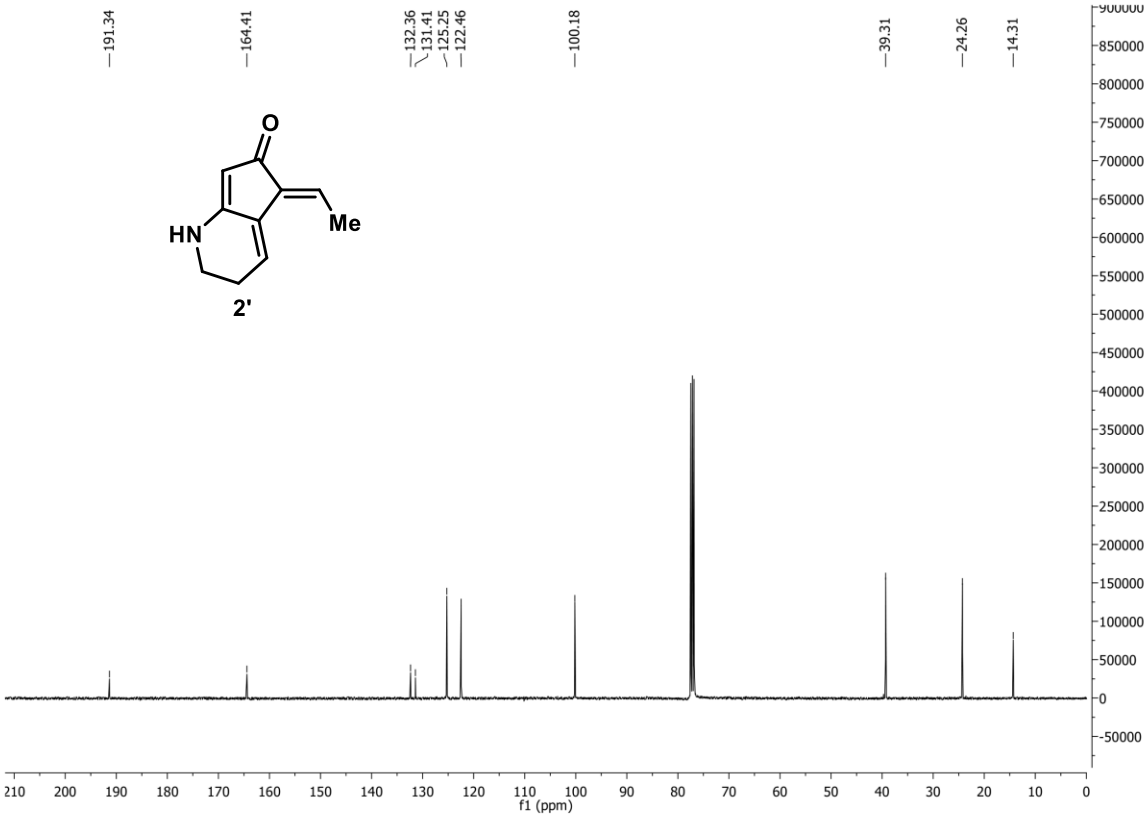
191.34
164.41
132.36
131.41
125.25
122.46
100.18
39.31
24.26
14.31
O
HN
Me
2'
f1 (ppm)

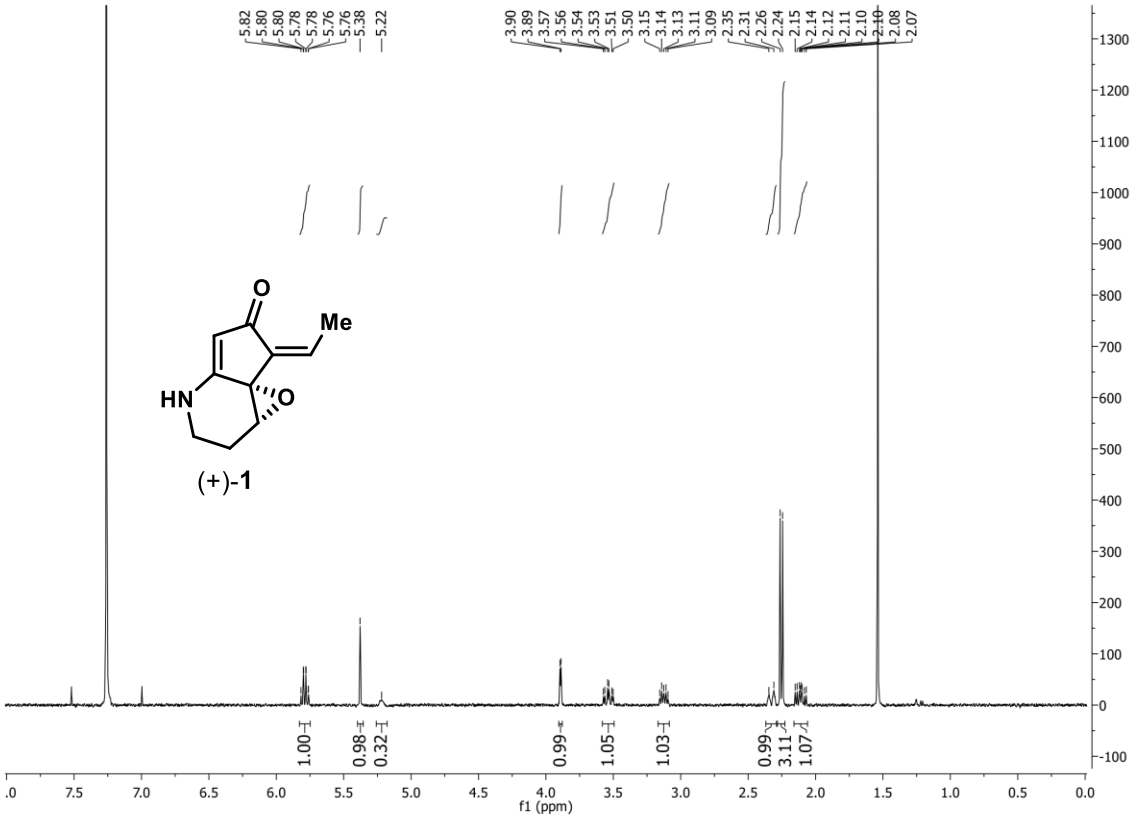
5.82
5.80
5.80
5.78
5.78
5.76
5.76
5.38
5.22
3.90
3.89
3.57
3.56
3.54
3.53
3.51
3.50
3.15
3.14
3.13
3.11
3.09
2.35
2.31
2.26
2.24
2.15
2.14
2.12
2.11
2.10
2.10
2.08
2.07
O
Me
HN
O
(+)-1
1.00
0.98
0.32
0.99
1.05
1.03
0.99
3.11
1.07
f1 (ppm)

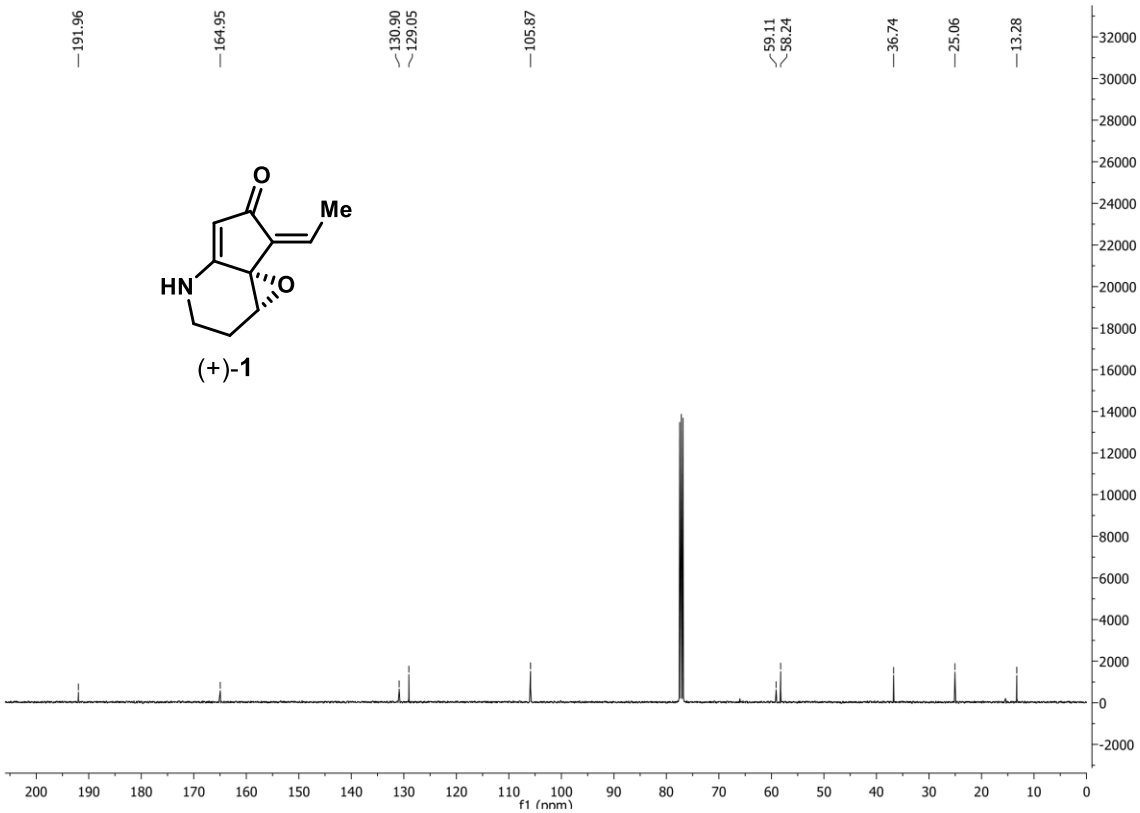
191.96
164.95
130.90
129.05
105.87
59.11
58.24
36.74
25.06
13.28
O
Me
HN
O
(+)-1
f1 (ppm)

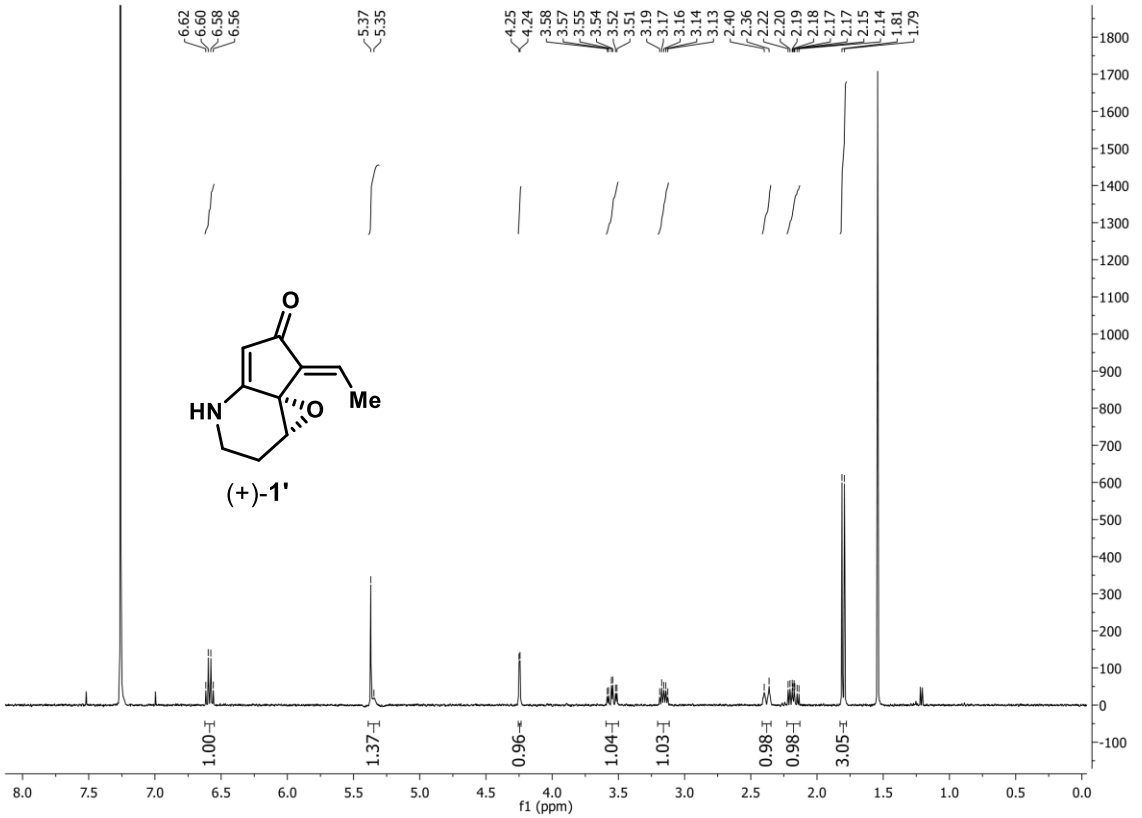
6.62
6.60
6.58
6.56
5.37
5.35
4.25
4.24
3.58
3.57
3.55
3.54
3.52
3.51
3.19
3.17
3.16
3.14
3.13
2.40
2.36
2.22
2.20
2.19
2.18
2.17
2.17
2.15
2.14
1.81
1.79
O
HN
O
Me
(+)-1'
1.00
1.37
0.96
1.04
1.03
0.98
0.98
3.05
f1 (ppm)

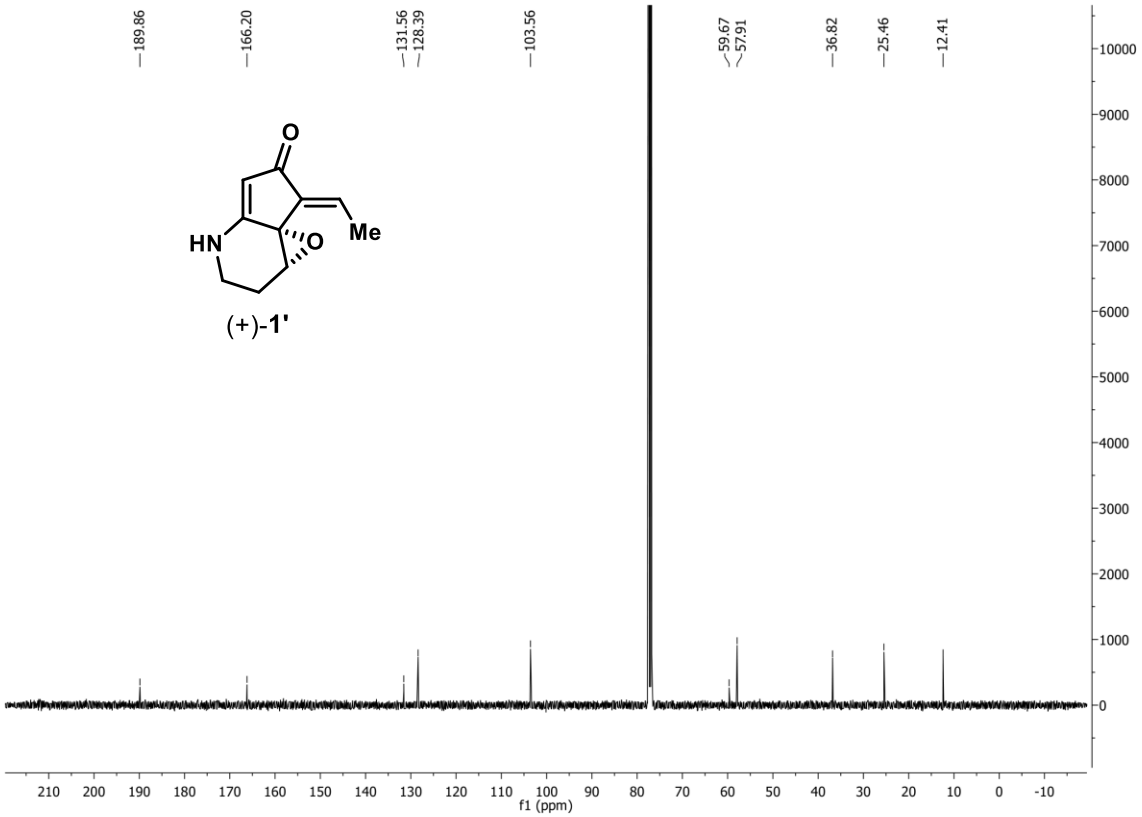
189.86
166.20
131.56
128.39
103.56
59.67
57.91
36.82
25.46
12.41
O
HN
O
Me
(+)-1'
f1 (ppm)

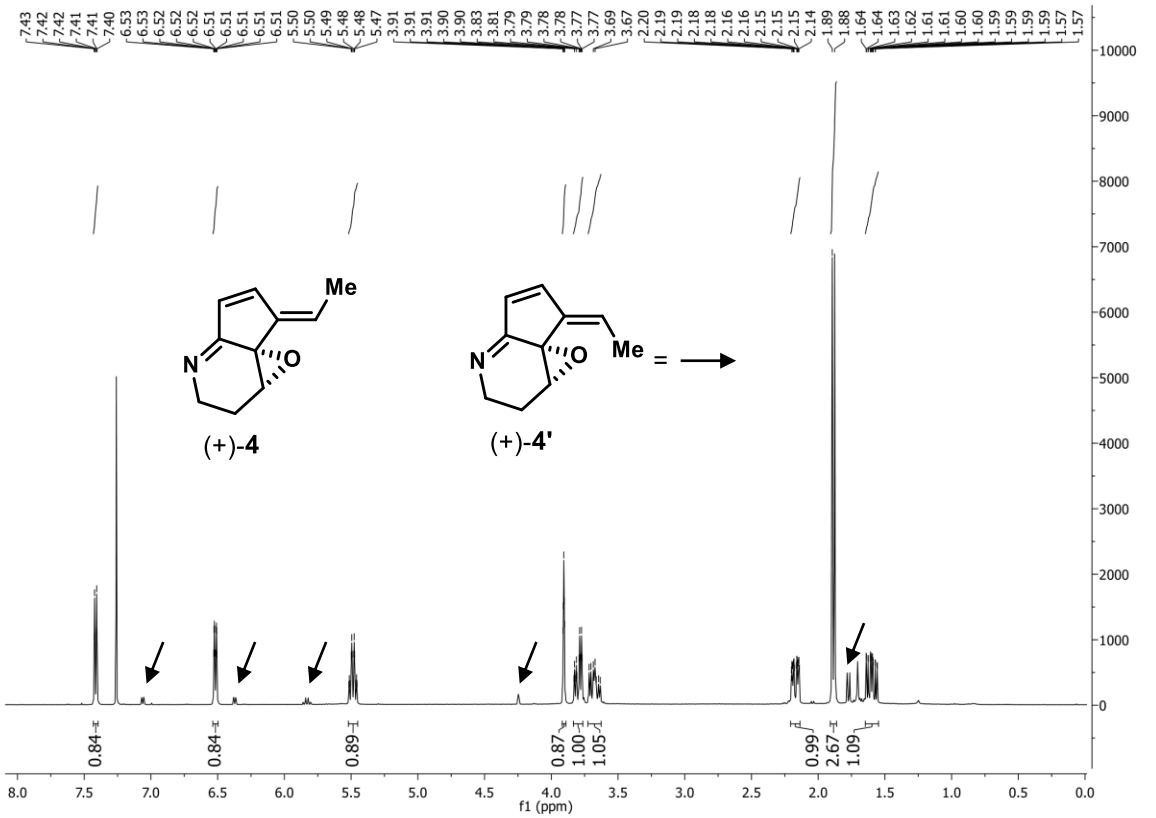
Me
N
O
(+)-4
Me
N
O
Me =
(+)-4'
0.84
0.84
0.89
0.87
1.00
1.05
0.99
2.67
1.09
f1 (ppm)

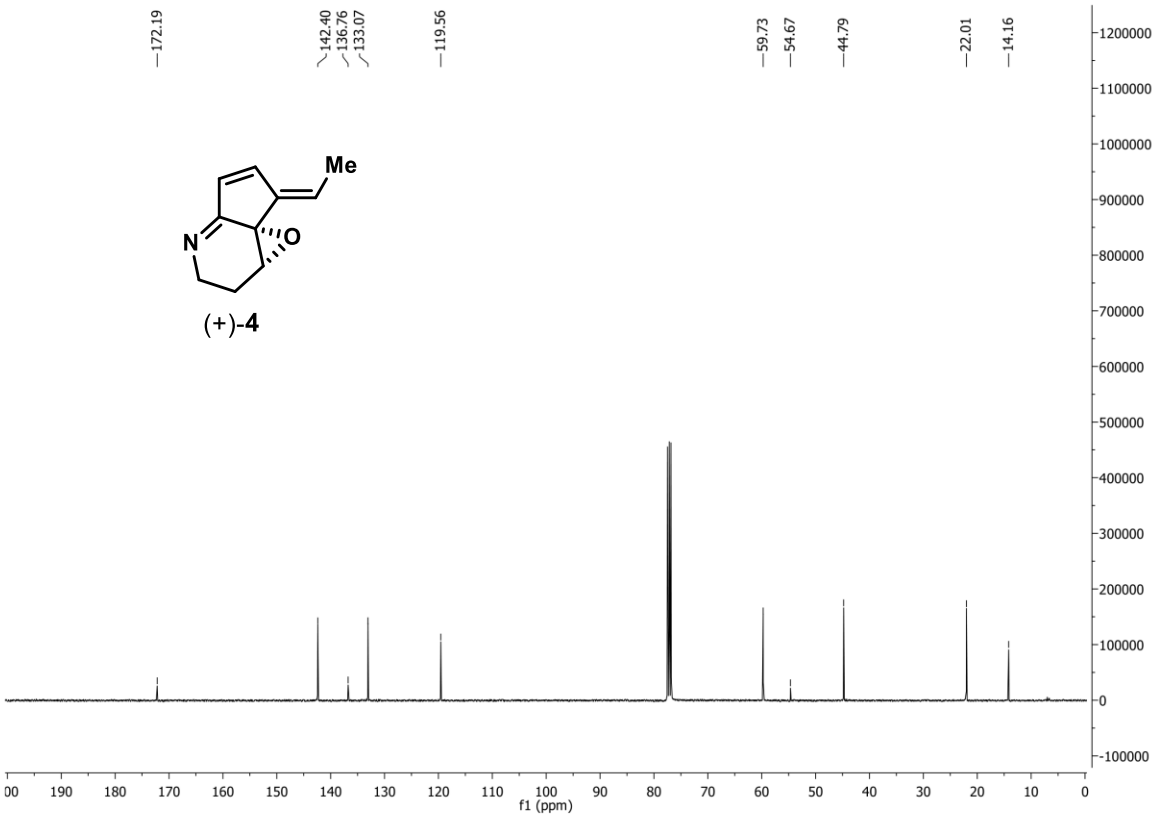
172.19
142.40
136.76
133.07
119.56
59.73
54.67
44.79
22.01
14.16
Me
N
O
(+)-4
f1 (ppm)

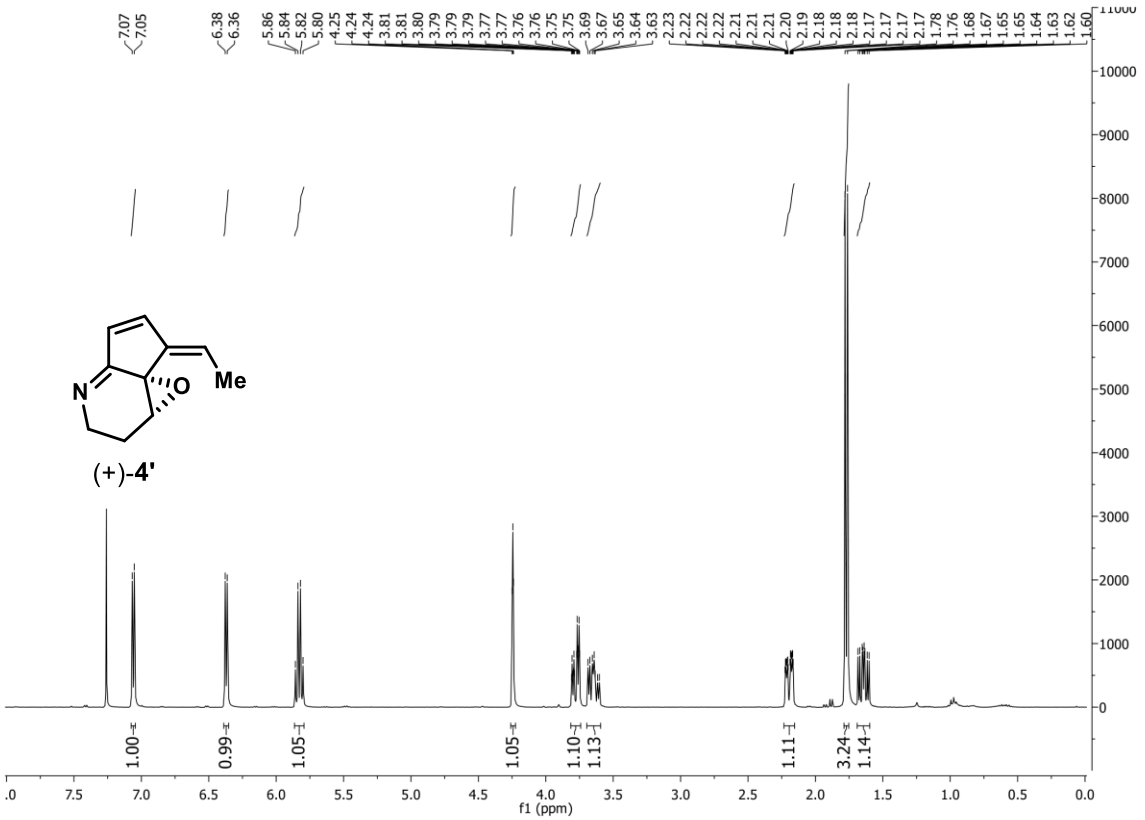
7.07
7.05
6.38
6.36
5.86
5.84
5.82
5.80
4.25
4.24
4.24
3.81
3.81
3.80
3.79
3.79
3.79
3.77
3.77
3.76
3.76
3.75
3.75
3.69
3.67
3.65
3.64
3.63
2.23
2.22
2.22
2.22
2.21
2.21
2.21
2.20
2.19
2.18
2.18
2.18
2.17
2.17
2.17
2.17
1.78
1.76
1.68
1.67
1.65
1.65
1.64
1.63
1.62
1.60
N
O
Me
(+)-4'
1.00
0.99
1.05
1.05
1.10
1.13
1.11
3.24
1.14
f1 (ppm)

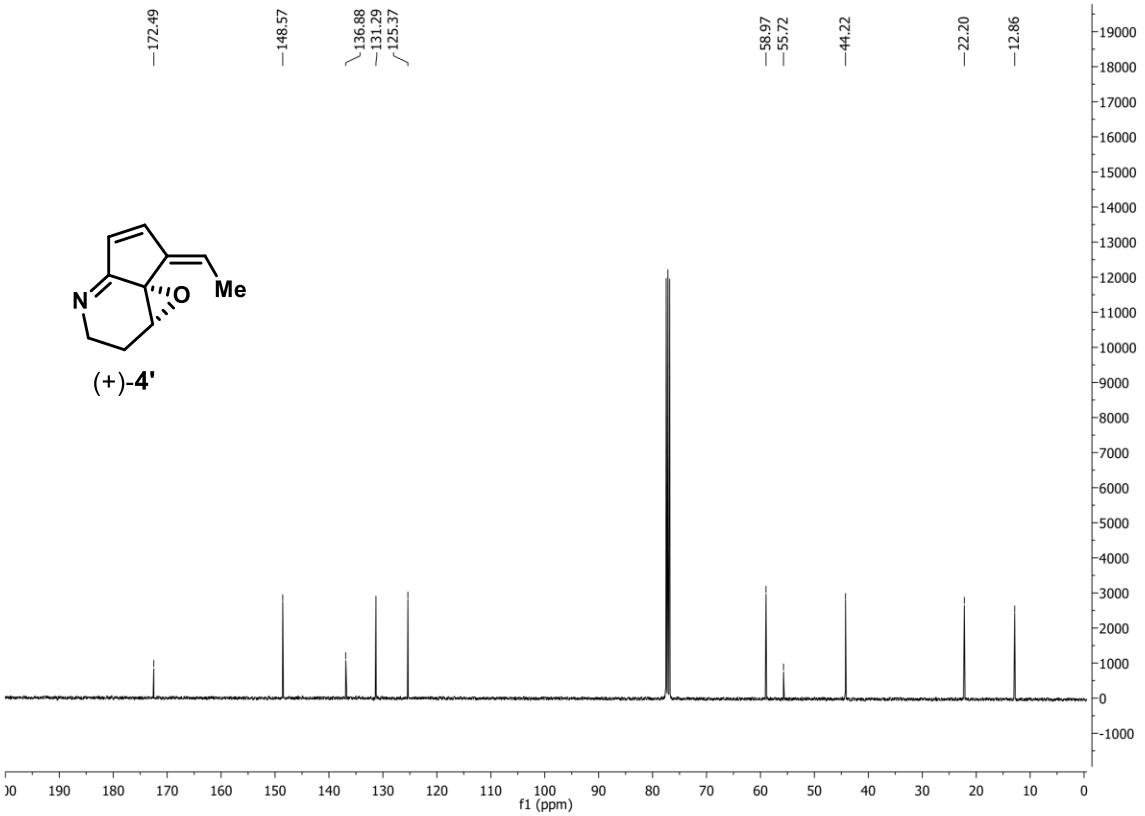
172.49
148.57
136.88
131.29
125.37
58.97
55.72
44.22
22.20
12.86
N
O
Me
(+)-4'
f1 (ppm)

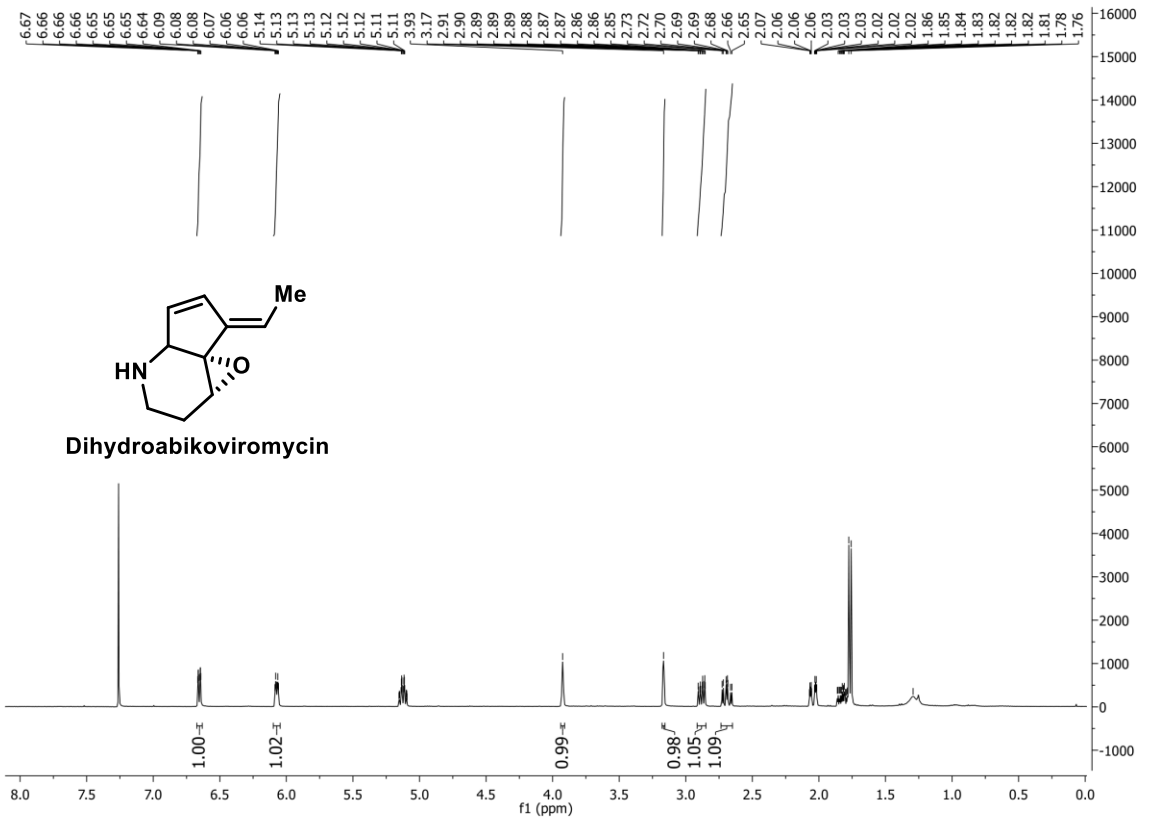
Me
HN
O
Dihydroabikoviromycin
f1 (ppm)

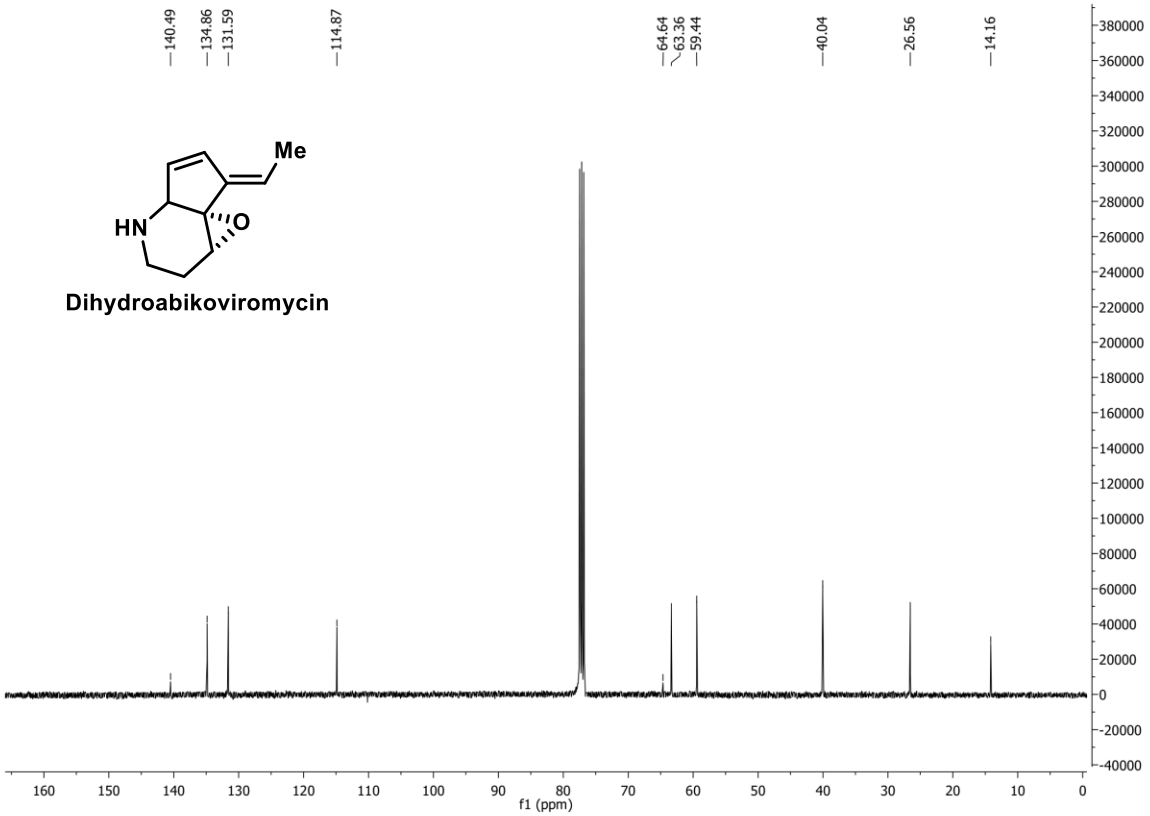
Me
HN
O
Dihydroabikoviromycin
f1 (ppm)

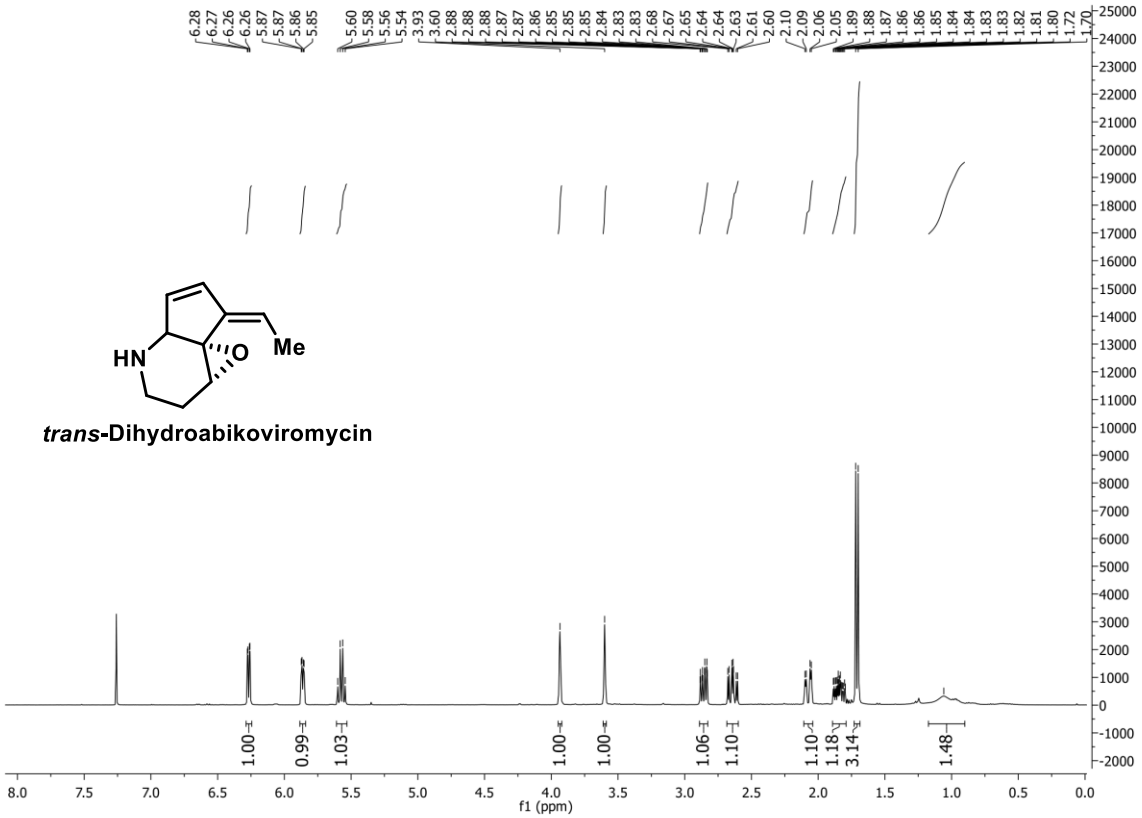
HN
O
Me
trans-Dihydroabikoviromycin
f1 (ppm)

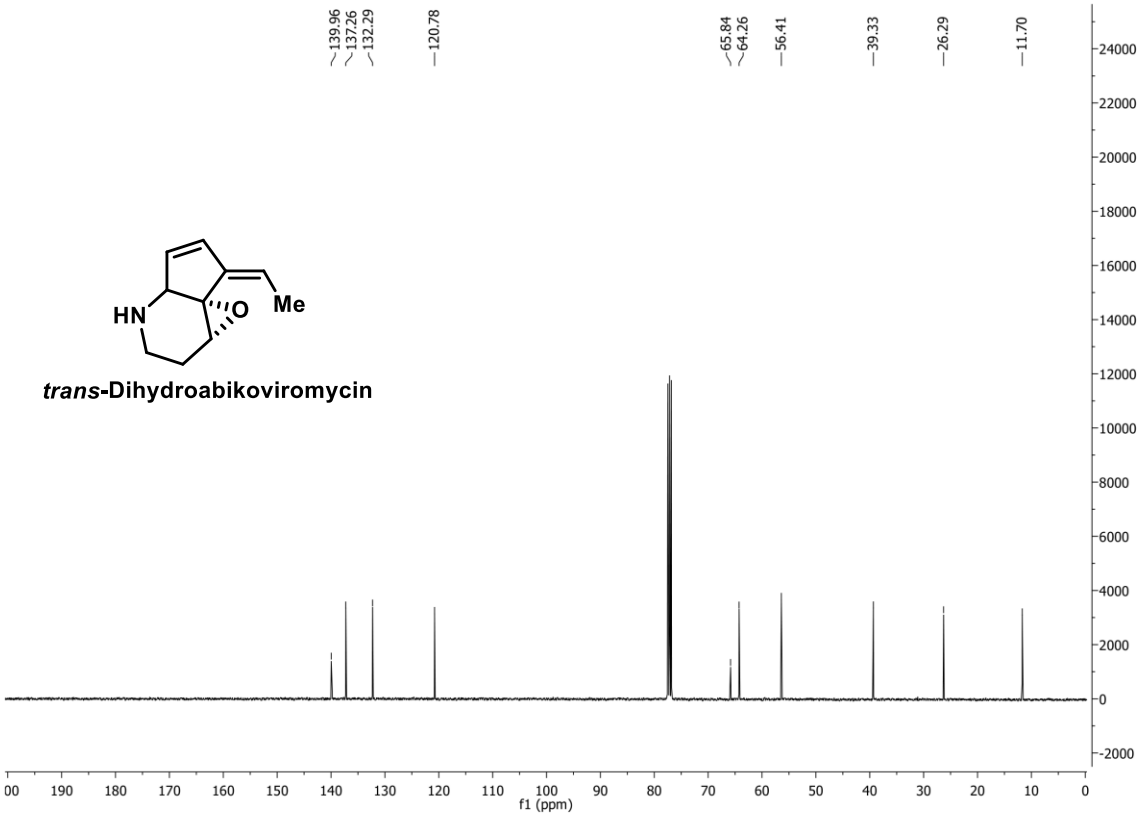
HN
O
Me
trans-Dihydroabikoviromycin
f1 (ppm)

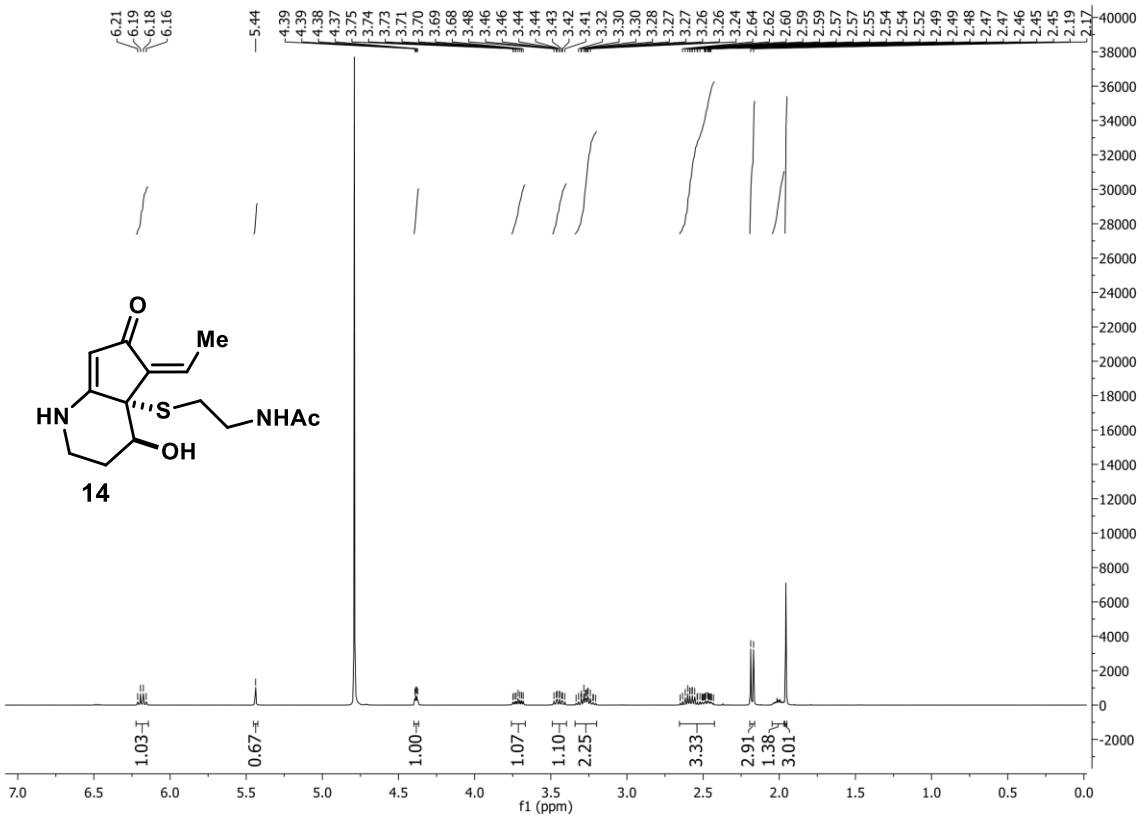
O
Me
HN
S
NHAc
OH
14
6.21
6.19
6.18
6.16
5.44
4.39
4.39
4.38
4.37
3.75
3.74
3.73
3.71
3.70
3.69
3.68
3.48
3.46
3.46
3.44
3.44
3.43
3.42
3.41
3.32
3.30
3.30
3.28
3.27
3.27
3.26
3.26
3.24
2.64
2.62
2.60
2.59
2.59
2.57
2.57
2.55
2.54
2.54
2.52
2.49
2.49
2.48
2.47
2.47
2.46
2.45
2.45
2.19
2.17
1.03
0.67
1.00
1.07
1.10
2.25
3.33
2.91
1.38
3.01
f1 (ppm)

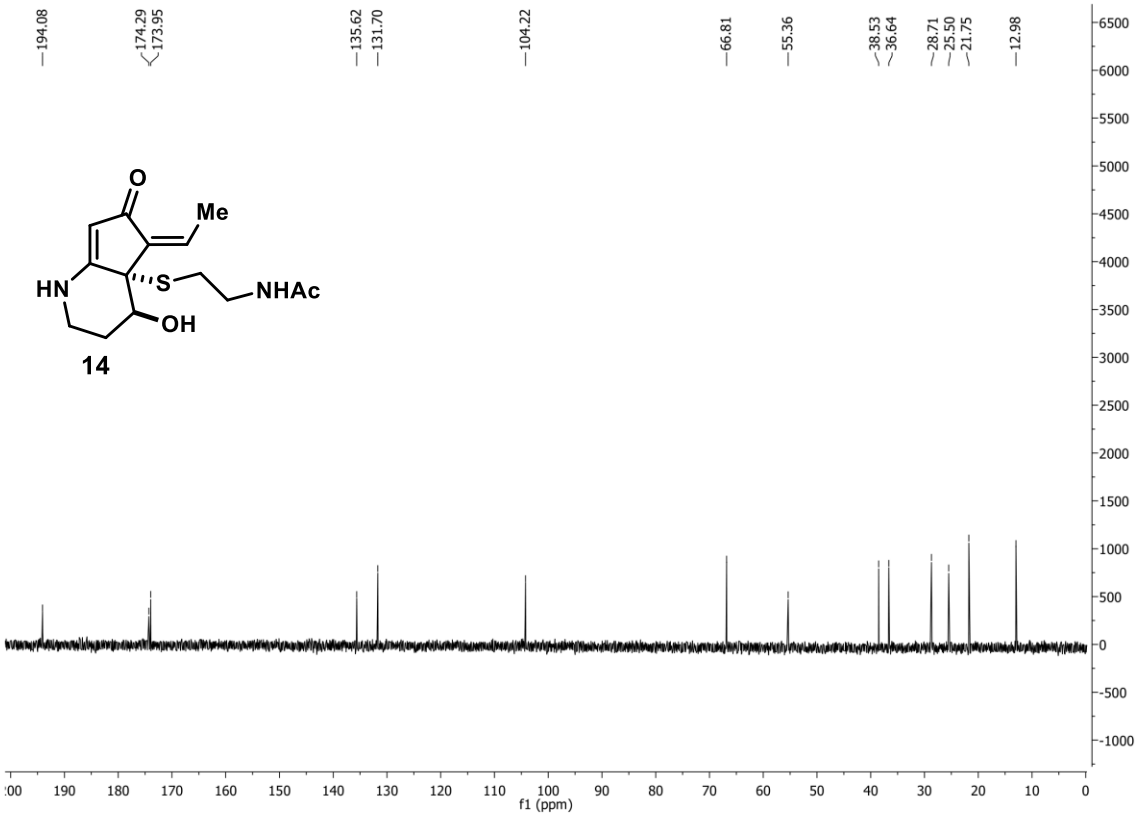
O
Me
HN
S
NHAc
OH
14
194.08
174.29
173.95
135.62
131.70
104.22
66.81
55.36
38.53
36.64
28.71
25.50
21.75
12.98
f1 (ppm)

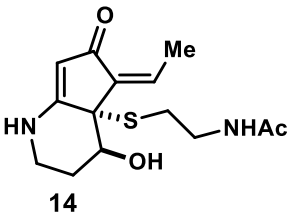

14

^{1}H-^{1}H COSY

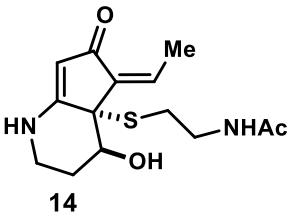

14

^{1}H-^{13}C HSQC

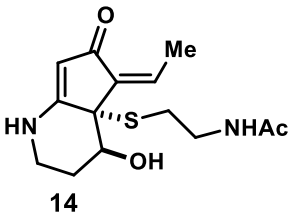

14

^{1}H-^{13}C HMBC

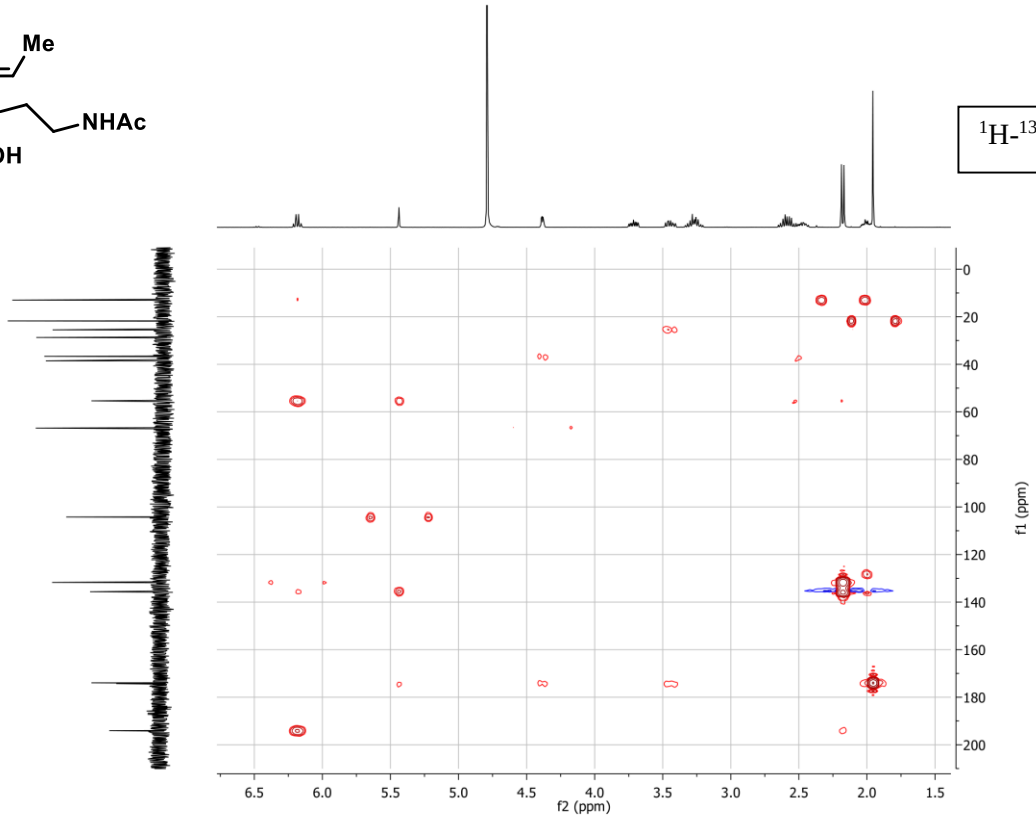

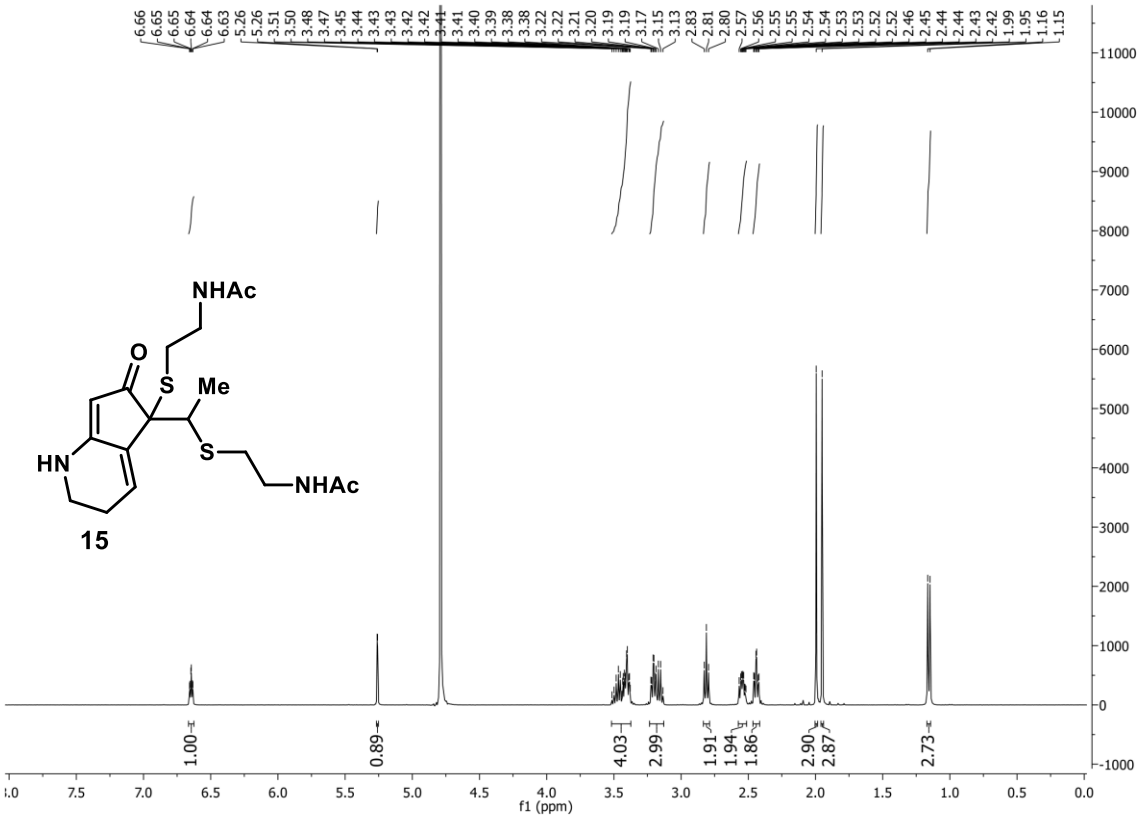
NHAc
O
S
Me
HN
S
NHAc
15
f1 (ppm)

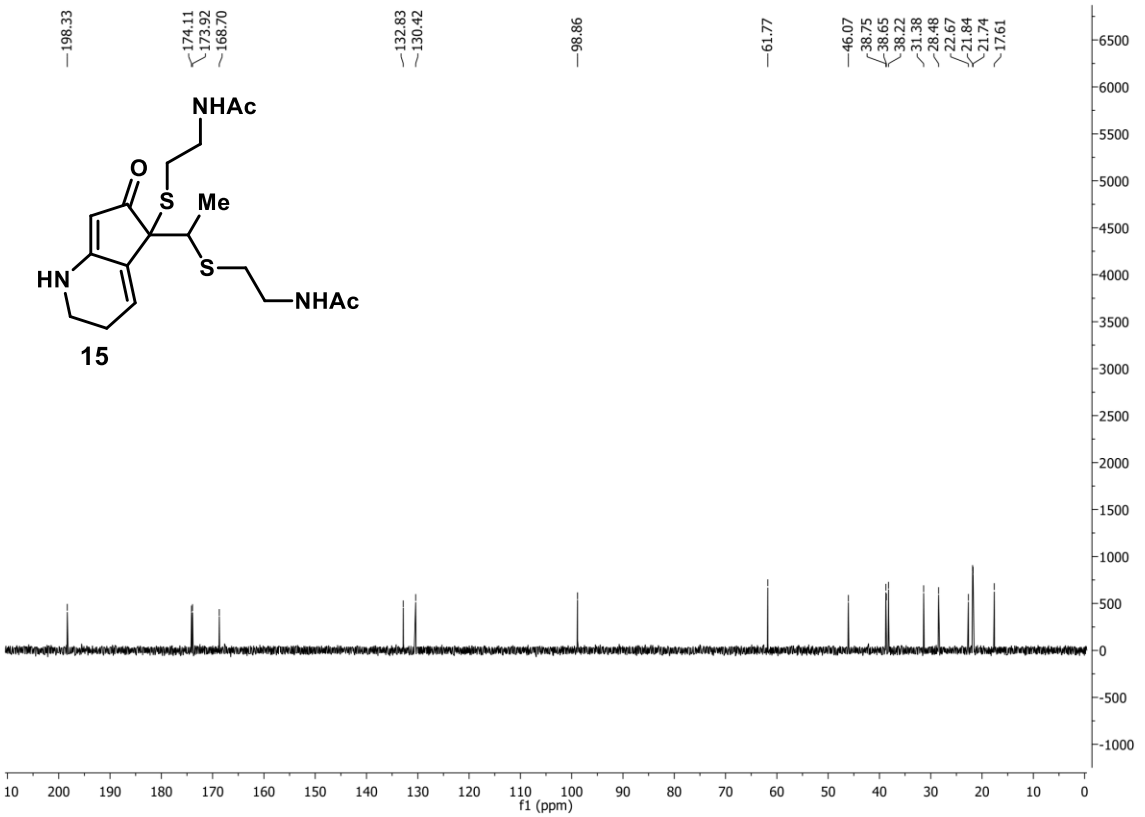
NHAc
O
S
Me
HN
S
NHAc
15
f1 (ppm)

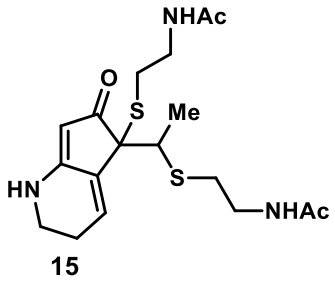

15

^{1}H-^{1}H COSY

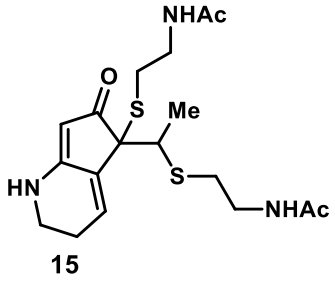

15

^{1}H-^{13}C HSQC

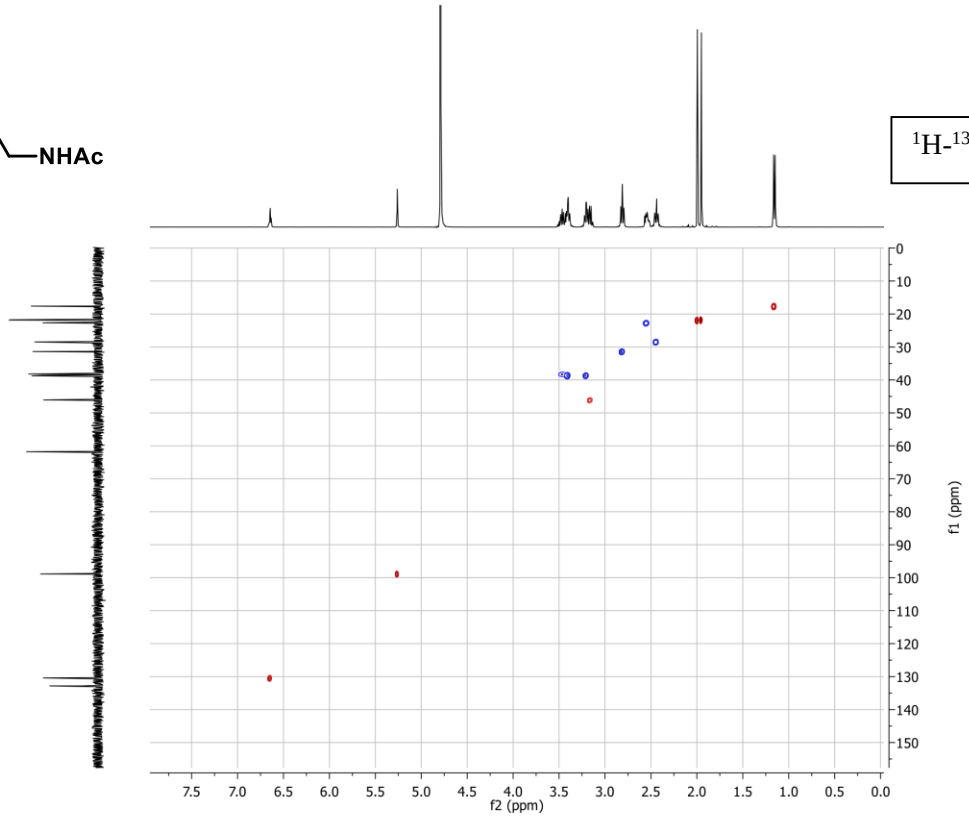

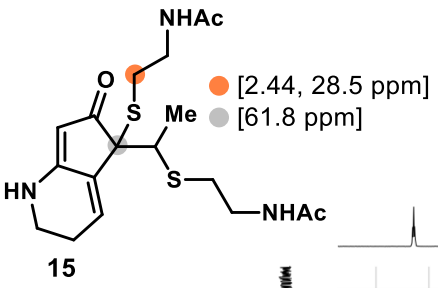

15

^{1}H-^{13}C HMBC

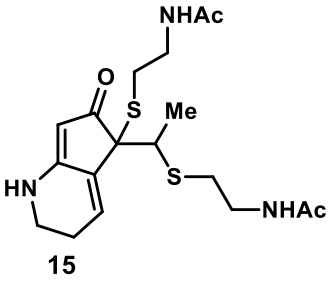

15

^{1}H-^{1}H NOESY

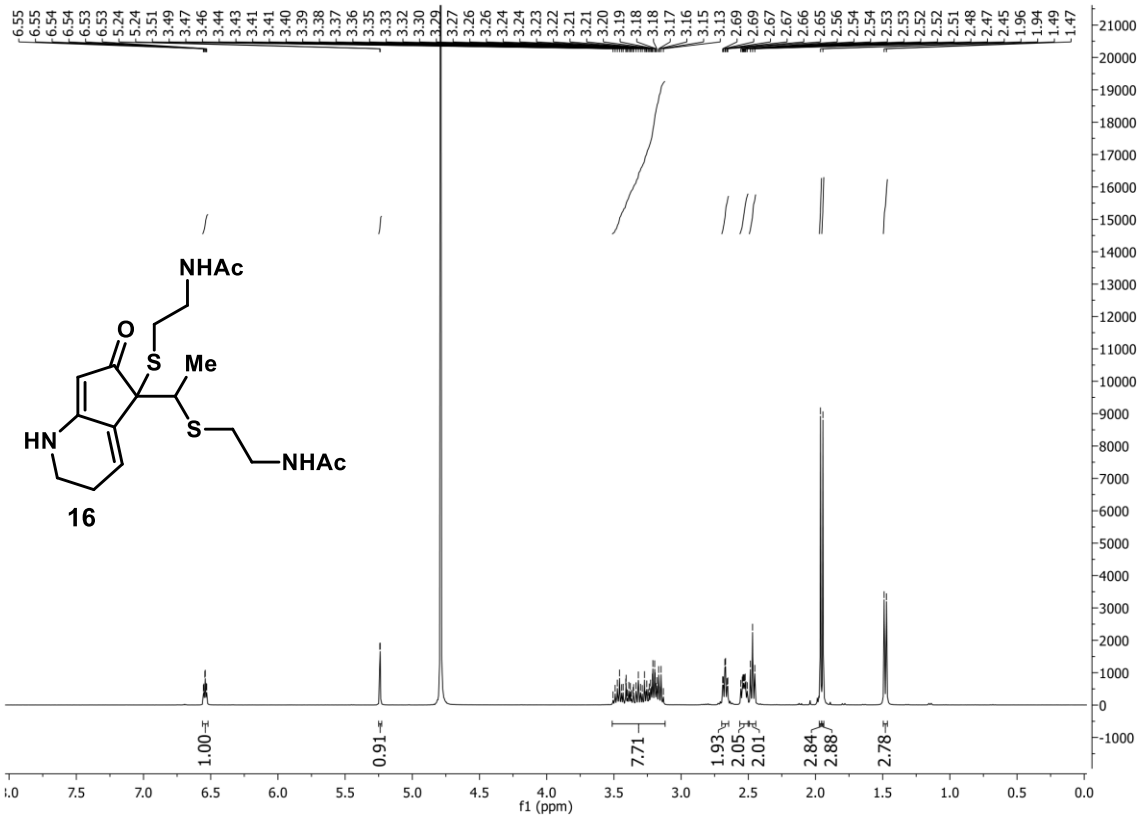
NHAc
O
S
Me
S
HN
NHAc
16
f1 (ppm)

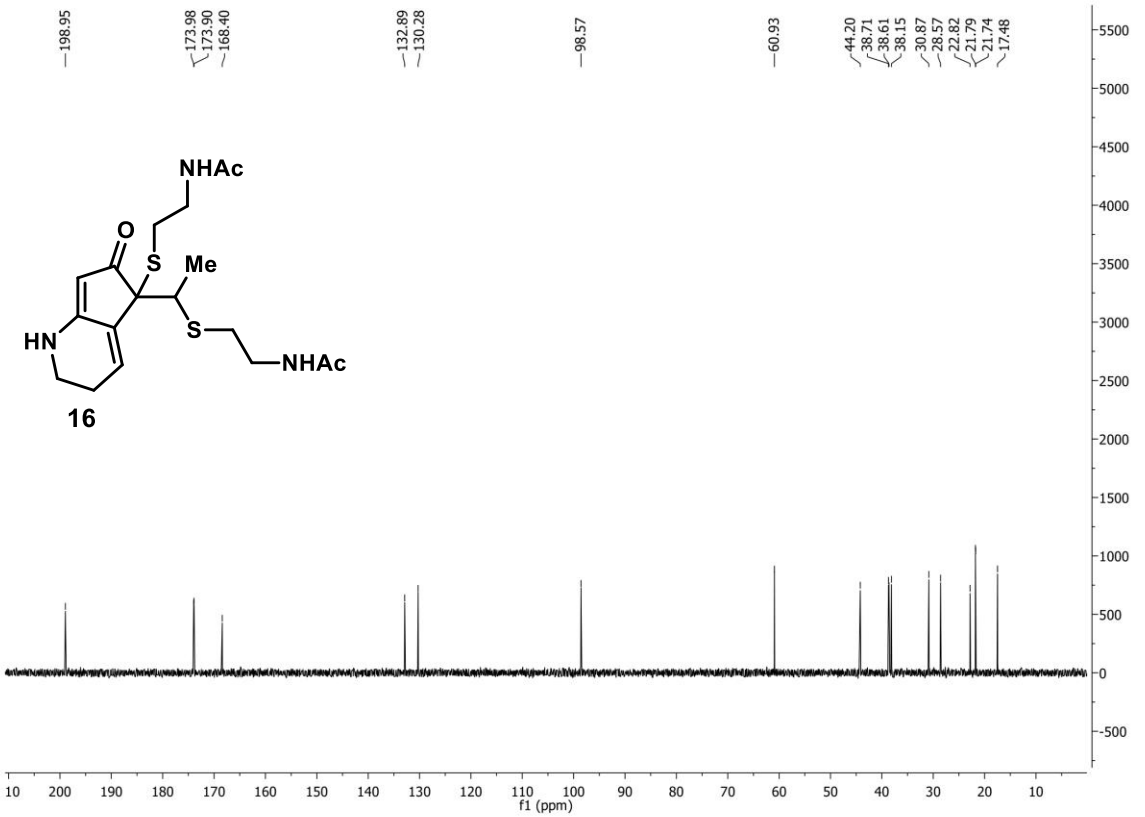
NHAc
O
S
Me
S
HN
NHAc
16
f1 (ppm)

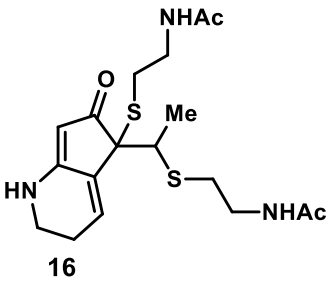

16

^{1}H-^{1}H COSY

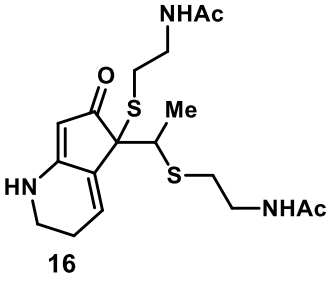

16

^{1}H-^{13}C HSQC

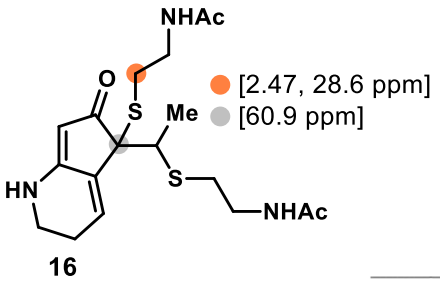

16

^{1}H-^{13}C HMBC

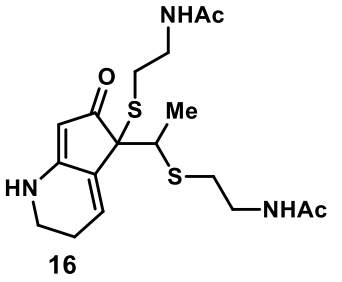

16

^{1}H-^{1}H NOESY

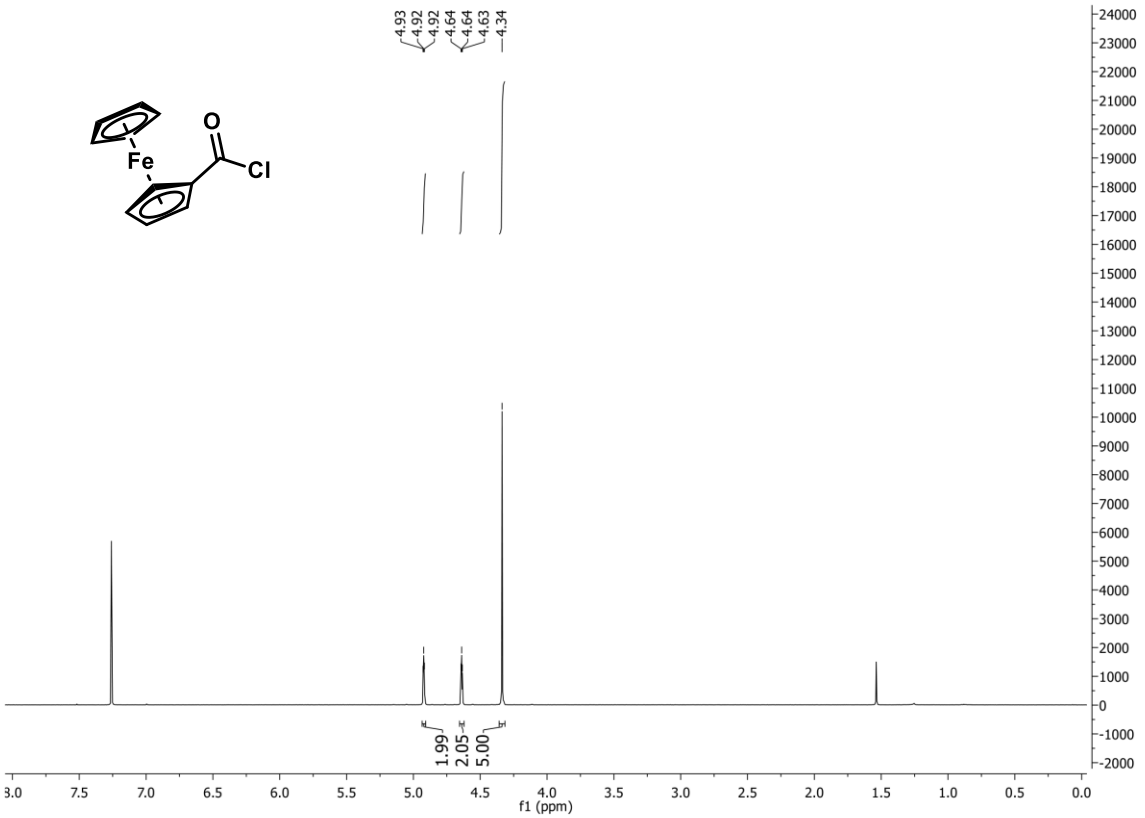
Fe
O
Cl
4.93
4.92
4.92
4.64
4.64
4.63
4.34
1.99
2.05
5.00
f1 (ppm)

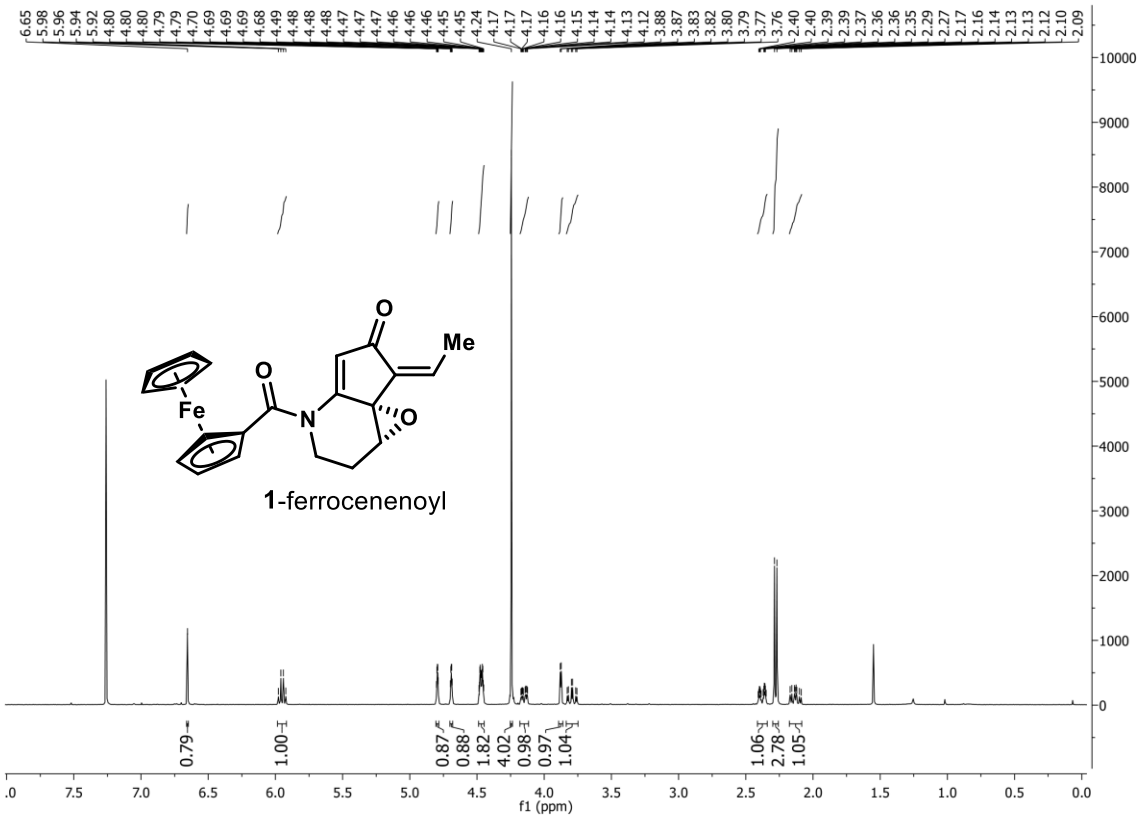
Me
O
Fe
N
O
1-ferrocenenoyl
f1 (ppm)

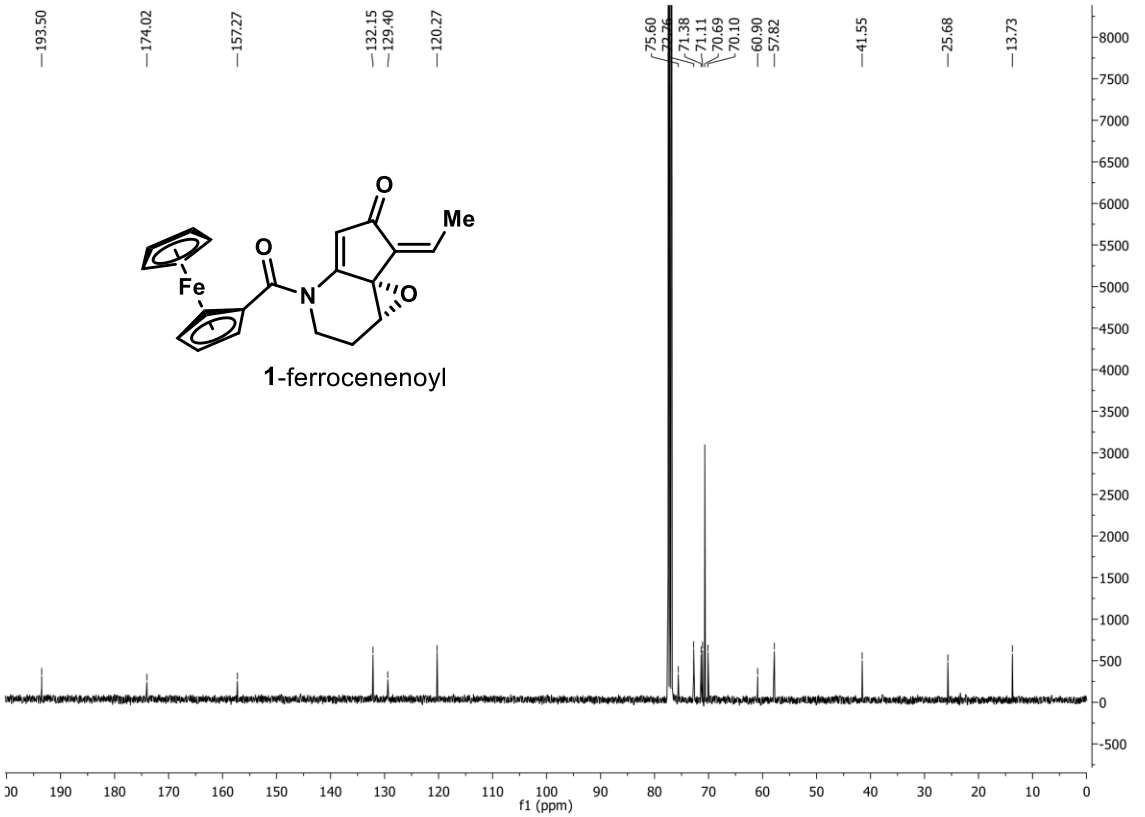
Me
O
Fe
N
O
1-ferrocenenoyl
f1 (ppm)

References

(1) Bruker. Apex2, SADABS (2016/2) and SAINT (Version 8.38A). (2016).

(2) Sheldrick, G. M. SHELXT – Integrated space-group and crystal-structure determination. *Acta Crystallogr. Sect. A Found. Adv*. **A71**, 3–8 (2015).

(3) Sheldrick, G. M. Crystal structure refinement with SHELXL. *Acta Crystallogr. Sect. C Struct. Chem.* **C71**, 3–8 (2015).

(4) Dolomanov, O. V., Bourhis, L. J., Gildea, R. J., Howard, J. A. K. & Puschmann, H. OLEX2 : a complete structure solution, refinement and analysis program. *J. Appl. Crystallogr*. **42**, 339–341 (2009).

(5) Rigaku Oxford Diffraction. CrysAlisPro 1.171.39.46. (2018).

(6) Li, M.; Dixon, D. J. Stereoselective Spirolactam Synthesis via Palladium Catalyzed Arylative Allene Carbocyclization Cascades. *Org. Lett*., **2010**, *12*, 17, 3784–3787.

(7) Skotnitzki, J.; Morozova, V.; Knochel, P. Diastereoselective Copper-Mediated Cross-Couplings between Stereodefined Secondary Alkylcoppers with Bromoalkynes. *Org. Lett*., **2018**, *20*, 8, 2365–2368.

(8) Jahnke, E.; Weiss, J.; Neuhaus, S.; Hoheisel, T. N.; Frauenrath, H. Synthesis of Diacetylene-Containing Peptide Building Blocks and Amphiphiles, Their Self-Assembly and Topochemical Polymerization in Organic Solvents. *Chem. Eur. J*., **2008**, *15*, 2, 388–404.

(9) Hems, E. S.; Wagstaff, B. A.; Saalbach, G.; Field, R. A. CuAAC Click Chemistry for the Enhanced Detection of Novel Alkyne-Based Natural Product Toxins. *Chem. Commun*., **2018**, *54* 86, 12234–12237.

(10) Puder, C.; Krastel, P.; Zeeck, A. Streptazones A, B_1, B_2, C, and D: New Piperidine Alkaloids from Streptomycetes. *J. Nat. Prod.,* **2000**, 63, 9, 1258–1260.

(11) Maruyama, H.; Okamoto, S.; Kubo, Y.; Tsuji, G.; Fujii, I.; Ebizuka, Y.; Furihata, K.; Hayakawa, Y.; Nagasawa, H.; Sakuda, S. Isolation of abikoviromycin and dihydroabikoviromycin as inhibitors of polyketide synthase involved in melanin biosynthesis by Colletotrichum lagenarium. *J. Antibiot.* **2003**, 56, 9, 801–804.

(12) Holmalahti, J.; Raatikainen O.; von Wright, A.; Laatsch, H.; Spohr, A.; Lyngberg, O. K.; Nielsen, J. Production of dihydroabikoviromycin by Streptomyces Anulatus: Production parameters and chemical characterization of genotoxicity. *J. App. Microbiol.* **1998**, *85*, 61–68.